December
2021
Vol. 16 – N. 2

SOCIETAS HERPETOLOGICA ITALICA

Acta Herpetologica

ISSN 1827-9635

Iscritto al Tribunale di Firenze con il n° 5450 del 03/11/2005
Poste Italiane S.p.A. - Spedizione in Abbonamento Postale 70% DCB Firenze

FIRENZE UNIVERSITY PRESS

Acta Herpetologica

Acta Herpetologica è la rivista ufficiale della *Societas Herpetologica Italica* (S.H.I.), un'associazione scientifica che promuove la ricerca erpetologica di base e applicata, la divulgazione delle conoscenze e la protezione degli Anfibi e Rettili e dei loro habitat.

Acta Herpetologica is the official journal of the *Societas Herpetologica Italica* (S.H.I.), a scientific association that promotes basic, applied, and conservation researches on Amphibians and Reptiles.

Sito ufficiale S.H.I. (Official S.H.I. website): http://www-3.unipv.it/webshi

Modalità di associazione
Le nuove domande di associazione sono esaminate periodicamente dal Consiglio Direttivo; solo successivamente i nuovi soci riceveranno la comunicazione di accettazione con le modalità per regolarizzare l'iscrizione (ulteriori informazioni sul sito: http://www.unipv.it/webshi). La quota annuale di iscrizione alla S.H.I. è di € 35,00. I soci sono invitati a versare la quota di iscrizione sul conto corrente postale n. 62198205 intestato a: SHI *Societas Herpetologica Italica*. In alternativa è possibile effettuare un bonifico bancario sul Conto Corrente Postale: n. conto 62198205 intestatario: SHI *Societas Herpetologica Italica* IBAN: IT-54-K-07601-03200-000062198205.

Membership
The S.H.I. Council will examine periodically new applications to S.H.I.: if accepted, new Members will receive confirmation and payment information (for more information contact the official website: http://www.unipv.it/webshi). Annual membership fee is € 35.00 (Euro). Payments are made on the postal account of SHI *Societas Herpetologica Italica* no. 62198205, or by bank transfer on postal account no. 62198205 IBAN: IT-54-K-07601-03200-000062198205 to SHI *Societas Herpetologica Italica.*

Versione on-line: http://www.fupress.com/ah

SOCIETAS
HERPETOLOGICA
ITALICA

Acta Herpetologica

Vol. 16, n. 2 - December 2021

Firenze University Press

Referee list. In alphabetical order the scientists that have accepted to act as editorial board members of Acta Herpetologica vol. 16 (2021).

Elenco dei revisori. In ordine alfabetico gli studiosi che hanno fatto parte del comitato editoriale di Acta Herpetologica vol. 16 (2021).

Edgar Lehr, Enrico Lunghi, Fabio Maria Guarino, Frederico Barroso, Giacomo Rosa, Giovanni Scillitani, Giovanni Scribano, Holly Woodward, Ilaria Bernabò, Iñigo Martínez-Solano, Kerim Çiçek Çiçek, Marco Alberto Luca Zuffi, Marco Sannolo, Mattia Falaschi, Natalia Ananjeva, Núbia Carla Santos Marques, Paolo Casale, Paul Székely, Roberto Sacchi, Romina Fusillo, Sandro Tripepi, Sebastiano Salvidio, Toni Mingozzi.

Acta Herpetologica 16(2): 63-87, 2021
DOI: 10.36253/a_h-10742

A new species of the genus *Noblella* (Amphibia: Strabomantidae) from Ecuador, with new information for *Noblella worleyae*

Carolina Reyes-Puig[1,2,3,4,*], Juan M. Guayasamin[2,5], Claudia Koch[6], David Brito-Zapata[1], Matthijs Hollanders[7], Melissa Costales[8], Diego F. Cisneros-Heredia[1,2,3]

[1] *Universidad San Francisco de Quito USFQ, Colegio de Ciencias Biológicas & Ambientales COCIBA & Instituto de Diversidad Biológica Tropical iBIOTROP, Museo de Zoología/ Laboratorio de Zoología Terrestre, Campus Cumbayá, Quito, Ecuador*
[2] *Universidad San Francisco de Quito USFQ, Colegio de Ciencias Biológicas y Ambientales COCIBA, Instituto BIOSFERA, Campus Cumbayá, Quito, Ecuador*
[3] *Instituto Nacional de Biodiversidad INABIO, Unidad de Investigación, Quito, Ecuador*
[4] *CIBIO/InBIO, Centro de Investigação em Biodiversidade e Recursos Genéticos da Universidade do Porto, Instituto de Ciências Agrárias de Vairão, R. Padre Armando Quintas, 4485-661 Vairão, Portugal*
[5] *Universidad San Francisco de Quito USFQ, Colegio de Ciencias Biológicas y Ambientales COCIBA, Laboratorio de Biología Evolutiva, Campus Cumbayá, Quito, Ecuador*
[6] *Zoologisches Forschungsmuseum Alexander Koenig ZFMK, Leibniz-Institut zur Analyse des Biodiversitätswandels, Bonn, Germany*
[7] *Southern Cross University, School of Environment, Science and Engineering, Lismore, Australia*
[8] *University of New Brunswick, Department of Biology, Fredericton, Canada*
**Corresponding autor*. E-mail: creyesp@usfq.edu.ec

Submitted on: 2021, 31st March; revised on: 2021, 22nd July; accepted on: 2021, 23rd July
Guest Editor: Aaron M. Bauer

Abstract. We describe a new species of terrestrial-breeding frog of the genus *Noblella* from the northwestern slopes of the Andes of Ecuador, in the province of Pichincha, Ecuador, and report a new locality for the recently described *N. worleyae*. We include a detailed description of the osteology of both species and discuss their phylogenetic relationships. The new species is differentiated from other species of *Noblella* by having discs of fingers rounded, without papillae; distal phalanges only slightly T-shaped; toes slightly expanded and rounded distally, without papillae; dorsum uniform brown with irregular suprainguinal dark brown marks; venter yellowish cream, ventral surfaces of legs and thighs reddish to brownish cream; and dark brown throat. The new locality for *N. worleyae* is located in Los Cedros Reserve, an area highly threatened by mining. We highlight the importance of protecting endemic species of small vertebrates in northwestern Ecuador.

Keywords. Frog, Los Cedros Biological Reserve**,** endemism, Imbabura, Mindo, Pichincha, phylogeny.

INTRODUCTION

The amphibian diversity in the tropical Andes is outstanding (Duellman, 1988; Myers et al., 2000; Hutter et al., 2013, 2017). Each year, several species are described from montane forests of this biodiversity hotspot (e.g., Rojas-Runjaic et al., 2018; Guayasamin et al., 2019; Paez and Ron, 2019; Reyes-Puig et al., 2019b; Santa-Cruz et al., 2019; Yanez-Muñoz et al., 2019; Acevedo et al., 2020; Ospina-Sarria et al., 2020; Lehr et al., 2021). Most described species from Ecuador belong to the hyper-diverse genus *Pristimantis* (Paez and Ron, 2019; Reyes-Puig et al., 2020a), but diversity in other anuran taxa has also increased considerably (e.g., *Osornophryne*, *Hyloscirtus*, *Noblella*, Centrolenidae; Mueses-Cisneros et al., 2010; Cisneros-Heredia and Gluesenkamp,

ISSN 1827-9635 (print)
ISSN 1827-9643 (online)

www.fupress.com/ah

2010; Yánez-Muñoz et al., 2010a; Páez-Moscoso and Guayasamin, 2012; Almendáriz et al., 2014; Guayasamin et al., 2017a, 2019; Reyes-Puig et al., 2019c).

Terrestrial-breeding frogs of the genus *Noblella* Barbour 1930 are minute-size anurans (SVL < 22 mm), morphologically differentiated by having terminal discs on digits not or barely expanded, discs and circumferential grooves present distally (except in *N. duellmani*), terminal phalanges narrowly T-shaped, pointed tips of at least Toes III–IV, and an inner tarsal tubercle (De La Riva et al., 2008; Hedges et al., 2008; Duellman and Lehr, 2009). However, phylogenetic relationships of *Noblella* are not fully resolved and its monophyly is uncertain (De la Riva et al., 2017; Santa-Cruz et al., 2019). As currently defined, *Noblella* includes 16 species, fourteen distributed in the Andes of Ecuador, Peru, and Bolivia, and two (*N. losamigos* and *N. myrmecoides*) in the Amazonian lowlands from southeastern Colombia, Ecuador, Peru, Bolivia, and western Brazil (Frost, 2021). During the last 15 years, the number of species in the genus has doubled; and four new species have been described since 2019 (Catenazzi and Ttito, 2019; Reyes-Puig et al., 2019c, 2020b; Santa-Cruz et al., 2019). Currently, the total number of species of the genus *Noblella* is 16, distributed in ten species in Peru, seven in Ecuador, three in Bolivia, and one in Colombia and Brazil (Frost, 2021).

Andean species of the genus *Noblella* show a high level of endemicity, with very restricted distributions. While some species of *Noblella* may apparently be able to survive in environments modified by humans (e.g., *N. duellmani*, *N. losamigos*, *N. lochites*, *N. naturetrekii*; Duellman and Lehr, 2009; Reyes-Puig et al., 2019c; Santa-Cruz et al., 2019); most species (e.g., *N. coloma, N. heyeri, N. personina, N. pygmaea*; Lynch, 1986; Guayasamin and Terán-Valdez, 2009; Harvey et al., 2013) seem to depend on undisturbed forest. Three species of *Noblella* have been described from western Ecuador, all from mature mountain forests: *Noblella heyeri* (Lynch, 1986) occurs in southwestern Ecuador and extreme northwestern Peru; *Noblella coloma* Guayasamin and Terán-Valdez, 2009 is known from its type locality and surroundings (Rio Guajalito and Chiriboga area; Ron et al., 2019); and *Noblella worleyae*, a recently described species is known just from seven specimens, all found in mature forest in the Río Manduriacu Reserve, province of Imbabura, Ecuador (Reyes-Puig et al., 2020b).

While the Ecuadorian Andes have suffered serious habitat destruction and fragmentation caused by expansion of deforestation, agriculture, mining, among others (Castellanos et al., 2011; Roy et al., 2018; Guayasamin et al., 2019; Lessmann et al., 2019; Ortega et al., 2021), there are still some areas with mature forests that have not been exploited due to their complex topography, difficult access, private protection, or preservation for touristic activities. Unfortunately, all such sites are under strong anthropogenic pressure, including mining concessions and the expansion of agricultural boundaries, among others (Cuesta et al., 2017; Roy et al., 2018; Guayasamin et al., 2019; Ortega et al., 2021). These privileged areas have proven to keep an extremely high cryptic diversity of small vertebrates and contain the last remnant populations of numerous threatened species (Cisneros-Heredia and Yanez-Muñoz, 2010; Reyes-Puig et al., 2010, 2019a, 2019b; Yánez-Muñoz et al., 2010b, 2018; Guayasamin et al., 2018, 2019, 2020; Sánchez-Nivicela et al., 2018; Barrio-Amorós et al., 2020).

During the last five years, we have carried out surveys on the western slopes of the Andes in the provinces of Imbabura and Pichincha, Ecuador. As a result of this continuous effort, we found a new species of leaf-litter frog of the genus *Noblella*, which we describe herein based on a combination of morphological, molecular, and osteological features. We also document new information on distribution, external morphology and osteology for the recently described *Noblella worleyae*, information that was not described in detail in the original description. We also include intraspecific variation that will allow complete full with members of the same genus in the future.

MATERIALS AND METHODS

Taxonomy

We followed the family taxonomy proposed by Heinicke et al. (2018) and, also we revised De la Riva et al. (2017) and Barrietos et al. (2021). For identifying species, we assumed the unified species concept (De Queiroz, 2005, 2007). Information for species comparisons was extracted from the original descriptions and cited once at the beginning of the comparison.

Study area and fieldwork

Over the last three years (i.e., 2018–2020), we have carried out field surveys at several localities in montane forests of northwestern Ecuador, mainly in the provinces of Imbabura and Pichincha. Specimens of two different species of *Noblella* were found in Mindo (province of Pichincha) and Los Cedros Biological Reserve (province of Imbabura). Mindo is a small town renowned for its adventure and nature-based touristic activities; thus the area has numerous reserves that protect cloud forests (Arteaga-Navarro et al., 2013). Los Cedros Biological Reserve is a protected area that contains 6,879 hectares

of premontane humid tropical forest and cloud mountain forest. This reserve is located south of the Cotocachi-Cayapas Ecological Reserve (state protected area), and is also recognized by its endemic microfauna (Hutter and Guayasamin, 2015). Collected specimens were euthanized with benzocaine, fixed in 8% formalin, and preserved in 75% ethanol. Liver and leg muscle tissue samples were collected from all individuals prior to preservation. Tissues were preserved in 95% ethanol and stored at -20°C at the Laboratorio de Biología Evolutiva USFQ. Specimens were deposited in the Museo de Zoología, Universidad San Francisco de Quito, Ecuador (ZSFQ).

DNA extraction, amplification, and sequencing

We obtained new DNA sequences of *Noblella* sp. nov. (ZSFQ 050–051). DNA was extracted from muscle or liver tissue following the protocol by Peñafiel et al. (2019). Standard polymerase chain reaction (PCR) was performed to amplify a fragment of the mitochondrial gene 16S rRNA, using a combination of the following primers: 16L10, 16H36E, 16L34, 16H47 (Heinicke et al., 2007). Amplicons were sequenced in both directions by the Macrogen Sequencing Team (Macrogen Inc., Seoul, Korea).

The new sequences were assembled and edited with Geneious 7.1.7 (GeneMatters Corp). After assemblage, the sequences were combined with sequences from GenBank for all species of *Noblella* and representatives of the genera within the Terrarana clade (sensu Hedges et al., 2008), including *Barycholos* Heyer 1969, *Bryophryne* Hedges, Duellman & Heinicke 2008, *Craugastor* Cope 1862, *Haddadus* Hedges, Duellman & Heinicke 2008, *Holoaden* Miranda-Ribeiro 1920, *Ischnocnema* Reinhardt & Lutken 1862, *Lynchius* Hedges, Duellman & Heinicke 2008, *Niceforonia* Goin & Cochran 1963, *Oreobates* Jiménez de la Espada 1872, *Qosqophryne* Catenazzi, Mamani, Lehr, von May 2020, *Phrynopus* Peters 2873, *Pristimantis* Jiménez de la Espada 1870, *Psychrophrynella* Hedges, Duellman & Heinicke 2008, and *Microkayla* De la Riva, Chaparro, Castroviejo-Fisher, Padial 2017. GenBank codes are shown in our inferred phylogenetic tree (Fig. 1).

Phylogenetic analyses

Phylogenetic relationships were inferred using maximum likelihood as the optimality criterion. The final matrix, with 52 terminals, was aligned with MAFFT v.7 (Multiple Alignment Program for Amino Acid or Nucleotide Sequences: http://mafft.cbrc.jp/alignment/software/), with the Q-INS-i strategy. MacClade 4.07 (Maddison and Maddison, 2005) was used to visualize the alignment, which contained a total of 492 bp. Phylogenetic analyses were performed under the ML criteria in GARLI 2.01 (Genetic Algorithm for Rapid Likelihood Inference; Zwickl, 2006) for the mitochondrial gene 16S. GARLI uses a genetic algorithm that finds the tree topology, branch lengths, and model parameters that maximize lnL simultaneously (Zwickl, 2006). Individual solutions were selected after 10,000 generations with no significant improvement in likelihood, with the significant topological improvement level set at 0.01. Then, the final solution was selected when the total improvement in likelihood score was lower than 0.05, compared to the last solution obtained. Default values were used for other GARLI settings, as per recommendations of the developer (Zwickl, 2006). Bootstrap support was assessed via 1,000 pseudoreplicates under the same settings used in tree search. Pairwise genetic distances between species (uncorrected-p) for gene 16S were calculated with PAUP 4a (Swofford et al., 1996).

External morphology

Diagnosis and description of the new species follow formats proposed by Duellman and Lehr (2009) and Lynch and Duellman (1997). For comparisons, we examined specimens of other species of *Noblella* (see Appendix I). We followed the sequence of characters proposed by Guayasamin and Terán-Valdez (2009). We measured preserved specimens using digital calipers to the nearest 0.01 mm. These measurements are: snout to vent length (SVL), from the tip of the snout to the cloaca; head length (HL), measured from tip of snout to anterior edge of tympanum; head width (HW), measured at midorbital region; horizontal diameter of the eye (ED); eye–nostril distance (EN), from anterior ocular angle to posterior edge of nostril; horizontal diameter of tympanum (TD); minimum interorbital distance (MIOD); minimum eyelid width (MWE); hand length (LH), from posterior edge of palmar tubercle to tip of third digit; shank length (LS), from the tip of the ankle to the knee; and foot length (LF), from posterior edge of external metatarsal tubercle to tip of Toe IV. We determined sexual maturity by the presence of vocal slits or extended vocal sacs in males and by the presence of eggs or convoluted oviducts in females. Detailed illustrations of the head, hands and feet were done with Adobe InDesign ©.

Osteology

Osteological descriptions were based on one specimen of the new species (ZSFQ 050) and one of *Noblella worleyae* (MZUTI 1709). Both specimens were scanned using a high-resolution micro-computed tomography (micro-CT) desktop device (Bruker SkyScan 1173, Kontich, Belgium) at the Zoologisches Forschungsmuseum Alexander Koenig (ZFMK, Bonn, Germany). To avoid movements during scanning, specimens were placed in a small plastic container and mounted with styrofoam. Acquisition parameters comprised: An X-ray beam (source voltage 43 kV and current 114 μA) without the use of a filter; 800 projections of 500 ms exposure time each with a frame averaging of 5 recorded over a 180° continuous rotation (rotation steps of 0.3 degrees), resulting in a scan duration of 49 min; a magnification setup generating data with an isotropic voxel size of 19.16 μm (MZUTI 1709) and 14.55 μm (ZSFQ 050), respectively. The CT-dataset was reconstructed with N-Recon software (Bruker MicroCT, Kontich, Belgium) and rendered in three dimensions using CTVox for Windows 64 bits version 2.6 (Bruker MicroCT, Kontich, Belgium). Osteological

terminology follows Trueb (1973), Duellman and Trueb (1994), Fabrezi and Alberch (1996), Guayasamin and Terán-Valdez (2009), Scherz et al. (2017), and Suwannapoom et al. (2018). Cartilage structures were omitted from the osteological descriptions because micro-CT does not render cartilage.

RESULTS

Phylogenetic relationships and genetic distances (Fig. 1)

The inferred phylogeny shows that the new species described herein is part of a clade composed of taxa distributed along the western slopes of the Ecuadorian Andes. This clade is composed by the new species *Noblella* sp. nov., *Noblella coloma* Guayasamin and Terán-Valdez, 2009, and *N. worleyae* Reyes-Puig, Maynard, Trageser, Vieira, Hamilton, Lynch, Culebras, Kohn, Brito and Guayasamin, 2020. Uncorrected p genetic distances are as follow: *N. coloma* (QCAZ 40579) and the new species (ZSFQ 050) = 5.1%; *N. coloma* (QCAZ 40579) and *N. worleyae* (ZSFQ 550–551) = 8.3%; *N. worleyae* (ZSFQ 550–551) and the new species (ZSFQ 050) = 1.2%.

Generic placement

We place the new species in the genus *Noblella* based on morphological and molecular evidence (Fig. 1). Morphologically, we assign the new species to the genus *Noblella,* as defined by Hedges et al. (2008), based on possession of the following traits: head not wider than body; cranial crests absent; tympanic membrane differentiated (undifferentiated in *N. duellmani*, *N. naturetrekii* and *N. madreselva*); dentigerous processes of vomers absent; terminal discs on digits not or barely expanded; discs and circumferential grooves present distally (absent in *N. duellmani*); terminal phalanges narrowly T-shaped; Finger I shorter than, or equal in length to, Finger II; Finger IV containing two phalanges in *Noblella carrascoicola* (De la Riva and Köhler, 1998), *N. lochites* (Lynch, 1976b), *N. losamigos* (Santa-Cruz et al., 2019), *N. myrmecoides* (Lynch, 1976b), *N. naturetrekii* (Reyes-Puig et al., 2019c), and *N. ritarasquinae* (Köhler, 2000) and three phalanges in *N. coloma* (Guayasamin and Terán-Valdez, 2009), *N. duellmani* (Lehr, Aguilar, and Lundberg, 2004), *N. heyeri* (Lynch, 1986), *N.* sp. nov., *N. lynchi* (Duellman, 1991), *N. madreselva* (Catenazzi, Uscapi, and von May, 2015), *N. personina* (Harvey, Almendáriz, Brito-M., and Batallas-R., 2013), *N. peruviana* (Noble, 1921), *N. pygmaea* (Lehr and Catenazzi, 2009), and *N. thiuni* (Catenazzi and Ttito, 2019); Toe III shorter than Toe V (except in *N. naturetrekii* and *N. worleyae*); tips of at least toes III–IV acuminate; subarticular tubercles not protruding; dorsum pustulate or shagreen; venter smooth; SVL less than 22 mm.

Systematic accounts

Noblella mindo new species.
Noblella coloma Arteaga et al. (2013).
Figs. 2–8
LSID urn:lsid: lsid:zoobank.org:act:3B7741EF-BF26-4589-B231-73F198AA1218
Proposed standard English name. Mindo Leaf Frog
Proposed standard Spanish name. Rana Noble de Mindo
Holotype. ZSFQ 050 (Fig. 2–6), adult female, collected in El Cinto, 11 Km E from Mindo town, Mindo (0.09022°S, 78.818581°W; 1,673 m; Fig. 2), province of Pichincha, República del Ecuador, by Melissa Costales, Matthijs Hollanders and Emilia Peñaherrera on 08 July 2017.
Paratypes (2 females, 2 males). Adult males (ZSFQ 049, 051) and adult females (ZSFQ 304–305) collected at the type locality (same data as holotype), by Melissa Costales on 04 October 2015.

Etymology

The specific name "mindo" is a word of unknown meaning in Panzaleo, an extinct pre-Columbian language of northern Ecuador (Jijón y Caamaño 1940). It is used as a noun in apposition, and alludes to the valley of Mindo, where the type locality of the new species is located. The remnant forests of this emblematic valley protect several species of endemic amphibians and reptiles such as *Pristimantis mindo, Noblella mindo*, and *Anolis proboscis*.

Diagnosis

Noblella mindo sp. nov. (Figs. 3–8) presents the following characteristics: (1) skin of dorsum finely shagreen, skin on venter smooth, discoidal fold slightly defined, discoidal and thoracic folds absent; (2) tympanic annulus and membrane visible externally, supratympanic fold inconspicuous (Figs. 3, 4); (3) snout short (eye-to-nostril distance 57% of eye diameter), rounded in dorsal and lateral views (Fig. 3); (4) eyelids without tubercles; (5) dentigerous processes of vomers absent; (6) vocal slits and sac present, nuptial pads not visible; (7) fingers not expanded distally, finger tips rounded, without papillae (Fig. 3); Finger I shorter than Finger II (Fig. 3); (8) distal phalanges slightly T-shaped, phalangeal formula of hands: 2-2-3-3 (Fig. 7); (9) supernumerary palmar tubercles present (slightly visible) mostly at the base

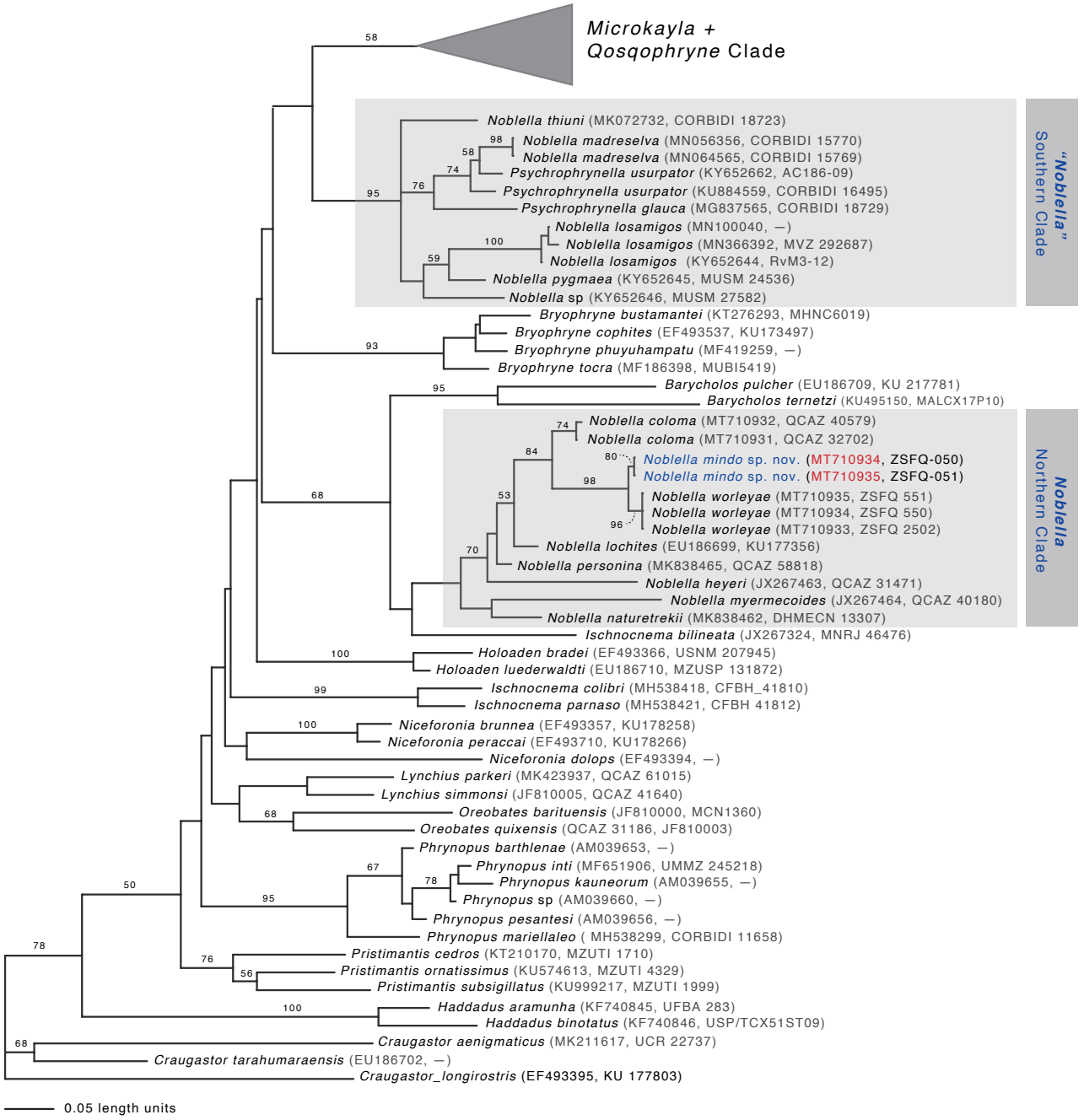

Fig. 1. Phylogeny of *Noblella* (light gray boxes) showing the relationships of *N. mindo* sp. nov. The phylogeny was inferred based on mitochondrial (16S) DNA sequences (16S; 52 terminals, 492 bp) and under the Maximum likelihood criterion. For each individual, museum catalog number or, if unavailable, GenBank accession number is shown.

of the digits, ulnar tubercles diminutive and rounded, subarticular tubercles rounded; circumferential grooves absent; (10) one tarsal tubercle elongated and subconical (Fig. 3); two prominent metatarsal tubercles (inner tubercle 3–4 times size of external); toes slightly expanded and rounded distally, without papillae; (11) Toe V shorter than Toe III, supernumerary plantar tubercles absent, distal portions of circumferential grooves not visible; (12) phalangeal formula of feet: 2-2-3-4-3 (Fig. 7); (13) in life, uniform brown dorsum, cream middorsal, longitudinal line distinct and present in all individuals, dark brown suprainguinal marks, white rictal gland,

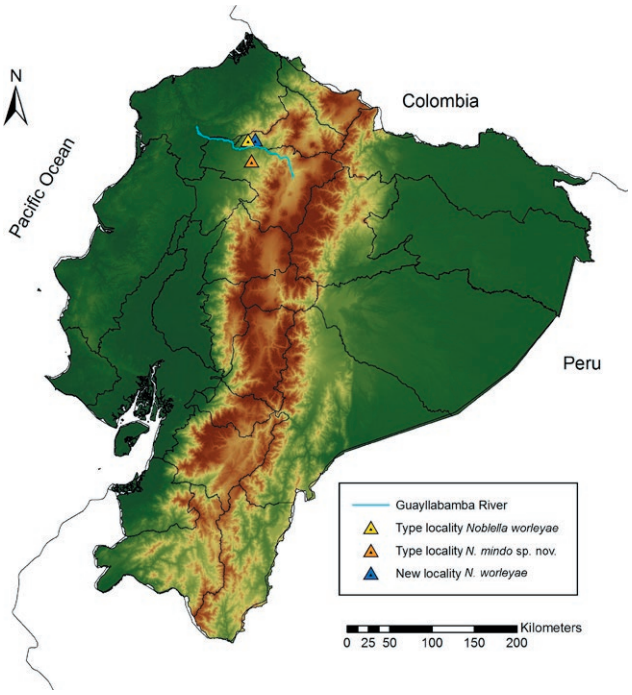

Fig. 2. Distribution of *Noblella mindo* sp. nov and *N. worleyae* in Ecuador.

flanks with dark brown band narrowing towards groin, dotted with white, light groin, with low concentration of melanophores, dark brown throat, chest and ventral surfaces of arms with a white cross formed by a longitudinal, fine line running from chin to chest crossing a similar line departing from midventral surface of each forelimb, yellowish-cream venter, reddish-copper iris with minute turquoise scattered dots (Fig. 4); (14) SVL in adult males 16.5–17.0 mm (mean 16.7 mm, n = 2), SVL in adult females 18.3–19.5 mm (mean 19.0 mm, n = 3).

Comparisons (Fig. 6, Table 1)

Noblella mindo sp. nov. differs from its congeners by the presence of rounded fingertips, without papillae; distal phalanges slightly T-shaped; toes slightly expanded and rounded distally, without papillae; dorsum uniform brown with middorsal cream line, suprainguinal marks dark brown, rictal gland white, light groin, throat and chest dark brown with white cross, and venter yellowish cream. *Noblella mindo* sp. nov. is most similar and closely related to *N. coloma* and *N. worleyae* (Fig. 1), but they differ as follows (characters of *N. mindo* sp. nov. in parentheses): *Noblella coloma* has all finger tips acuminate (all rounded), dark middorsal line (light), dark rictal gland (white), orange to reddish-venter (yellowish-cream), dark groin (light), uniform dark brown throat, chest and ventral surfaces of arms (dark brown with white cross), ulnar tubercles absent (diminutive and rounded), and smaller body size of 16.0 mm SVL in adult female (18.3–19.5 mm SVL in adult females); the new species (characters of *N. mindo* sp. nov. in parentheses) is distinguished from *Noblella worleyae* has finger tips slightly acuminate on Fingers I and IV and acuminate on Fingers II and III (rounded), T-shaped distal phalanges (slightly T-shaped), prootic and exoccipital fused to form otoccipital (separated), sphenethmoid well-ossified and ventrally fused at midline (moderately ossified, ventrally fused at midline in posterior half and separated in anterior half). For more comparison's information see Table 1.

Noblella mindo sp. nov. has three phalanges on Finger IV like *N. duellmani* (Lehr, Aguilar and Ludenberg, 2004), *N. heyeri* (Lynch, 1986), *N. lynchi* (Duellman, 1991), *N. madreselva* (Catenazzi, Uscapi and von May, 2015), *N. personina* (Harvey, Almendáriz, Brito, and Batallas, 2013), *N. peruviana* (Noble, 1921), *N. pygmaea* (Lehr and Catenazzi, 2009), and *N. thiuni* (Catenazzi and Ttito, 2019), but they differ as follows (characters of *N. mindo* sp. nov. in parentheses): *Noblella duellmani* has dorsal skin pustular (finely shagreen), tympanum membrane and annulus absent (present), upper eyelid bearing small tubercles (absent), ulnar tubercles coalesced into low folds (diminutive and round, not forming a fold), outer edge of tarsus bearing row of low and elongate tubercles (absent), tips of Fingers I-II slightly expanded and tips of Fingers III–IV slightly acuminate (all finger tips rounded), venter brown with tan mottling (yellowish-cream), and larger body size of 20.0 mm SVL in adult female (18.3–19.5 mm SVL in adult females); *Noblella heyeri* has dorsal skin weakly pustulate (finely shagreen), snout subacuminate in dorsal view (round), ulnar tubercles distinct and round (diminutive, round), toe tips slightly acuminate (round), venter brown with cream fleck (yellowish-cream), and smaller body size of 13.1–15.9 mm SVL in adult females (18.3–19.5 mm SVL in adult females); *Noblella lynchi* has dorsal skin pustular (finely shagreen), snout subacuminate in dorsal view (round), ulnar tubercles coalesced into low folds (diminutive and rounded, not forming a fold), outer edge of tarsus bearing row of low and elongate tubercles (absent), toe tips weakly acuminate (round), and venter brown with fine cream flecks (yellowish cream); *Noblella madreselva* has dorsal skin with small tubercles (finely shagreen), tympanic membrane not differentiated and tympanic annulus barely visible below skin (well-differentiated), upper eyelid with minute tubercles (absent), toe tips weakly acuminate (rounded), venter black with large and irregularly shaped white mark (yellowish-cream), and smaller body size of 17.6 mm SVL in adult female (18.3–19.5 mm SVL in adult females); *Noblella*

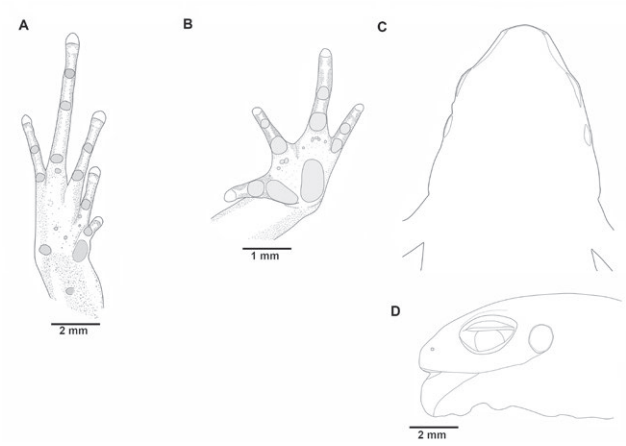

Fig. 3. *Noblella mindo* sp. preserved holotype, ZSFQ 050, adult female, SVL = 18.3 mm. **(A)** Foot in ventral view. **(B)** Hand in ventral view. **(C)** Head in dorsal view. **(D)** Head in lateral view. Illustrations by Carolina Reyes-Puig.

personina has dorsal skin smooth with pustules (finely shagreen), snout subtruncate in profile (round), finger and toe tips acuminate with papillae (round, lacking papillae), venter white (yellowish-cream), and smaller body size of 15.6–17.9 mm SVL in adult females (18.3–19.5 mm SVL in adult females); *Noblella peruviana* has tympanic membrane not differentiated (differentiated), toe tips slightly acuminate (round), and venter tan (yellowish cream); *Noblella pygmaea* has dorsal skin tubercular (finely shagreen), thoracic fold present (absent), dorsolateral fold on anterior half of body present (absent), upper eyelid bearing small tubercles (absent), minute tubercle on heel present (absent), toe tips pointed (round), venter pale grayish brown (yellowish-cream), and smaller body size of 11.3–12.4 mm SVL in adult females (18.3–19.5 mm SVL in adult females); *Noblella thiuni* has thin dorsolateral folds visible on anterior half of body (absent), tympanic membrane not differentiated (differentiated), fingertips bulbous (round), ulnar tubercles absent (present, diminutive and round), venter copper reddish with a profusion of silvery spots (yellowish cream), and smaller body size of 11.0 mm SVL in male (16.5–17 mm in adult females). *Noblella carrascoicola* (De la Riva and Köhler, 1998), *N. lochites* (Lynch, 1976b), *N. losamigos* (Santa-Cruz et al., 2019), *N. myrmecoides* (Lynch, 1976b), *N. naturetrekii* (Reyes-Puig et al., 2019c), and *N. ritarasquinae* (Köhler, 2000) are easily differentiated from *N. mindo* sp. nov. by having two phalanges on Finger IV instead of three.

Description of the holotype

Adult female (ZSFQ 050); head narrower than body, its length 40.8% of SVL; head longer than wide; head width 31.1% of SVL; snout round in dorsal and lateral

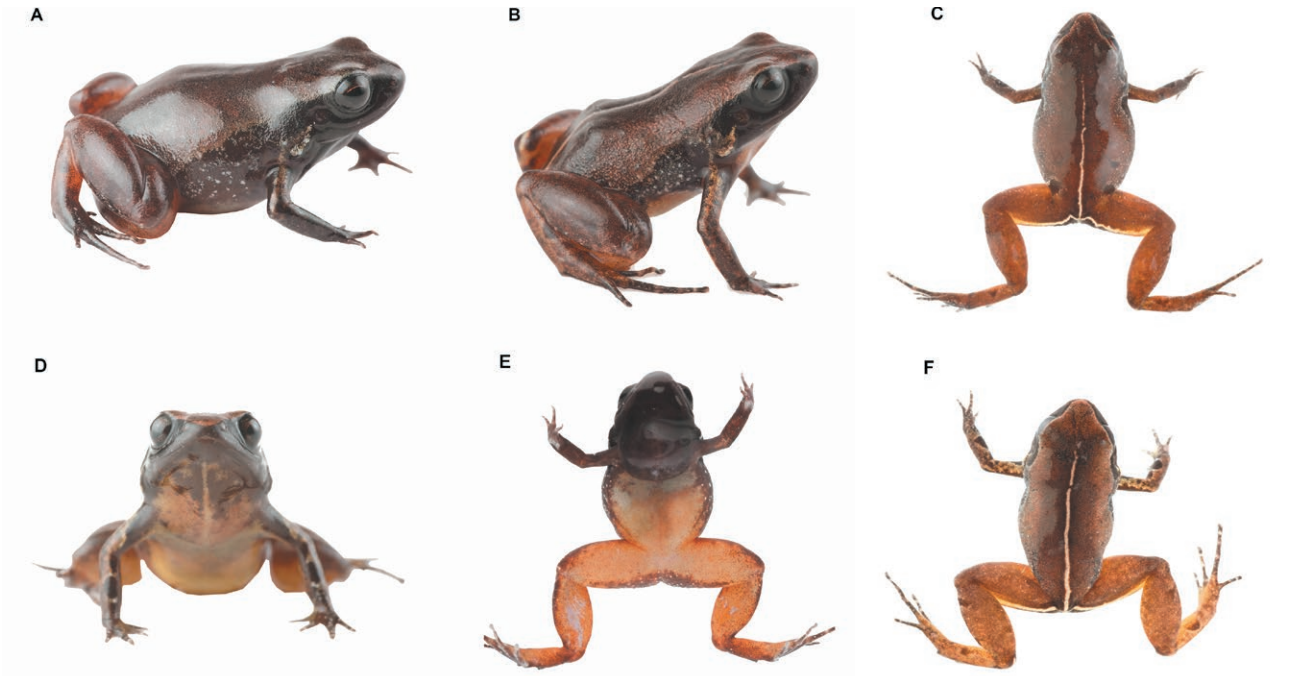

Fig. 4. Color patterns of *Noblella mindo* sp. nov. in life. **(A, C)** Dorso-lateral and ventral patterns of holotype, ZSFQ 050, adult female, SVL = 18.3 mm. **(B, D)** Dorsolateral and ventral patterns of paratype, ZSFQ 051, adult male, SVL = 16.9 mm. Photos by Matthijs Hollanders.

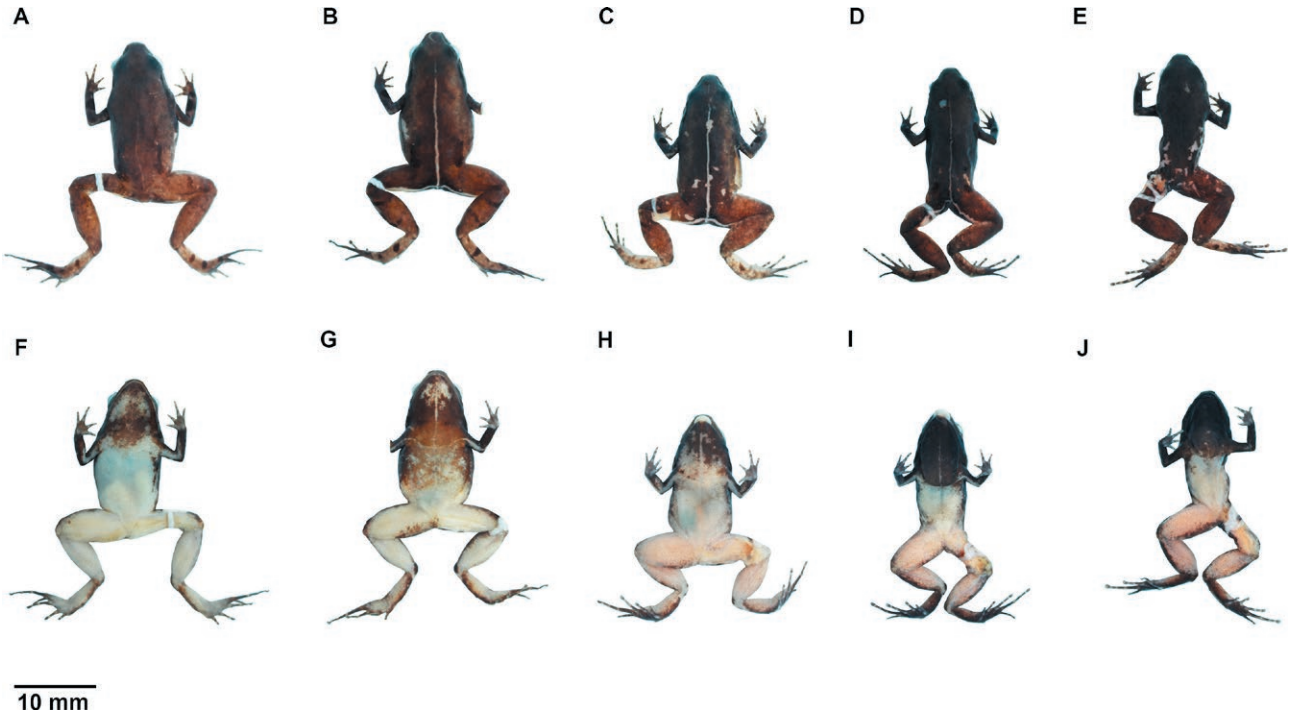

Fig. 5. Color variation of preserved *Noblella mindo* sp. nov. in (**A–E**) dorsal and (**F–J**) ventral views: **(A, F)** ZSFQ 305, paratype, adult female, SVL = 19.5 mm; **(B, G)** ZSFQ 304, paratype, adult female, SVL = 19.2 mm; **(C, H)** ZSFQ 050, holotype, adult female, SVL = 18.3 mm; **(D, I)** ZSFQ 051, paratype, adult male, SVL = 17.0 mm; **(E, J)** ZSFQ 049, paratype, adult male, SVL = 16.5 mm. Photos by David Brito-Zapata and Carolina Reyes-Puig.

views; canthus rostralis straight, slightly concave in profile; loreal region slightly concave; upper eyelid 45.6% of interorbital distance; eye-nostril distance 54.8% of eye diameter; tympanum visible externally, tympanic membrane differentiated from surrounding skin; supratympanic fold indistinct. Dentigerous processes of vomers absent and vomerine teeth absent; choanae laterally oriented; tongue longer than wide, elongated, partially notched posteriorly.

Skin of dorsum finely shagreen, evident tubercles absent; skin on flanks smooth; venter smooth; discoidal fold slightly visible, dorsolateral folds and thoracic folds absent; diminutive rounded ulnar tubercles; palmar tubercle oval, about 2 times the size of the thenar tubercle; supernumerary palmar tubercles present, mainly at the base of the digits; proximal subarticular tubercles prominent, rounded; phalangeal formula 2-2-3-3; fingers not expanded distally, finger tips rounded, circumferential grooves absent; relative lengths of fingers: I < II < IV < III; forearm lacking evident tubercles.

Hindlimb lengths moderate, tibia length 49.3% of SVL; foot length 46.1% of SVL; dorsal surfaces of hindlimbs shagreen; tubercles on the heel absent; one prominent elongated tarsal tubercle on ventral surface of tarsus; two metatarsal tubercles, inner elongated conspicuous, outer subconical; proximal and distal subarticular tubercles well-defined; supernumerary tubercles absent. Toes slightly expanded and rounded distally; distal portions of circumferential grooves not visible; phalangeal formula 2-2-3-4-3; relative lengths of toes: I < II < V < III < IV.

Measurements of holotype (in mm)

SVL= 18.3, HL= 7.5, HW= 5.7, ED= 2.4, EN= 1.3, MWE= 1.5, TD= 0.9, MIOD= 3.4, LH= 3.4, LS= 9.0, LF= 8.4. For measurements of the type series (mm) see Table 2.

Color of holotype in life (Fig. 4)

Dorsum brown, grayish brown towards the flanks; well-defined cream middorsal stripe, extending from interparietal region to cloaca and continuing along posterior surfaces of hindlimb. Loreal region black, extending as homogeneous dark band to upper insertion of arm and into body flanks, narrowing towards groin and limited dorsally with a lighter brown line; flanks strongly light flecked; groin dark. Rictal gland white. Venter and ventral surfaces of hindlimbs yellowish cream; throat dark brown with large irregular yellowish cream marks and

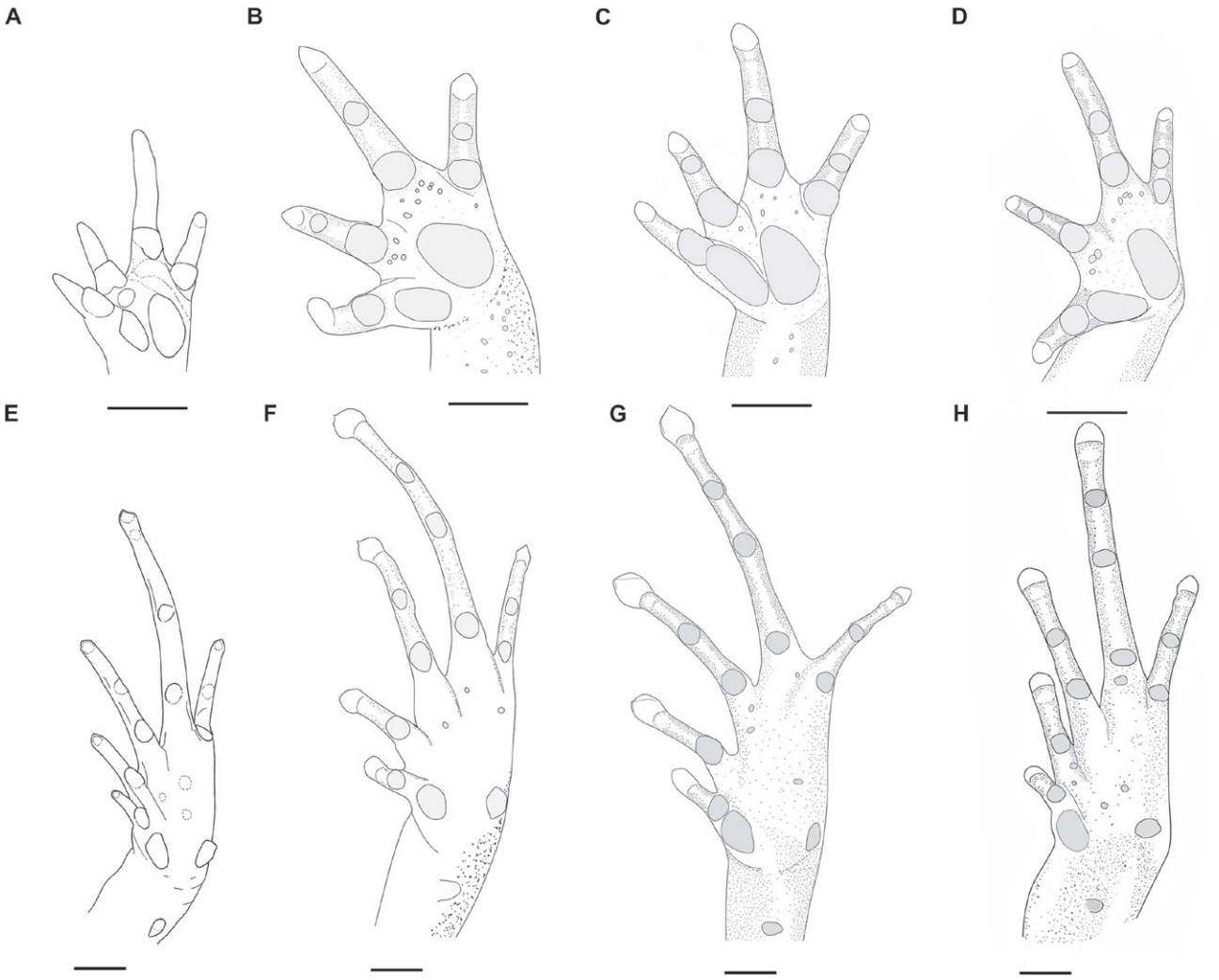

Fig. 6. Ventral views of **(A–D)** hands and **(E–H)** feet from three species of *Noblella*: **(A, E)** *Noblella coloma*, extracted from Guayasamin and Terán-Valdez (2009); **(B, F)** *N. worleyae* (holotype); **(C, G)** *N. worleyae* (ZSFQ 3851); **(D, H)** *N. mindo* sp. nov. (holotype). Scale bars = 1 mm. Illustrations by Carolina Reyes-Puig.

medium longitudinal line. Forelimbs ventrally yellowish cream with dark brown marks, dorsally light brown with dark brown marks; iris reddish copper with minute scattered turquoise dots. Hindlimbs like dorsum.

Color of holotype in ethanol (Fig. 5)

Dorsum brown, darker towards middorsum, well-defined middorsal line cream, extending from interparietal region to cloaca where stripe continues along posterior surface of thighs and pes. Dorsal surfaces of forelimbs brown with black spots. Labial bars absent; rictal gland light brown. Loreal region black, extending as homogeneous dark band to upper insertion of arm and into body flanks, narrowing towards groin; flanks strongly light flecked; groin dark. Dorsal surfaces of hindlimbs lighter brown than dorsum to cream with dark fleck and spots. Throat dark brown with cream irregular marks and medium longitudinal stripe. Chest, venter and ventral surfaces of thigh and crus cream.

Variation of color patterns and external morphology (Figs. 4–5)

Adult females ZSFQ 050, 304–305 and the adult male ZSFQ 051 exhibit a cream middorsal stripe extending from interparietal region to cloaca; stripe of ZSFQ 305 is thinner and faintly defined. Dark suprainguinal marks are faint in ZSFQ 049. Throat, chest and ventral surfaces of forelimbs are dark brown with a white cross formed by a longitudinal, fine line running from chin to chest, crossing a similar line departing from midventral

Table 1. Main diagnostic characters of three species of *Noblella* from northwestern Ecuador.

Species	Characters										Source
	Finger tips	Toe tips	Distal phalanges	Toes papillae	Ulnar tubercles	Venter and throat coloration	Prootic and exoccipital	Sphenethmoid	Length of transverse processes of Presacrals	Neural arch of Presacrals	
Noblella coloma	Acuminate	Slightly expanded and acuminate distally	T-shaped	Absent	Absent	Venter orange with minute white and brown spots	Separated	Well-ossified, ventrally not fused at midline	II, VIII<V–VII<IV<III	Presacrals III–V with raised medial ridge	Terán-Valdez and Guayasamin, 2009
N. worleyae	Slightly acuminate on Fingers I and IV and acuminate on Fingers II and III	Slightly expanded and slightly acuminate on Toes I and V, and cuspidate tips on Toes II–IV	T-shaped	Absent	Present	Venter yellowish cream with minute speckling; throat with irregular brown marks to homogeneously brown	Fused to form otoccipital	Well-ossified, ventrally fused at midline	II<V–VIII<IV<III	With raised medial ridge in all presacrals	Reyes-Puig et al., 2020 and this paper
N. mindo sp. nov.	Rounded	Slightly expanded and rounded distally	slightly T-shaped	Absent	Present	Throat, chest and ventral surfaces of arms dark brown with a white cross, venter yellowish cream	Separated	Moderately ossified, ventrally fused at midline in posterior half and separated in anterior half	V–VIII<II–IV<III	Presacrals III–VIII with raised medial ridge	This paper

Table 2. Measurements (in mm) of type series of *Noblella mindo* sp. nov. Ranges followed by mean and standard deviation in parentheses.

Characters	*Noblella mindo* sp. nov.	
	Females (n = 3)	Males (n = 2)
SVL	18.3–19.5 (19.0 ± 0.6)	16.5–17.0 (16.7 ± 0.3)
HL	7.1–7.5 (7.2 ± 0.2)	6.2–7.0 (6.6 ± 0.6)
HW	5.7–6.7 (6.3 ± 0.5)	5.37–5.4 (5.38 ± 0.02)
ED	2.2–2.5 (2.4 ± 0.2)	1.9–2.0 (1.95 ± 0.1)
EN	1.26–1.29 (1.28 ± 0.01)	1.21–1.22 (1.215 ± 0.01)
MWE	1.2–1.5 (1.3 ± 0.2)	1.1–1.2 (1.15 ± 0.01)
TD	0.8–1.2 (0.9 ± 0.2)	0.78–0.82 (0.8 ± 0.02)
MIOD	3.3–3.4 (3.3 ± 0.1)	3.0–3.4 (3.2 ± 0.3)
LH	3.5–3.9 (3.7 ± 0.2)	3.0–3.2 (3.1 ± 0.2)
LS	9.0–9.3 (9.1 ± 0.2)	7.7–8.0 (7.8 ± 0.2)
LF	8.4–9.0 (8.6 ± 0.4)	7.3–7.5 (7.4 ± 0.1)

surface of each forelimb (ZSFQ 050, 304, 774), longitudinal line on throat of ZSFQ 773 is faint, while cross is almost unnoticeable in holotype due to extensive light color of throat. Venter and ventral surfaces of hindlimbs are cream (ZSFQ 305), dirty cream with diffused irregular brown marks (ZSFQ 304), or pinkish cream (ZSFQ 049–051). The throat in females is cream (ZSFQ 304–305) or pinkish cream (ZSFQ 050) with large irregular dark brown marks; meanwhile in males it is homogenously dark brown with a slightly defined medium longitudinal stripe (ZSFQ 049, 051).

Osteology

Osteological description of *Noblella mindo* sp. nov. is based on micro-CT images of the adult female holotype (ZSFQ 050). Details of skull morphology and osteological aspects of hand and foot are presented in Fig. 7 and main skeletal features are shown in Fig. 8.

Skull (Fig. 7)

Skull slightly longer than wide; widest part is at about where quadratojugal meets maxilla and is 89% of skull length. Rostrum short; distance from anterior edge of frontoparietals to anterior face of premaxilla is 16% of skull length. At level of midorbit, braincase is about 38% of maximum skull width. Braincase combines well- and poorly ossified elements. Frontoparietals are well-developed bones, distinctly longer than broad, slightly narrower anteriorly than posteriorly; narrowly separated along most of their length and only fused in anterior region. Boarder between frontoparietals and prootics not well-resolved in micro-CT scan. Ventrally, prootics in contact with parasphenoid alae. Prootics well-separated from each other. Exoccipitals approximate one another ventromedially and dorsomedially but still clearly separated with about same distance ventrally and dorsally; separated from frontoparietals. Anterolaterally, frontoparietals in contact with sphenethmoid. Sphenethmoid ventrally at midline separated in anterior half and fused in posterior half; posterior margin does not reach midpoint of orbit and is broadly separated from prootic and in ventral contact with parasphenoid. Cultriform process of parasphenoid well-ossified posteriorly, thinning anteriorly, and about 28% width of braincase at mid-orbit. Lateral margins of process approximately parallel. Parasphenoid alae long but poorly ossified at their lateral ends. Neopalatines very thin and long, articulate with sphenethmoid and approximate but not contact maxilla. Columella (or stapes) large and well-ossified. Due to tiny size and fine structure, septomaxilla is not well-resolved in micro-CT scan. Dorsal investing bones moderately developed. Nasals thin and broadly separated from one another, posteriorly in contact with anterior end of frontoparietals and posterolaterally in thin contact with maxilla. They curve ventrally towards their lateral edges. Small prevomers broadly separated from one another medially, their anterior edge almost contacts a long and thin posterior projecting ramus of septomaxilla. Maxillary arcade bears many small, poorly resolved teeth on premaxillae and maxillae. Premaxillae separated medially, and their anterodorsal alary processes rise divergent from midline but still distinctly separated from nasals. Premaxilla and maxilla in lateral contact, with anterior edge of maxilla slightly overlapping lateral edge of premaxilla. Pars palatina of premaxilla broad, with two well-defined processes: medial process thin and acuminate, running about parallel to its counterpart, being distinctly separated from it; lateral process about the same length, but slightly broader, especially at its truncate posterior ending. Maxilla long, its posterior end acuminate and in contact with quadratojugal. Triradiate pterygoid bears a long, curved anterior ramus oriented anterolaterally toward maxilla, with which it articulates at ventral boarder slightly anterior to midline of orbit. Posterior ramus of pterygoid about same length as medial ramus and both about half length of anterior ramus; however, posterior ramus more robust than other two. Edge of medial ramus overlaps lateral edge of prootic. Quadratojugal slender, almost straight and articulating anteriorly with maxilla and posterodorsally with ventral ramus of squamosal. Squamosal T-shaped, with a long laminar otic ramus; zygomatic ramus much shorter and slender; ventral ramus about same length as otic ramus, laminar and broad, increasing in width ventrally. Mandible slim and edentate. Mentomeckelians small, medial-

ly, and laterally slightly broadened, and separated medially by a narrow gap. Dentary long and thin, reaching to about anterior corner of orbit; it is posteriorly acuminate and overlapping angulospenial, seeming to be in contact with this bone for about the posterior half of its length; anteroventrally it contacts mentomeckelian bones. Angulosplenial long and arcuate. Coronoid process is a moderately long and slightly raised ridge. The only ossified portions of hyoid apparatus are two posteromedial processes, which are anteriorly slightly and posteriorly moderately expanded, approaching each other at anterior ends but being still moderately separated.

Postcranium (Fig. 8)

Eight presacral vertebrae. All presacrals non-imbricate. Presacral I longer than posterior vertebrae. All except Presacral I bear well-developed diapophyses. Transverse processes of Presacrals V–VIII similar in size, being the shortest and thinnest, those of Presacrals II and IV also about similar in size and being slightly larger, and those of Presacral III being the longest and widest of all transverse processes. Transverse processes of Presacrals II and VIII have slightly anterolateral orientation, those of Presacral III are laterally oriented and the others are slightly posterolaterally oriented. Neural arch of Presacrals III–VIII bears a raised medial ridge. Sacrum bears slightly expanded diapophyses. Urostyle long, slender, slightly shorter than presacral portion of vertebral column and bearing a well-pronounced dorsal ridge along most of its length, beginning at its anterior end. The bone has a bicondylar articulation with the sacrum. Pectoral girdle with well-ossified coracoids, clavicles, scapulae and cleithra. Suprascapular and sternum unossified and not visible in micro-CT scan, and omosternum hardly visible. Clavicles long and slim, oriented anteromedially, slightly curved, with medial tips touching each other. Laterally, clavicles firmly articulating with scapulae. Coracoids stout and glenoidal and sternal ends about equally expanded. Anterior edges of coracoids slightly curved, posterior edges almost straight. Medial tips of coracoids broadly separated from another. Scapula long, with a prominent pars acromialis not separated from pars glenoidalis. Cleithrum long, broader, and thicker at scapular boarder, thinning posteriorly. In pelvic girdle, long, slender iliac shafts bearing conspicuous dorsolateral ridges along most of their length, except anteriormost region. Ilia are fused posteriorly with ischium and pubis. Ischium stout, whereas pubis is thin and blade-like.

Manus and pes (Fig. 7)

All phalanges are ossified with a phalangeal formula for fingers and toes: 2-2-3-3 and 2-2-3-4-3, respectively. Order of finger length: I < II < IV < III, and that of toes: I < II < V < III < IV. Distal knobs present on terminal phalanges of all fingers and toes. Terminal phalanges of all toes and fingers narrower than penultimate phalanges of all toes and fingers, respectively. Carpus and tarsus not well-resolved in micro-CT scan. However, carpus seems to be composed of a radiale, ulnare, Element Y, ossified prepollex element, Carpal 2 and a large post-axial element probably representing a fusion of Carpals 3–5. Tarsus seems to be composed of two tarsal elements: Tarsal 1 and Tarsal 2 + 3, with latter being distinctly larger than Tarsal 1. A moderately large centrale and small ossified prehallux are also present. In ventral view, three sesamoids of subequal sizes are overlaying proximal end of Metatarsals IV–V, a further smaller sesamoid is overlaying parts of Tarsal 1.

Distribution and Natural History

Noblella mindo sp. nov. is only known from El Cinto (0.09022°S, 78.81858°W; 1,673 m), Mindo, province of Pichincha, Ecuador (Fig. 2). *Noblella mindo* sp. nov. inhabits secondary cloud forests, with the presence of palmito (*Bactris gasipaes*) plantations and trees that have emerged after the massive logging of forests in the area. These forests have a high humidity index, dense leaf litter layer, and abundant epiphytes. It has a restricted distribution; sampling activities were carried out in a range up to 3km around the type locality, and no individuals nor calls of *N. mindo* sp. nov. were recorded. The gecko *Lepidoblepharis conolepis* was found in sympatry. The locality is surrounded by livestock areas and within the type locality forest, there are trails used by farmers to move their livestock. The population of *Noblella mindo* sp. nov. could be impacted if livestock activity or deforestion expands. Three individuals (ZSFQ 049–051) were found active during the day between 10:00 and 11:00 am; all frogs were on the ground in a 2-meter depth hole.

Noblella worleyae Reyes-Puig, Maynard, Trageser, Vieira, Hamilton, Lynch, Culebras, Kohn, Brito, and Guayasamin 2020: New locality

Figs. 2, 9–12

New records (3 females, 1 male). All individuals were collected at different localities inside Los Cedros Biological Reserve: ZSFQ 3851 (Figs. 9–10), adult female and ZFSQ 3852, adult male, collected at 0.31501°N, 78.77943°W, 1,612 m (WGS84; Fig. 2), García Moreno, Cotacachi, province of Imbabura, by David Brito-Zapata and Martín Obando on 26 October 2019. MZUTI 1708, adult female, collected at 0.31125°N, 78.78095°W, 1,417 m, by Giusseppe Gagliardi and JMG on 13 March

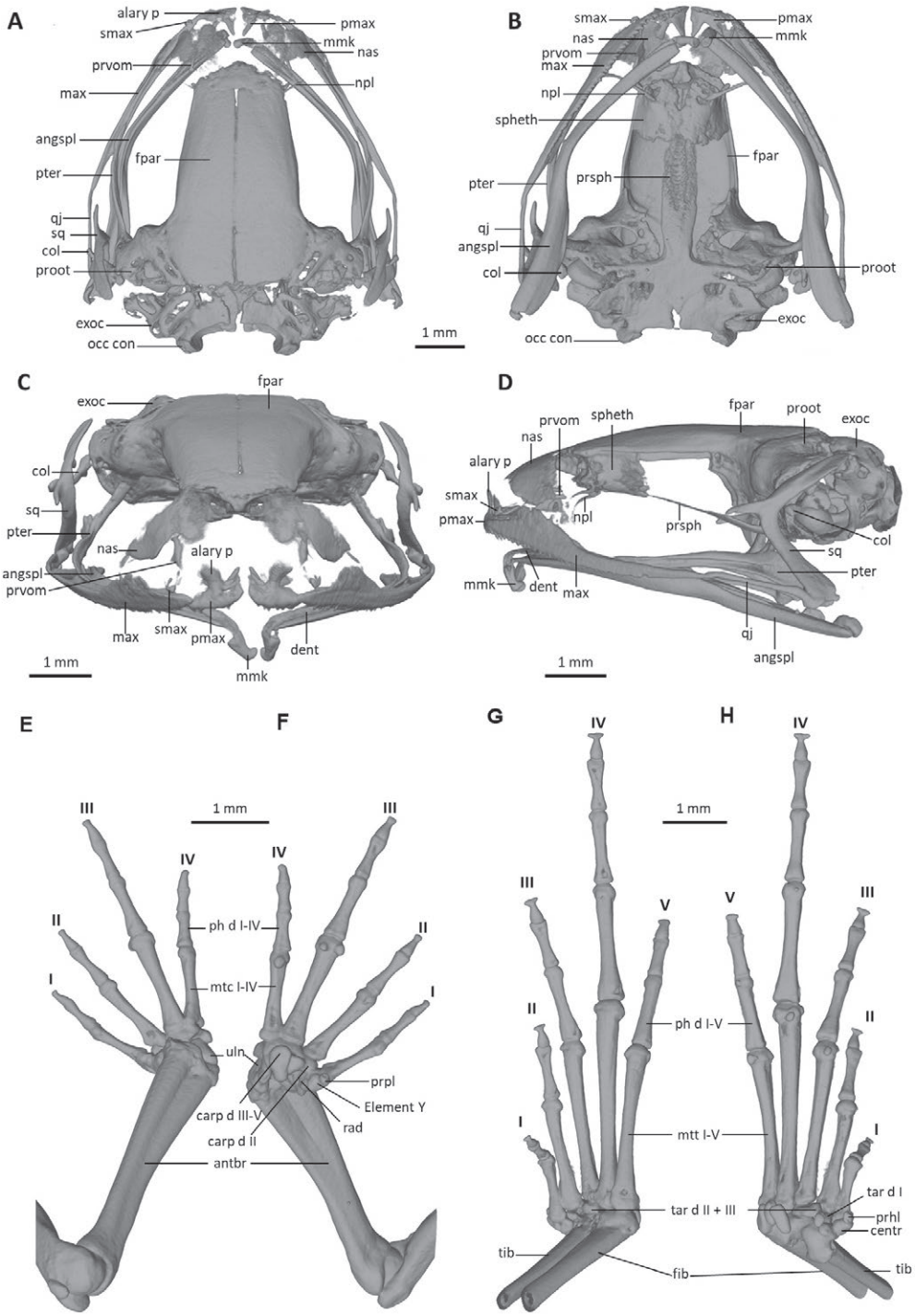

Fig. 7. Details of **(A–D)** skull morphology and osteological aspects of **(E–F)** hand and **(G–H)** foot of *Noblella mindo* sp. nov., ZSFQ 050, holotype, adult female. The skull is shown in **(A)** dorsal, **(B)** ventral, **(C)** frontal, and **(D)** lateral views. alary p = alary process, angspl = angulosplenial, col = columella, dent = dentary, fpar = frontoparietal, max = maxilla, mmk = mentomeckelian bone, nas = nasal, npl = neopalatine, occ con = occipital condyle, otoc = otoccipital (fused prootic and exoccipital), pmax = premaxilla, prsph = parasphenoid, prvom = prevomer, pter =pterygoid, qj = quadratojugal, smax = septomaxilla, spheth = sphenethmoid, sq = squamosal. The right hand is shown in **(E)** dorsal, and **(F)** palmar aspects; and the left foot in **(G)** dorsal, and **(H)** plantar aspects. Digits numbered I–V. antbr = os antebrachii (radius + ulna), carp d = carpale distale, cent = centrale, fib = fibulare, mtc = metacarpalia, mtt = metatarsalia, ph d I–IV = finger phalanges F1–F4, ph d I–V = toe phalanges F1–F5, prhl =prehallux, prpl = prepollex, rad = radius, tar d = tarsale distale, tib = tibiale, uln = ulnare. Images prepared by Claudia Koch.

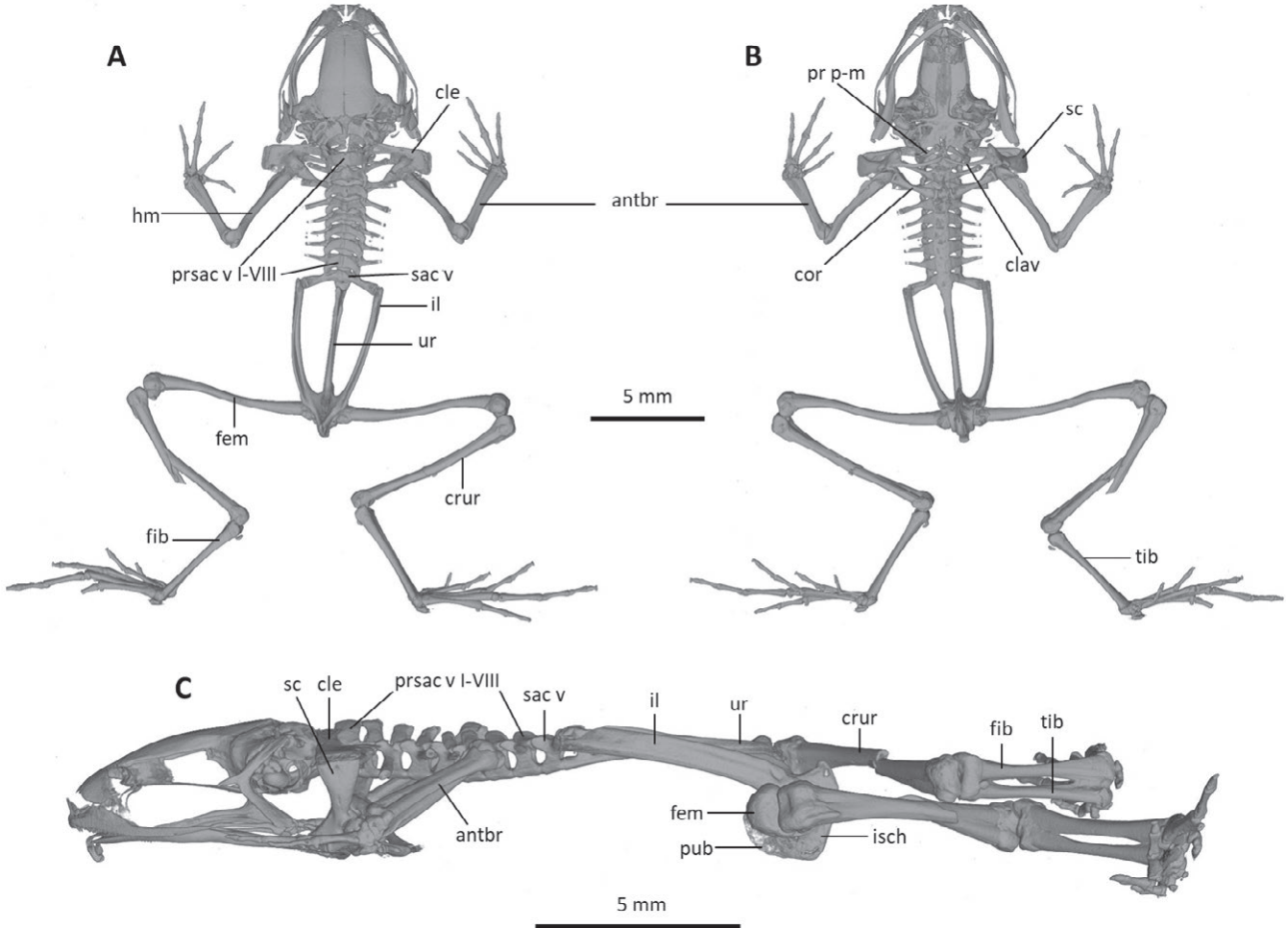

Fig. 8. Osteology of *Noblella mindo* sp. nov., ZSFQ 050, holotype, adult female. The full skeleton is shown in **(A)** dorsal, **(B)** ventral, and **(C)** lateral views. antbr = os antebrachii (radius + ulna), clav = clavicle, cle = cleithrum, cor = coracoid bone, crur = os cruris (tibia + fibula), fem = femoral bone, fib = fibulare, hm = humeral bone, il = ilium, isch = ischium, pr p-m = processus postero-medialis, prsac v = presacral vertebrae, pub = pubis, sac v = sacral vertebra, sc = scapula, ur = urostyle, tib = tibiale. Images prepared by Claudia Koch.

2012; MZUTI 1709, adult female, collected at 0.3184°N, 78.7837°W, 1,790 m, by Jaime Culebras and JMG on 15 March 2012.

Diagnosis

Specimens collected in Los Cedros reserve show morphological characters described for *Noblella worleyae* (Reyes-Puig et al., 2020; Figs. 6, 9–10) as follow (variation from original description in bold): (1) skin of dorsum finely shagreen, skin on venter smooth; (2) tympanic annulus and membrane visible externally, supratympanic fold inconspicuous; (3) snout, rounded in dorsal and lateral views; (4) eyelids without tubercles; (5) dentigerous processes of vomers absent; (6) vocal slits and vocal sac present, nuptial pads not visible; (7) fingers not expanded or slightly expanded distally, tips of Fingers I and IV rounded and tips of Fingers II and III slightly acuminate (originally described as tips of Fingers I and IV slightly acuminate, Fingers II and III acuminate), without papillae (Fig. 6), Finger I shorter than Finger II,(8); distal phalanges T-shaped (originally described as slightly T-shaped)**,** phalangeal formula of hands: 2-2-3-3 (Fig. 11); (9) supernumerary palmar tubercles few but present, ulnar tubercles diminutive and round (decreased by preservation effects), subarticular tubercles rounded, discs lacking circumferential grooves; (10) one tarsal tubercle, elongated and subconical, two metatarsal tubercles (inner tubercle 2 times size of external); toes slightly expanded distally and rounded on Toes I and V, cuspidate tips on Toes II–IV, papillae present on Toes II–IV (Fig. 6); (11) Toe V shorter than Toe III distal portions of circumferential grooves present on Toes II–V, supernumerary tubercles absent (12) phalangeal formula of feet: 2-2-3-4-3 (Fig. 11); (13) in life, dorsum brown, with two suprain-

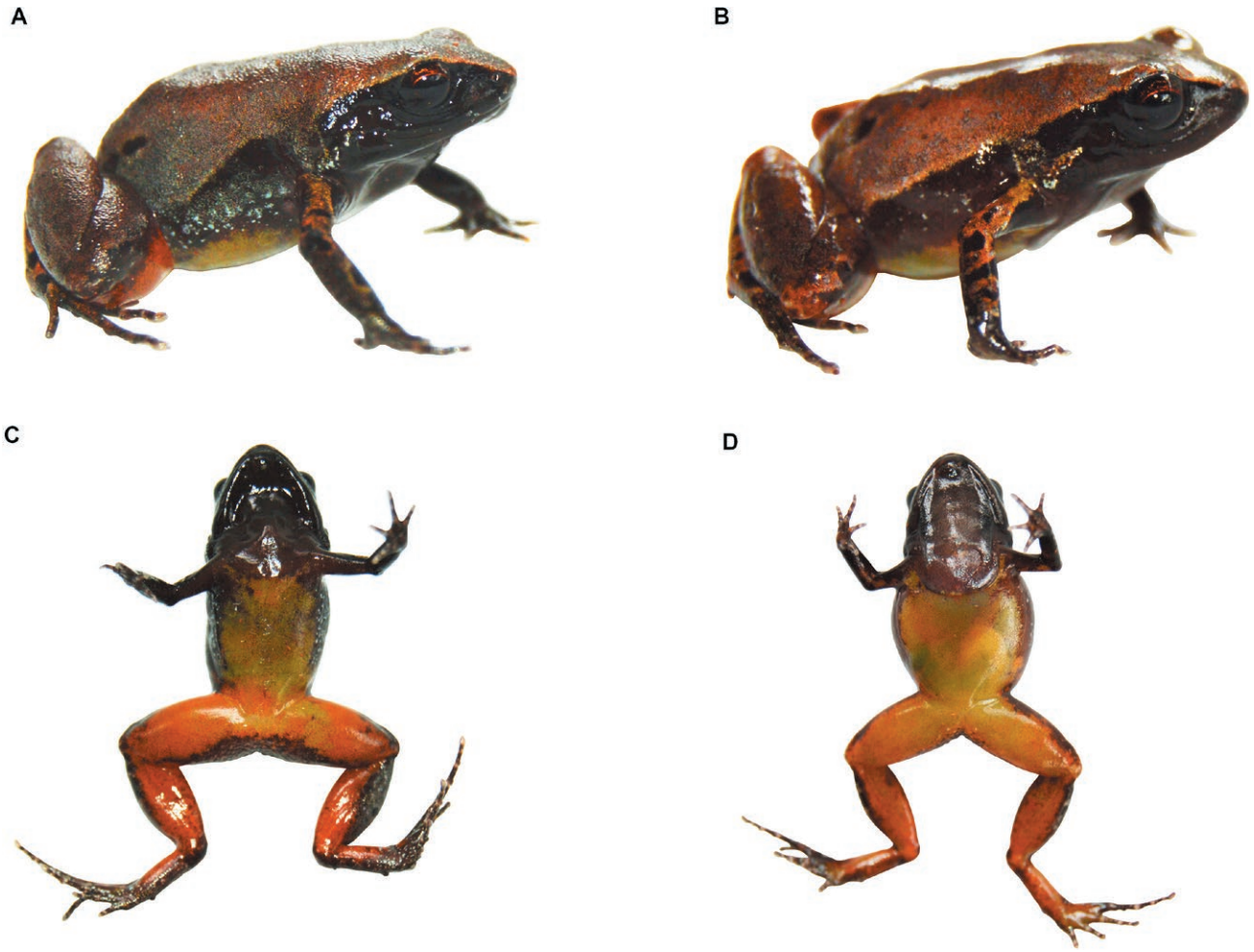

Fig. 9. Color pattern of *Noblella worleyae* in life: **(A, C)** Dorso-lateral and ventral patterns of ZSFQ 3851, adult female, SVL = 19.1 mm; **(B, D)** Dorsal and ventral patterns of ZSFQ 3852, adult male, SVL = 16.1 mm. Photos by David Brito-Zapata.

guinal dark brown marks; middorsal, longitudinal line faint cream; rictal gland dark brown; flanks with dark brown band narrowing towards groin and with clusters of turquoise specks towards ventral side; groin dark, with high concentration of melanophores; throat, chest and ventral surfaces of arms dark brown; venter yellowish cream, with brownish-orange tones on ventral surfaces of legs and thighs, iris reddish copper; (14) SVL in one adult male 16.1 mm; in adult females 19.1–20.4 mm (mean 19.8 mm, n = 3) (range originally described 18.1–19.1 mm).

Variation of color patterns and external morphology (Figs. 9–10)

Specimens of *Noblella worleyae* from Los Cedros Reserve vary from brown (MZUTI 1708–1709) to dark brown (ZSFQ 3851–3852). In preservative, specimen ZSFQ 3852 has a grayish-brown dorsal coloration. Black suprainguinal spots vary in size and may be diffused but are always present. All specimens exhibit a faint, cream middorsal stripe extending from the head to cloaca, but only in one specimen (MZUTI 1709) this line continues onto posterior surfaces of thigh, disappears in crus, and reappears in posterior surfaces of pes. Specimens MZUTI 1708 and ZSFQ 3852 have a homogenously dark brown throat like the holotype, but in MZUTI 1709 the throat is brown with scattered irregular cream marks. Ventral surfaces of thighs and crus of ZSFQ 3852 retain pinkish-cream color in preservative. Male ZSFQ 3852 exhibits an evident discoidal fold.

Osteology description

Osteological description of *Noblella worleyae* is based on micro-CT images of an adult female (MZUTI 1709). Details of skull morphology and osteological aspects of hand and foot are presented in Fig. 11 and main skeletal features are shown in Fig. 12.

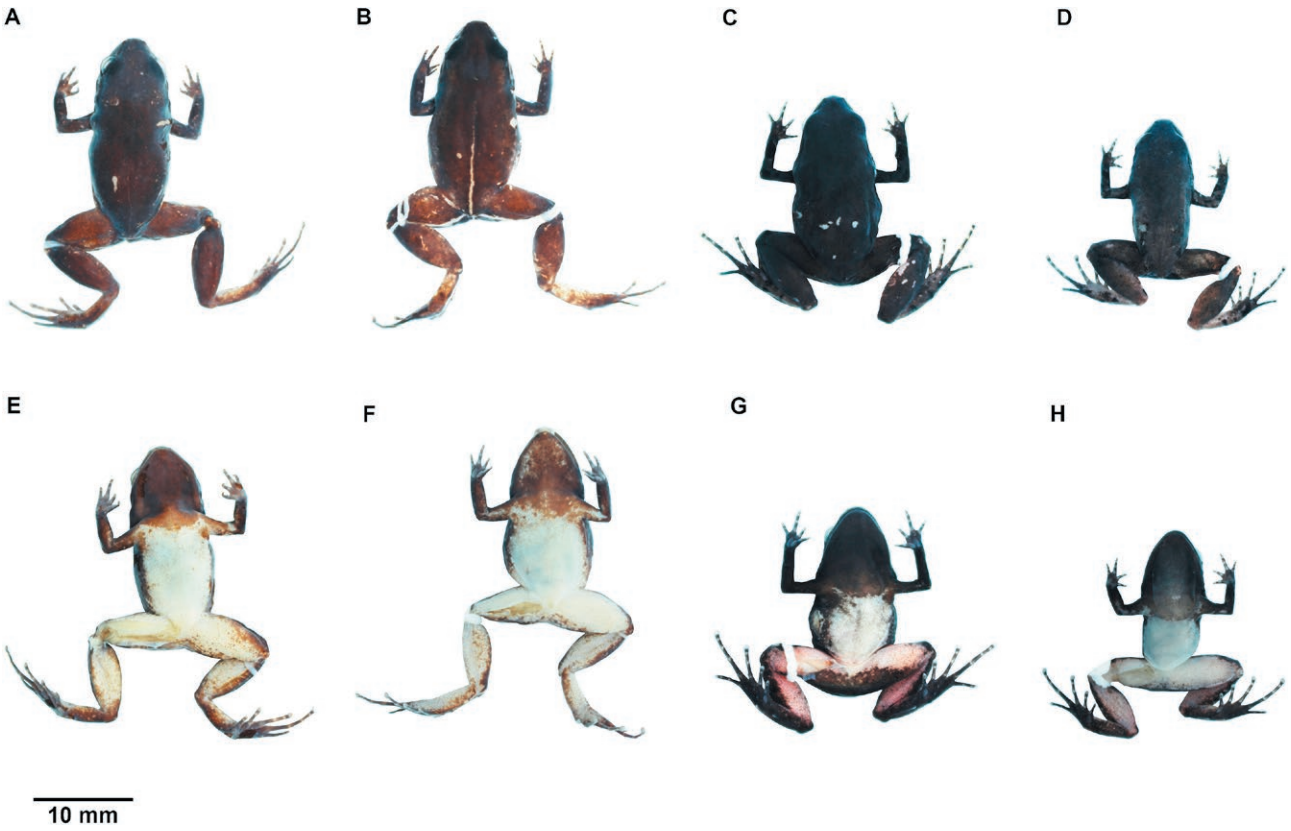

Fig. 10. Color variation of preserved *Noblella worleyae* in (**A–D**) dorsal and (**E–H**) ventral views: **(A, E)** MZUTI 1708, adult female, SVL = 20.4 mm; **(B, F)** MZUTI 1709, adult female, SVL = 19.9 mm; **(C, G)** ZSFQ 3851, adult female, SVL = 19.1 mm; **(D, H)** ZSFQ 3852, adult male, SVL = 16.1 mm. Photos by David Brito-Zapata and Carolina Reyes-Puig.

Skull (Fig. 11)

Skull almost as wide as long; widest part is at about where quadratojugal meets maxilla and is 97% of skull length. Rostrum short; distance from anterior edge of frontoparietals to anterior face of premaxilla is 18% of skull length. At level of midorbit, braincase is about 34% of maximum skull width. Braincase combines well- and poorly ossified elements. Prootic and exoccipital seem to be fused to form otoccipital. Frontoparietals are well-developed bones, distinctly longer than broad, slightly narrower anteriorly than posteriorly; narrowly separated along most of their length and only fused in anterior region. Posterior portion of braincase seems to be fully enclosed by partial fusion of frontoparietals with otoccipitals. However, there might still exist some traces of boarders between bones, but these parts are not well-resolved in micro-CT scans. Ventrally, otoccipitals are in contact with parasphenoid alae. Prootic part of otoccipitals are well-separated from each other. Exoccipital parts approximate one another ventromedially and dorsomedially but are still clearly separated with a broader ventral than dorsal gap between them. Anterolaterally, frontoparietals are in contact with sphenethmoid. Sphenethmoid is well-ossified and ventrally fused at midline; posterior margin almost reaches midpoint of orbit but is still broadly separated from prootic part of otoccipitals and is in ventral contact with cultriform process of parasphenoid. Cultriform process of parasphenoid is well-ossified posteriorly, thinning anteriorly, and about 31% of width of braincase at mid-orbit. Lateral margins of process are approximately parallel. Parasphenoid alae are long and well-ossified. Neopalatines are very thin and long, articulating with sphenethmoid dorsomedially and maxilla laterally. Columella (or stapes) is large and well-ossified. Because of tiny size and fine structure, septomaxilla is not well-resolved in micro-CT scan. Dorsal investing bones are moderately developed. Nasals are thin and broadly separated from one another, posteriorly in contact with anterior end of frontoparietals and posterolaterally in very thin contact with maxilla. They curve ventrally towards their lateral edges. Small prevomers are broadly separated from one another medially, their anterior edge approximates a long and thin posterior projecting ramus of septomax-

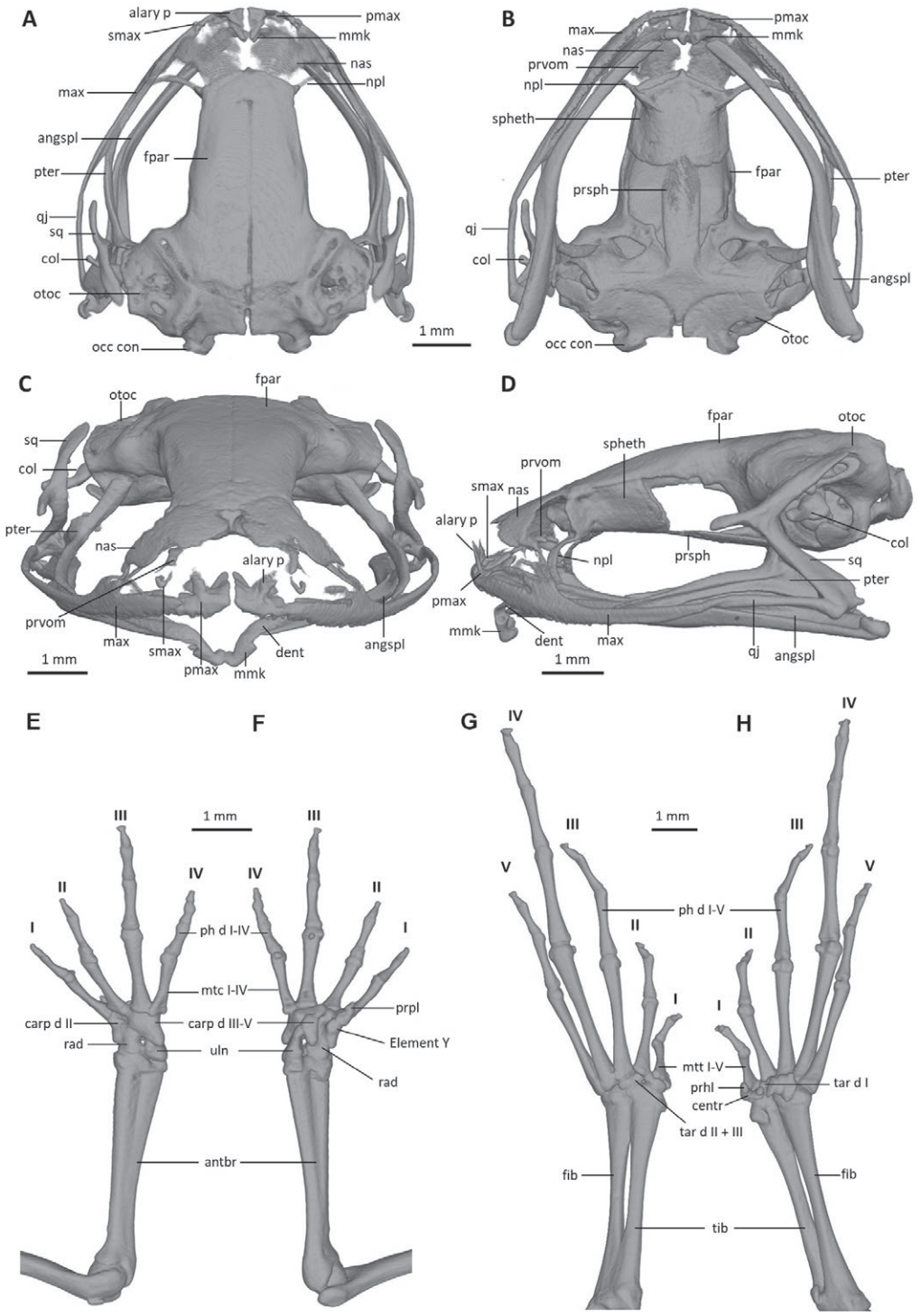

Fig. 11. Details of **(A–D)** skull morphology and osteological aspects of **(E–F)** hand and **(G–H)** foot of *Noblella worleyae*, MZUTI 1709. The skull is shown in **(A)** dorsal, **(B)** ventral, **(C)** frontal, and **(D)** lateral views. alary p = alary process, angspl = angulosplenial, col = columella, dent = dentary, fpar = frontoparietal, max = maxilla, mmk = mentomeckelian bone, nas = nasal, npl = neopalatine, occ con = occipital condyle, otoc = otoccipital (fused prootic and exoccipital), pmax = premaxilla, prsph = parasphenoid, prvom = prevomer, pter =pterygoid, qj = quadratojugal, smax = septomaxilla, spheth = sphenethmoid, sq = squamosal. The right hand is shown in **(E)** dorsal, and **(F)** palmar aspects; and the left foot in **(G)** dorsal, and **(H)** plantar aspects. Digits numbered I–V. antbr = os antebrachii (radius + ulna), carp d = carpale distale, cent = centrale, fib = fibulare, mtc = metacarpalia, mtt = metatarsalia, ph d I–IV = finger phalanges F1–F4, ph d I–V = toe phalanges F1–F5, prhl =prehallux, prpl = prepollex, rad = radius, tar d = tarsale distale, tib = tibiale, uln = ulnare. Images prepared by Claudia Koch.

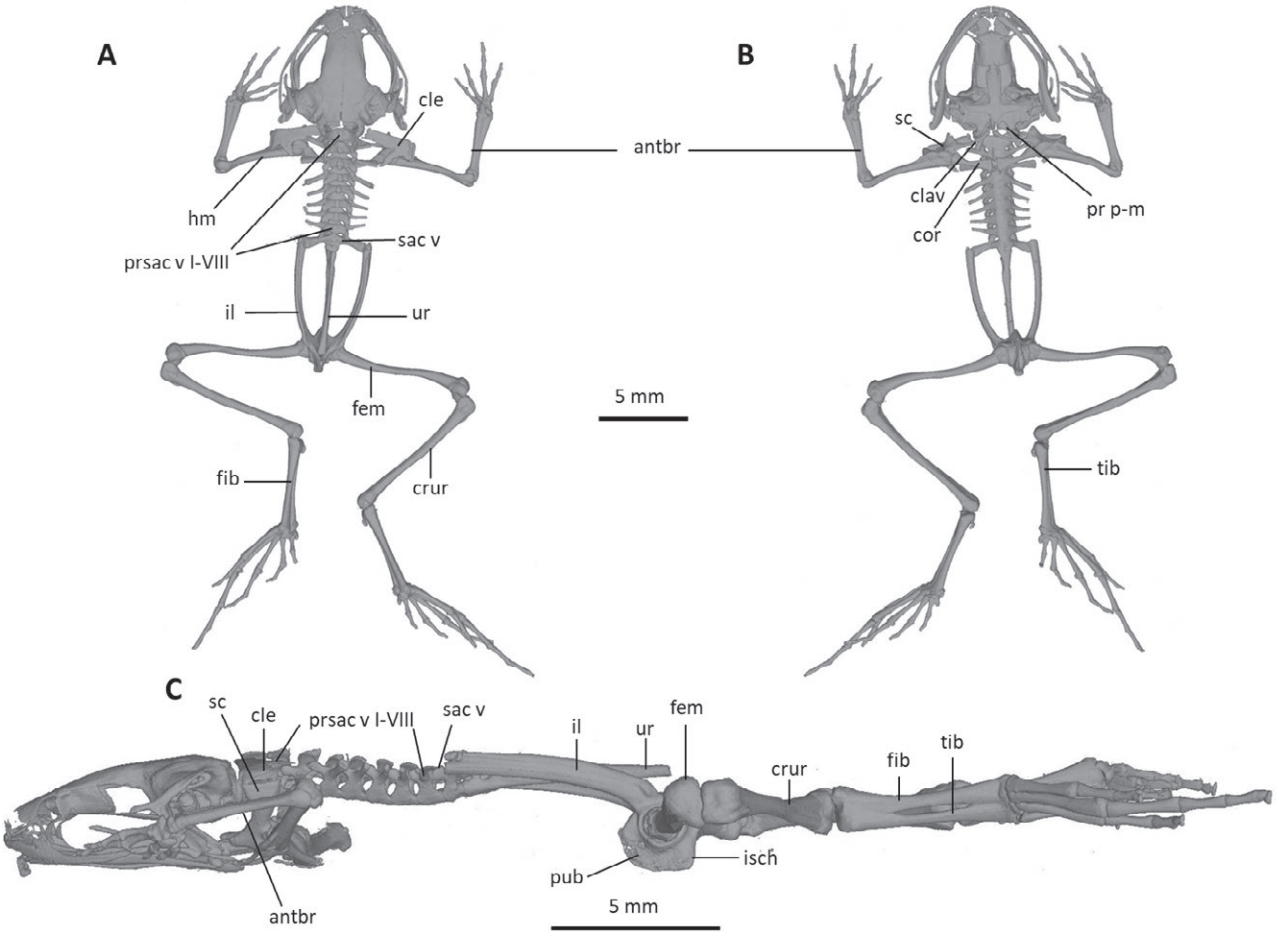

Fig. 12. Osteology of *Noblella worleyae,* MZUTI 1709, adult female. The full skeleton is shown in **(A)** dorsal, **(B)** ventral, and **(C)** lateral views. antbr = os antebrachii (radius + ulna), clav = clavicle, cle = cleithrum, cor = coracoid bone, crur = os cruris (tibia + fibula), fem = femoral bone, fib = fibulare, hm = humeral bone, il = ilium, isch = ischium, pr p-m = processus postero-medialis, prsac v = presacral vertebrae, pub = pubis, sac v = sacral vertebra, sc = scapula, ur = urostyle, tib = tibiale. Images prepared by Claudia Koch.

illa. Maxillary arcade bears many small, poorly resolved teeth on premaxillae and maxillae. Premaxillae are separated medially, and their anterodorsal alary processes rise divergent from midline but are still distinctly separated from nasals. Premaxilla and maxilla are in lateral contact, with anterior edge of maxilla slightly overlapping lateral edge of premaxilla. Pars palatina of premaxilla is broad, with two well-defined processes: medial process acuminate, and runs about parallel to its counterpart, being distinctly separated from it; lateral process is slightly shorter and broader. Maxilla is long, its posterior end acuminate and in contact with quadratojugals. Triradiate pterygoid bears a long, curved anterior ramus that is oriented anterolaterally towards maxilla, with which it articulates at ventral boarder anterior to midline of orbit. Posterior ramus of pterygoid is about same length as medial ramus and both are about half length of anterior ramus; however, posterior ramus is more robust than the other two. Edge of medial ramus overlaps lateral edge of prootic part of otoccipital. Quadratojugal is slender, slightly curved and articulates anteriorly with maxilla and posterodorsally with ventral ramus of squamosal. Squamosal is T-shaped with long laminar otic ramus; zygomatic ramus is much shorter and more slender; ventral ramus is about same length as otic ramus, laminar and broad, increasing in width ventrally. Mandible is slim and edentate. Mentomeckelians are small, medially and laterally slightly broadened, and medially contacting each other. Dentary is long and thin, reaching to about anterior corner of orbit; posteriorly acuminate and overlapping angulospenial, seeming to be in contact with this bone for most of its length, except the most anterior part; anteroventrally it contacts mentomeckelian bones. Angulosplenial is long and arcu-

ate. Coronoid process is a moderately long and strongly raised ridge. The only ossified portions of hyoid apparatus are two posteromedial processes, which are anteriorly slightly more expanded than posteriorly, approaching each other at anterior ends but being still distinctly separated.

Postcranium (Fig. 12)

Eight presacral vertebrae. All presacrals are non-imbricate. First presacral vertebra is longer than posterior vertebrae. All except Presacral I bear well-developed diapophyses. Transverse processes of Presacrals V–VIII similar in size and being the thinnest and second shortest, those of Presacral II being the shortest, and those of Presacral III being the longest and widest of all transverse processes. Transverse processes of Presacrals II and VIII have slightly anterolateral orientation, those of Presacrals III and VII are laterally oriented and others are slightly posterolaterally oriented. Neural arch of all presacrals bears a raised medial ridge. Sacrum bears slightly expanded diapophyses. Urostyle is long, slender, about similar in length as presacral portion of vertebral column and bearing a well-pronounced dorsal ridge along about two-thirds of its length, beginning at its anterior end, with a lateral foramen in anterior region. The bone has a bicondylar articulation with the sacrum. Pectoral girdle with well-ossified coracoids, clavicles, scapulae and cleithra. Suprascapular, omosternum, and sternum unossified and not visible in micro-CT scan. Clavicles are long and slim, oriented anteromedially, slightly curved, with medial tips approaching but not touching each other. Laterally, clavicles firmly articulating with scapulae. Coracoids are stout and glenoidal and sternal ends are about equally expanded. Anterior edges of coracoids are curved, the posterior edges are almost straight. Medial tips of coracoids are broadly separated from another. Scapula is long with a prominent pars acromialis that is not separated from pars glenoidalis. Cleithrum is long, broader and thicker at scapular boarder, thinning posteriorly. In pelvic girdle, long, slender iliac shafts bear conspicuous dorsolateral ridges along most of their length, except the anterior most region. Ilia is fused posterirly with ischium and pubis. Ischium is stout, whereas pubis is thinner and blade-like.

Manus and pes (Fig. 11)

All phalanges are ossified, with phalangeal formula for fingers and toes: 2-2-3-3 and 2-2-3-4-3, respectively. Order of finger length: I < II < IV < III, and that of toes: I < II < V < III < IV. Distal knobs seem to be absent on Finger I but are present on terminal phalanges of all other fingers and toes. Nevertheless, they are not well-resolved in micro-CT scans and are sensitive to thresholds used during reconstruction. Terminal phalanges of all toes and fingers are narrower than penultimate phalanges of all toes and fingers, respectively. Carpus and tarsus are not well-resolved in micro-CT scan. However, carpus seems to be composed of a radiale, ulnare, Element Y, ossified prepollex element, Carpal 2 and a large post-axial element probably representing a fusion of Carpals 3–5. Tarsus seems to be composed of two tarsal elements: Tarsal 1 and Tarsal 2 + 3, with latter being larger than Tarsal 1. A moderately large centrale and small ossified prehallux are also present. In ventral view, three sesamoids of subequal sizes overlaying proximal end of Metatarsals II–IV, a further smaller sesamoid overlaying parts of Tarsal 1 and proximal end of Metatarsal I.

Natural History

We report a new locality for *Noblella worleyae*: Los Cedros Biological Reserve, province of Imbabura, Ecuador (Fig. 2), at approximately 8.4 km in a straight line between the type locality of *N. worleyae* (i.e., Manduriacu Reserve). The individuals were found at several point-localities between 1,417–1,790 m of elevation. The reserve presents an important track of mature Low Montane Evergreen Forest. All specimens were collected at night between 7:00 and 11:50 pm and were found on the ground, in areas covered with abundant leaf litter. Individuals appeared inactive, because they were located by movement only when litter was removed. Syntopic species were *Pristimantis mutabilis* (Guayasamin et al., 2017b), *P. crenunguis*, (Lynch, 1976a) and *Alopoglossus viridiceps* (Torres-Carvajal and Lobos, 2014). *Noblella worleyae* seems to be a rare species at Los Cedros Biological Reserve. Only two individuals were found in two different surveys with known sampling effort. The first sampling was carried out between 22–25 August 2019, with five people for approximately nine hours per day. The second sampling was carried out between 26–30 October 2019, with two people for about nine hours per day. Individuals were found in the lower forest stratum, camouflaged extremely well in leaflitter and having an evasive behavior, similar to other *Noblella* species (Reyes-Puig et al., 2019c).

DISCUSSION

Our phylogenetic analyses (Fig. 1) agree with previous studies that have shown that southern species of *Noblella* (*N. losamigos*, *N. madreselva*, *N. pygmaea*, *N. thiuni*) are more closely related to species of *Psychrophrynella*, rather than to northern species of *Noblel-*

la (*N. coloma*, *N. heyeri*, *N. lochites*, *N. mindo* sp. nov., *N. myrmecoides*, *N. personina*, *N. worleyae*) (Reyes-Puig et al., 2019c, 2020; Santa-Cruz et al., 2019). *Noblella peruviana* is the type species of the genus, which, based on geography, is most likely part of the Southern Clade. However, since there are no sequences of *N. peruviana,* we refrain from proposing a new generic arrangement.

Species richness of the genus *Noblella* has increased dramatically over the last decade (Frost, 2020). About a decade ago, only three species of *Noblella* were known in Ecuador and no species had been described from the northwestern slopes of the Andes of Ecuador (Cisneros-Heredia and Reynolds, 2007). Nowadays, there are eight species of *Noblella* reported from Ecuador, including three from the western Ecuadorian Andes (*N. coloma*, *N. mindo* sp. nov., and *N. worleyae*) that form a distinct clade among the northern *Noblella* (Fig 1). The diversity of the genus *Noblella* has also increased in the Peruvian Andes, where in recent years three species been described, forming a clade with the previously described *Psychrophrynella* and *Noblella* (Catenazzi et al., 2015; Santa Cruz et al., 2019; Catenazzi and Ttito, 2019).

Our new records of *Noblella worleyae* from Los Cedros reserve add important intraspecific variation to the original description, in terms of its body size, coloration and shape of tips of the digits. In particular, variation in the fingertips was found, with tips of Fingers I and IV varying from slightly acuminate (original description) to rounded (data presented herein), and tips of Fingers II and III from acuminate (original description) to slightly acuminate (data presented herein). We also strengthen the original publication (Reyes-Puig et al., 2020) with a detailed description of the osteology of the species.

Diversification in *Noblella* seems be related with the linearity of the Andes, with allopatric and parapatric populations being separated by ecological and geographic barriers. In Ecuador, all species of *Noblella* are allopatric and most of them are restricted to very specific geographic areas. *Noblella mindo* sp. nov. occurs in low montane forest in the valley of Mindo, in the Nambillo River watershed, western slopes of the Pichincha Massif, northwestern Andes, at 1,673 m; while *N. worleyae* inhabits low montane forest in the Manduriacu-Los Cedros watersheds, southern slopes of the Toisan massif; and *N. coloma* is restricted to the cloud forests of the Río Guajalito watershed, western slopes of the Atacazo volcano. *Noblella worleyae* is separated from *N. coloma* and *N. mindo* sp. nov. by the Guayllabamba River Valley (Fig. 2), an important biogeographic barrier, especially for frog species with low vagility (Hillman et al., 2014). Although the valley of Mindo (type locality of *N. mindo* sp. nov.) and the valley of Guajalito (type locality of *N. coloma*) are ca. 20 km apart in straight line, they are in different watersheds, separated by the Nambillo River and complex orogeny caused by the Pichincha massif and the Atacazo volcano.

All species currently recognized under the genus *Noblella* are miniaturized frogs, among the smallest Neotropical vertebrates (Duellman and Lehr, 2009). They are cryptic and adapted to live amidst or under leaf litter in forests, where they are often overlooked by amphibian visual surveys, being easier to locate by their calls or through pitfall traps (Reyes-Puig et al., 2019c). Although some species may be abundant locally, most species appear to have low densities. For example, yearly surveys between 2000–2012 at the type locality of *N. coloma* produced only three records, while up to 20 individuals of *N. lochites* were found in 2014 at a single locality in the province of Zamora-Chinchipe (D. F. Cisneros-Heredia pers. obs.).

Most remnants of mature forests in the Andes of Ecuador are nowadays either inside public or private protected areas or persist due to their inaccessibility. Private conservation initiatives have become extremely important in Ecuador (Betancourt et al., 2018; Guayasamin et al., 2018, 2019; Reyes-Puig et al., 2019a, 2019b, 2019c), where public protected areas do not cover all critically important regions for biodiversity (Lessmann et al., 2014; Cuesta et al., 2017; Reyes-Puig et al., 2017).

Unfortunately, habitat loss due to unsustainable expansion of the agricultural frontier, mining and infrastructure projects have placed a heavy burden on several private reserves (Roy et al., 2018; Guayasamin et al., 2019). In the early 2000s, the region of Mindo was heavily threatened by the construction of an oil pipeline (Oleoducto de Crudos Pesados OCP). Fortunately, local, national and international protests managed to promote some actions to mitigate the largest impacts of the pipeline development. Eventually Mindo has transformed into one of the most popular ecotourism destinations in northwestern Ecuador, allowing several private protected areas to preserve large tracks of mature forest (Welford and Yarbrough, 2015). Unfortunately, twenty years later, history repeats itself, now at Los Cedros reserve, but this time with mining concessions, exploration and exploitation (Roy et al., 2018). Thus, biodiversity conservation is facing an uncertain future.

The increasing descriptions of new species within the Ecuadorian territory have a practical application in the conservation of biodiversity. By highlighting the presence of new vertebrates with restricted distributions in the Andes, the visualization of this unique biodiversity is indisputable.

ACKNOWLEDGEMENTS

We conducted this research under research permits and agreement for genetic resources access (MAE-DNB-CM-2018-0106, 019-2018-IC-FAU-DNB/MAE) issued by Ministerio del Ambiente del Ecuador. We carried out this study following the guidelines for treatment and management of live amphibians and reptiles in field and laboratory investigations (Beaupre et al., 2004), recommended by the American Society of Ichthyologists and Herpetologists, the Herpetologists' League and the Society for the Study of Amphibians and Reptiles.

This study was developed as part of "Proyecto Descubre Napo", an initiative of Universidad San Francisco de Quito in association with Wildlife Conservation Society, and funded by the Gordon and Betty Moore Foundation, as part of the project "WCS Consolidating Conservation of Critical Landscapes (mosaics) in the Andes". We express our gratitude to the following people for their support: Ana Nicole Acosta-Vásconez, Susana Cárdenas, Mariela Domínguez, Jonathan Guillemot, Andrés León-Reyes, Emilia Peñaherrera, Carolina Proaño, Robert P. Reynolds, Alejandra Robledo, Ana Sevilla, Rebecca Zug. Work at Los Cedros Biological Reserve was developed as part of project "Muestreo de Grupos Ecológicos Clave", research program "Evaluación biológica rápida del corredor norte de la Reserva de Mashpi", a joint initiative of Fundación Futuro and Universidad San Francisco de Quito USFQ (Instituto ECOLAP, Museo de Zoología, Instituto iBIOTROP). This research was supported by Universidad San Francisco de Quito USFQ through research funds for the Museo de Zoología & Laboratorio de Zoología Terrestre, Instituto de Diversidad Biológica y Tropical iBIOTROP granted to DFCH; USFQ Collaboration Grants and COCIBA Grants (project HUBI ID 34, 39, 48, 1057, 7703, 12268, 13524) granted to DFCH and CRP; and Collaboration Grants and COCIBA Grants (project HUBI ID 5521, 5467, 5447, 11164, 16871) granted by USFQ to JMG. Work by DFCH was supported by Programa "Becas de Excelencia", Secretaría de Educación Superior, Ciencia, Tecnología e Innovación (SENESCYT), Ecuador; the Smithsonian Women's Committee, the 2002 Research Training Program, National Museum of Natural History, Smithsonian Institution; María Elena Heredia and Laura Heredia. We thank the Inédita Program from the Ecuadorian Science Agency SENESCYT (Respuestas a la Crisis de Biodiversidad: La Descripción de Especies como Herramienta de Conservación; INEDITA PIC-20-INE-USFQ-001) that funded the molecular component of this study. We are grateful for the comments of Edgar Lehr and an anonymous reviewer to improve the manuscript.

REFERENCES

Acevedo, A.A., Armesto, O., Palma, R.E. (2020): Two new species of *Pristimantis* (Anura: Craugastoridae) with notes on the distribution of the genus in northeastern Colombia. Zootax **4750**: 499-523.

Albernaz, A. (2007): Letter from Mindo: the residents of a tiny Ecuadorian town strike a balance between tourism and ecology, and find that it suits their nature just right. Science & Spirit **18**: 13-16.

Almendáriz, A., Brito, J., Batallas, D., Ron, S. (2014): Una especie nueva de rana arbórea del género *Hyloscirtus* (Amphibia: Anura: Hylidae) de la Cordillera del Cóndor. Pap. Avuls. Zool. **54**: 33-49.

Arteaga, A., Bustamante, L., Guayasamin, J.M. (2013): The Amphibians and Reptiles of Mindo: Life in the Cloudforest. Universidad Tecnológica Indoamérica, Quito, Ecuador.

Barbour, T. (1930): A list of Antillean reptiles and amphibians. Zoologica **11**: 61-116.

Barrientos, L.S., Streicher, J.W., Miller, E.C., Pie, M.R., Wiens, J.J., Crawford, A.J. (2021): Phylogeny of terraranan frogs based on 2,665 loci and impacts of missing data on phylogenomic analyses. Syst. Biodiv. **19**: 1-16.

Beaupre, S.J., Jacobson, E.R., Lillywhite, H.B., Zamudio, K. (2004): Guidelines for use of live amphibians and reptiles in field and laboratory research. American Society of Ichthyologists and Herpetologists, Lawrence.

Barrio-Amorós, C.L., Costales, M., Vieira, J., Osterman, E., Kaiser, H., Arteaga, A. (2020): Back from extinction: rediscovery of the harlequin toad *Atelopus mindoensis* Peters, 1973 in Ecuador. Herpetol. Notes **13**: 325-328.

Betancourt, R., Reyes-Puig, C., Lobos, S.E., Yánez-Muñoz, M.H., Torres-Carvajal, O. (2018): Sistemática de los saurios *Anadia* Gray, 1845 (Squamata: Gymnophthalmidae) de Ecuador: límite de especies, distribución geográfica y descripción de una especie nueva. Neotrop. Biodiv. **4**: 83-102.

Castellanos, A., Laguna, A., Clifford, S. (2011): Suggestions for mitigating cattle depredation and resulting human-bear conflicts in Ecuador. Interntl. Bear News **20**: 16-18.

Catenazzi, A., Ttito, A. (2019): *Noblella thiuni* sp. n., a new (singleton) species of minute terrestrial-breeding frog (Amphibia, Anura, Strabomantidae) from the montane forest of the Amazonian Andes of Puno, Peru. PeerJ **7**: e6780.

Catenazzi, A., Uscapi, V., von May, R. (2015): A new species of *Noblella* (Amphibia, Anura, Craugastori-

dae) from the humid montane forests of Cusco, Peru. ZooKeys **516**: 71–84.

Catenazzi, A., Mamani, L., Lehr, E., von May, R. (2020): A new genus of terrestrial-breeding frogs (Holoadeninae, Strabomantidae, Terrarana) from southern Peru. Diversity **12**: 1–17

Cisneros-Heredia, D.F., Ryenolds, R.P. (2007): New records of *Phyllonastes* Heyer, 1977 from Ecuador and Peru. Herpetozoa **19**: 184-186.

Cisneros-Heredia, D.F., Gluesenkamp, A.G. (2010): A new Andean toad of the genus *Osornophryne* (Amphibia: Anura: Bufonidae) from northwestern Ecuador, with taxonomic remarks on the genus. ACI Av. Cienc. Ing. **2**: B64-B73.

Cisneros-Heredia, D.F., Yanez-Munoz, M.H. (2010): A new poison frog of the genus *Epipedobates* (Dendrobatoidea: Dendrobatidae) from the north-western Andes of Ecuador. Av. Cienc. Ing. **2**: 83-86.

Cope, E. (1862): On some new and little known American Anura. Proc. Acad. Nat. Sci. Philadelphia **14**: 151-159.

Cuesta, F., Peralvo, M., Merino-Viteri, A., Bustamante, M., Baquero, F., Freile, J.F., Muriel, P., Torres-Carvajal, O. (2017): Priority areas for biodiversity conservation in mainland Ecuador. Neotrop. Biodiv. **3**: 93-106.

De la Riva, I., Chaparro, J.C., Castroviejo-Fisher, S., Padial, J.M. (2017): Underestimated anuran radiations in the high Andes: five new species and a new genus of Holoadeninae, and their phylogenetic relationships (Anura: Craugastoridae). Zool. J. Linnean Soc. **182**: 129-172.

De La Riva, I., Chaparro, J.C., Padial, J.M. (2008): The taxonomic status of *Phyllonastes* Heyer and *Phrynopus peruvianus* (Noble) (Lissamphibia, Anura): resurrection of *Noblella* Barbour. Zootaxa **1685**: 67-68.

De la Riva, I., Köhler, J. (1998): A new minute leptodactylid frog, genus *Phyllonastes*, from humid montane forests of Bolivia. J. Herpetol. **32**: 325-329.

De Queiroz, K. (2005): Ernst Mayr and the modern concept of species. Proc. Natl. Acad. U.S.A. **102**: 6600–6607.

De Queiroz, K. (2007): Species concepts and species delimitation. Syst. Biol. **56**: 879-886.

Duellman, W.E. (1988): Patterns of species diversity in anuran amphibians in the American tropics. Ann. Missouri Bot. Gard. **75**: 79–104.

Duellman, W.E. (1991): A new species of leptodactylid frog, genus *Phyllonastes*, from Peru. Herpetologica **47**: 9-13.

Duellman, W.E., Lehr, E. (2009): Terrestrial-breeding frogs (Strabomantidae) in Peru. Natur und Tier Verlag, Münster, Germany.

Duellman, W.E., Trueb, L. (1994): Biology of Amphibians. Johns Hopkins University Press, Baltimore.

Fabrezi, M., Alberch, P. (1996): The carpal elements of anurans. Herpetologica **32**: 188-204.

Frost, D.R. (2021): Amphibian Species of the World: an Online Reference. Version 6.1. American Museum of Natural History, New York. Available online at: https://amphibiansoftheworld.amnh.org/index.php. [*Accessed 7 July 2021*].

Goin, C.J., Cochran, D.M. (1963): Two new genera of leptodactylid frogs from Colombia. Proc. California Acad. Sci., 4th Series **31**: 499-505.

Guayasamin, J.M., Arteaga, A., Hutter, C.R. (2018): A new (singleton) rainfrog of the *Pristimantis myersi* Group (Amphibia: Craugastoridae) from the northern Andes of Ecuador. Zootaxa **4527**: 323-334.

Guayasamin, J.M., Cisneros-Heredia, D.F., Maynard, R.J., Lynch, R.L., Culebras, J., Hamilton, P.S. (2017a): A marvelous new glassfrog (Centrolenidae, Hyalinobatrachium) from Amazonian Ecuador. ZooKeys **673**: 1-20.

Guayasamin, J.M., Cisneros-Heredia, D.F., Vieira, J., Kohn, S., Gavilanes, G., Lynch, R.L., Hamilton, P.S., Maynard, R.J. (2019): A new glassfrog (Centrolenidae) from the Choco-Andean Rio Manduriacu Reserve, Ecuador, endangered by mining. PeerJ **7**: e6400.

Guayasamin, J.M., Terán-Valdez, A. (2009): A new species of *Noblella* (Amphibia: Strabomantidae) from the western slopes of the Andes of Ecuador. Zootaxa **2161**: 47-59.

Guayasamin, J.M., Cisneros-Heredia, D.F., McDiarmid, R.W., Peña, P., Hutter, C.R. (2020): Glassfrog of Ecuador: diversity, evolution, and conservation. Diversity **12**: 222.

Guayasamin, O.L., Couzin, I.D., Miller, N.Y. (2017b): Behavioural plasticity across social contexts is regulated by the directionality of inter-individual differences. Behav. Process. **141**: 196-204.

Harvey, M., Almendariz, A., Brito, J., Batallas, D. (2013): A new species of *Noblella* (Anura: Craugastoridae) from the amazonian slopes of the Ecuadorian Andes with comments on *Noblella lochites* (Lynch). Zootaxa **3635**: 1-14.

Hedges, S.B., Duellman, W.E., Heinicke, M.P. (2008): New World direct-developing frogs (Anura: Terrarana): Molecular phylogeny, classification, biogeography, and conservation. Zootaxa **1737**:1-182.

Heinicke, M.P., Duellman, W.E., Hedges, S.B. (2007): Major Caribbean and Central American frog faunas originated by ancient oceanic dispersal. Proc. Natl. Acad. Sci. U.S.A. **104**: 10092-10097.

Heinicke, M.P., Lemmon, A.R., Lemmon, E.M., McGrath, K., Hedges, S.B. (2018): Phylogenomic support for

evolutionary relationships of New World direct-developing frogs (Anura: Terraranae). Mol. Phylogenet. Evol. **118**: 145-155.

Heyer, W. (1969): Studies on the genus *Leptodactylus* (Amphibia, Leptodactylidae) III. A redefinition of the genus *Leptodactylus* and a description of a new genus of leptodactylid frogs. Contrib. Sci. Nat. Hist. Mus. Los Angeles Co. **155**: 1-14.

Hillman, S.S., Drewes, R.C., Hedrick, M.S., Hancock, T.V. (2014): Physiological vagility: correlations with dispersal and population genetic structure of amphibians. Physiol. Biochem. Zool. **87**: 105-112.

Hutter, C.R., Guayasamin, J.M. (2015): Cryptic diversity concealed in the Andean cloud forests: two new species of rainfrogs (*Pristimantis*) uncovered by molecular and bioacoustic data. Neotrop. Biodiv. **1**: 36-59.

Hutter, C.R., Guayasamin, J.M., Wiens, J.J. (2013): Explaining Andean megadiversity: the evolutionary and ecological causes of glassfrog elevational richness patterns. Ecol. Lett. **16**: 1135-1144.

Hutter, C.R., Lambert, S.M., Wiens, J.J. (2017): Rapid diversification and time explain amphibian richness at different scales in the Tropical Andes, Earth's most biodiverse hotspot. Amer. Nat. **190**: 828-843.

INHAMI. (2020): Instituto Nacional de Meteorología e Hidrología. Gobierno de la República de Ecuador, Quito, Ecuador. Available online at: http://www.inamhi.gob.ec/. [*Accessed 7 July 2021*].

Jiménez de la Espada, M. (1872): Nuevos batrácios Americanos. An. Soc. Esp. Hist. Nat. Madrid **1**: 84-88.

Jiménez de la Espada, M. (1870): Fauna neotropicalis species quaedam nondum cognitae. J. Sci., Math., Phys. Nat., Lisboa **3**: 57-65.

Köhler, J. (2000): A new species of *Phyllonastes* Heyer from the Chapare region of Bolivia, with notes on *Phyllonastes carrascoicola*. Spixiana **23**: 47-53.

Lehr, E., Aguilar, C., Lundberg, M.A. (2004): A New species of *Phyllonastes* from Peru (Amphibia, Anura, Leptodactylidae). J. Herpetol. **38**: 214-218.

Lehr, E., Catenazzi, A. (2009): A New species of minute *Noblella* (Anura: Strabomantidae) from southern Peru: The smallest frog of the Andes. Copeia **2009**: 148-156.

Lehr, E., Lyu, S., Catenazzi, A. (2021): A new, critically endangered species of *Pristimantis* (Amphibia: Anura: Strabomantidae) from a mining area in the Cordillera Occidental of northern Peru (Región Cajamarca). Salamandra **57**: 15-26.

Lessmann, J., Muñoz, J., Bonaccorso, E. (2014): Maximizing species conservation in continental Ecuador: A case of systematic conservation planning for biodiverse regions. Ecol. Evol. **2014**: 2410-2422.

Lessmann, J., Troya, M.J., Flecker, A.S., Funk, W.C., Guayasamin, J.M., Ochoa-Herrera, V., Poff, N.L., Suarez, E., Encalada, A.C. (2019): Validating anthropogenic threat maps as a tool for assessing river ecological integrity in Andean-Amazon basins. PeerJ **7**: e8060.

Lips, K.R., Reaser, J.K., Young, B.E. (2001): Amphibian Monitoring in Latin America: a Protocol Manual/ Monitoreo de Anfibios en América Latina: Manual de Protocolos. Society for the Study of Amphibians and Reptiles [Herpetological Circular 30].

Lynch, J. (1986): New species of minute leptodactylid frogs from the Andes of Ecuador and Peru. J. Herpetol. **20**: 423-431.

Lynch, J.D. (1976a): New species of frogs (Leptodactylidae: *Eleutherodactylus*) from the Pacific versant of Ecuador. Occ. Pap. Mus. Nat. Hist., Univ. Kansas **55**: 1-33.

Lynch, J.D. (1976b): Two new species of frogs of the genus *Euparkerella* (Amphibia: Leptodactylidae) from Ecuador and Perú. Herpetologica **32**: 48-53.

Lynch, J.D., Duellman, W.E. (1997): Frogs of the genus *Eleutherodactylus* (Leptodactylidae) in Western Ecuador: Systematics, Ecology, and Biogeography. Natural History Museum, University of Kansas, Lawrence.

Maddison, D.R., Maddison, W.P. (2005): MacClade 4.07 for OS X. Sinauer Associates, Inc., Sunderland, Massachusetts.

MECN. (2009): Ecosistemas del Distrito Metropolitano de Quito (DMQ). Publ. Misc. **6**: 1-51.

Miranda-Ribeiro, A. de. (1920): Algumas consideracões sobre *Holoaden lüderwaldti* e generos correlatos. Rev. Mus. Paulista **12**: 319-320.

Mueses-Cisneros, J.J., Yánez-Muñoz, M.H., Guayasamin, J.M. (2010): Una nueva especie de sapo del género *Osornophryne* (Anura: Bufonidae) de las estribaciones amazónicas de los Andes de Ecuador. Pap. Avuls. Zool. **50**: 269-279.

Myers, N., Mittermeier, R.A., Mittermeier, C.G., da Fonseca, G.A.B., Kent, J. (2000): Biodiversity hotspots for conservation priorities. Nature **403**: 853-858.

Noble, G.K. (1921): Five new species of Salientia from South America. Amer. Mus. Novit. **29**: 1-7.

Ortega-Andrade, H. M., Rodes Blanco, M., Cisneros-Heredia, D. F., Guerra Arévalo, N., López de Vargas-Machuca, K. G., Sánchez-Nivicela, J. C., Armijos-Ojeda, D., Cáceres, J.F., Reyes-Puig, C., Quezada, A., Székely, P., Rojas Soto, O., Székely, D., Guayasamin, J.M., Siavichay F., Amador, L., Betancourt, B., Ramírez-Jaramillo, S., Timbe-Borja, B., Gomez, M., Webster, J.F., Oyagata, L., Chávez, D., Posse, V., Valle-Piñuela, C., Padilla, D., Reyes-Puig, J.P., Terán-

Valdez, A. Coloma, L., Pérez, M.B., Carvajal-Endara, S. Urgilés, M., Yánez Muñoz, M.H. (2021): Red List assessment of amphibian species of Ecuador: A multidimensional approach for their conservation. PLoS ONE **16**: e0251027.

Ospina-Sarria, J. J., Angarita-Sierra, T. (2020): A new species of *Pristimantis* (Anura: Strabomantidae) from the eastern slope of the cordillera oriental, Arauca, Colombia. Herpetologica **76**: 83-92.

Páez-Moscoso, D. J., Guayasamin, J.M. (2012): Species limits in the Andean toad genus *Osornophryne* (Bufonidae). Mol. Phylogenet. Evol **65**: 805-822.

Paez, N.B., Ron, S.R. (2019): Systematics of *Huicundomantis*, a new subgenus of *Pristimantis* (Anura, Strabomantidae) with extraordinary cryptic diversity and eleven new species. ZooKeys **868**: 1-112.

Peñafiel, N., Flores, D.M., Rivero De Aguilar, J., Guayasamin, J.M., Bonaccorso, E. (2019): A cost-effective protocol for total DNA isolation from animal tissue. Neotrop. Biodiv. **5**: 69-74.

Peters, W.C.H. (1873): Über zwei Giftschlangen aus Afrika und über neue oder weniger bekannte Gattungen und Arten von Batrachiern. Mber. K. Preuss.Akad. Wiss. Berlin **1873**: 411-418.

Reinhardt, J.T., Lütken, C.F. (1862 "1861"): Bidrag til Kundskab om Brasiliens Padder og Krybdyr. Förste Afdeling: Padderne og Öglerne. Vidensk. Meddel. Dansk Naturhist. Foren. Kjøbenhavn, Serie 2, **3**: 143-242.

Reyes-Puig, C., Almendáriz, A., Torres-Carvajal, O. (2017): Diversity, threat, and conservation of reptiles from continental Ecuador. Amphib. Reptile Conserv. **11**: 51-58.

Reyes-Puig, C., Bittencourt-Silva, G.B., Torres-Sánchez, M., Wilkinson, M., Streicher, J.W., Maddock, S.T., Kotharambath, R., Müller, H., Angiolani Larrea, F.N., Almeida-Reinoso, D., Cisneros-Heredia, D.F., Ron, S.R. (2019a): Rediscovery of the endangered Carchi Andean toad, *Rhaebo colomai* (Hoogmoed, 1985), in Ecuador, with comments on its conservation status and extinction risk. Check List **15**: 415-419.

Reyes-Puig, C., Maynard, R.J., Trageser, S.J., Vieira, J., Hamilton, P.S., Lynch, R., Culebras, J., Kohn, S., Brito, J., Guayasamin, J.M. (2020b): A new species of *Noblella* (Amphibia: Strabomantidae) from the Río Manduriacu Reserve on the Pacific slopes of the Ecuadorian Andes. Neotrop. Biodiv. **6**: 162-171.

Reyes-Puig, C., Pablo Reyes-Puig, J., Velarde-Garcez, D., Dávalos, N., Mancero, E., Navarrete, M., Yanez-Munoz, M., Cisneros-Heredia, D., Ron, R.S. (2019b): A new species of terrestrial frog *Pristimantis* (Strabomantidae) from the upper basin of the Pastaza River, Ecuador. ZooKeys **832**: 113-133.

Reyes-Puig, C., Yánez-Muñoz, M.H., Ortega, J.A., Ron, S.R. (2020a): Relaciones filogenéticas del subgénero *Hypodictyon* (Anura: Strabomantidae: *Pristimantis*) con la descripción de tres especies nuevas de la región del Chocó. Rev. Mex. Biodiv. **91**: 1-38.

Reyes-Puig, J.P., Reyes-Puig, C., Ron, S., Ortega, J.A., Guayasamin, J.M., Goodrum, M., Recalde, F., Vieira, J.J., Koch, C., Yanez-Munoz, M.H. (2019c): A new species of terrestrial frog of the genus *Noblella* Barbour, 1930 (Amphibia: Strabomantidae) from the Llanganates-Sangay Ecological Corridor, Tungurahua, Ecuador. PeerJ **7**: e7405.

Reyes-Puig, J.P., Yánez-Muñoz, M.H., Cisneros-Heredia, D.F., Ramírez-Jaramillo, S.R. (2010): Una nueva especie de rana *Pristimantis* (Terrarana: Strabomantidae) de los bosques nublados de la cuenca alta del río Pastaza, Ecuador. ACI Av. Cienc. Ing. **2**: B72-B82.

Rojas-Runjaic, F.J., Infante-Rivero, E.E., Salerno, P.E., Meza-Joya, F.L. (2018): A new species of *Hyloscirtus* (Anura, Hylidae) from the Colombian and Venezuelan slopes of Sierra de Perijá, and the phylogenetic position of *Hyloscirtus jahni* (Rivero, 1961). Zootaxa **4382**: 121-146 .

Ron, S.R., Merino-Viteri, A. Ortiz, D.A. (Eds). Anfibios del Ecuador. Version 2019.0. Museo de Zoología, Pontificia Universidad Católica del Ecuador, Quito, Ecuador. Available online at: https://bioweb.bio/ faunaweb/amphibiaweb/FichaEspecie/Noblella%20myrmecoides. [*Accessed 13 June 2021*].

Roy, B.A., Zorrilla, M., Endara, L., Thomas, D.C., Vandegrift, R., Rubenstein, J.M., Policha, T., Ríos-Touma, B., Read, M. (2018): New mining concessions could severely decrease biodiversity and ecosystem services in Ecuador. Trop. Conserv. Sci. **11**: 1-20.

Sánchez-Nivicela, J.C., Celi-Piedra, E., Posse-Sarmiento, V., Urgiles, V.L., Yánez-Muñoz, M., Cisneros-Heredia, D.F. (2018): A new species of *Pristimantis* (Anura, Craugastoridae) from the Cajas Massif, southern Ecuador. ZooKeys **751**: 113-128.

Santa-Cruz, R., von May, R., Catenazzi, A., Whitcher, C., López Tejeda, E., Rabosky, D. (2019): A new species of terrestrial-breeding frog (Amphibia, Strabomantidae, *Noblella*) from the Upper Madre De Dios watershed, Amazonian Andes and lowlands of Southern Peru. Diversity **11**: 1-20.

Scherz, M.D., Hawlitschek, O., Andreone, F., Rakotoarison, A., Vences, M., Glaw, F. (2017): A review of the taxonomy and osteology of the *Rhombophryne serratopalpebrosa* species group (Anura: Microhylidae) from Madagascar, with comments on the value of volume rendering of micro-CT data to taxonomists. Zootaxa **4273**: 301-340.

Suwannapoom, C., Sumontha, M., Tunprasert, J., Ruangsuwan, T., Pawangkhanant, P., Korost, D.V., Poyarkov, N.A. (2018): A striking new genus and species of cave-dwelling frog (Amphibia: Anura: Microhylidae: Asterophryinae) from Thailand. PeerJ **6**: e4422.

Swofford, D.L., Olsen, G.J., Waddell, P.J., Hillis, D.M. (1996): Phylogenetic inference. In: Molecular Systematics, pp. 407-514. Hillis, D.M., Moritz, C., Mable, B.K., Eds, Sinauer Associates, Sunderland, Massachusetts.

Terán-Valdez, A., Guayasamin, J.M. (2009): The smallest terrestrial vertebrate of Ecuador: A new frog of the genus *Pristimantis* (Amphibia: Strabomantidae) from the Cordillera del Cóndor. Zootaxa **2447**: 53-68.

Torres-Carvajal, O., Lobos, S.E. (2014): A new species of *Alopoglossus* lizard (Squamata, Gymnophthalmidae) from the tropical Andes, with a molecular phylogeny of the genus. Zookeys **410**: 105-120.

Trueb, L. (1973): Bones, frogs, and evolution. In: Evolutionary Biology of the Anurans: Contemporary Research on Major Problems, pp. 65-132. Vial, J.L., Ed, University of Missouri Press, Columbia, Missouri.

Welford, M.R., Yarbrough, R.A. (2015): Serendipitous conservation: Impacts of oil pipeline construction in rural northwestern Ecuador. Extract. Indust. Soc **2**: 766-774.

Yánez-Muñoz, M.H., Altamirano-Benavides, M., Cisneros-Heredia, D.F., Gluesenkamp, A.G. (2010a): Nueva especie de sapo andino del género *Osornophryne* (Amphibia: Bufonidae) del norte de Ecuador, con notas sobre la diversidad del género en Colombia. ACI Av. Cienc. Ing. **2**: B46-B53.

Yánez-Muñoz, M.H., Meza-Ramos, P.A., Cisneros-Heredia, D.F., Reyes-Puig, J.P. (2010b): Descripción de tres nuevas especies de ranas del género *Pristimantis* (Anura: Terrarana: Strabomantidae) de los bosques nublados del Distrito Metropolitano de Quito. ACI Av. Cienc. Ing. **2**: B16-B27.

Yánez-Muñoz, M.H., Reyes-Puig, C., Reyes-Puig, J.P., Velasco, J.A., Ayala-Varela, F., Torres-Carvajal, O. (2018): A new cryptic species of *Anolis* lizard from northwestern South America (Iguanidae, Dactyloinae). ZooKeys **794**: 135-163.

Yanez-Muñoz, M.H., Veintimilla-Yanez, D., Batallas, D., Cisneros-Heredia, D.F. (2019): A new giant *Pristimantis* (Anura, Craugastoridae) from the paramos of the Podocarpus National Park, southern Ecuador. ZooKeys **852**: 137-156.

Zwickl, D.J. (2006): Genetic algorithm approaches for the phylogenetic analysis of large biological sequence datasets under the maximum likelihood criterion. Ph.D. dissertation. The University of Texas at Austin. [GARLI: Genetic Algorithm for Rapid Likelihood Inference. Available for download at: http://www.bio.utexas.edu/faculty/antisense/garli/Garli.html.

APPENDIX I

Examined specimens.

*Noblella lochites***.** Ecuador, Napo: ZSFQ 346, Archidona, Reserva Narupa, 1176 m; ZSFQ 347, Reserva Narupa, 1152 m; ZSFQ 348, Reserva Narupa, 1167 m; Zamora Chinchipe: ZSFQ 1119, Yantzaza, Concesión La Zarza, 1385 m; ZSFQ 1124, Concesión La Zarza, 1357 m; ZSFQ 1186, ZSFQ 1187, ZSFQ 1188, Yantzaza, Río Blanco, 1654 m; ZSFQ 1188, Río Blanco, 1830 m.

Noblella cf. *lochites*. Ecuador, Zamora Chinchipe: ZSFQ 3262 – 326, Yantzaza, Estación Experimental El Padmi UNL, 775 m. Noblella myrmecoides: Ecuador, Napo: ZSFQ 670, Mera, Parque Nacional Llanganates, 1325 m; ZSFQ 671, Parque Nacional Llanganates, 1352 m; ZSFQ 672, Parque Nacional Llanganates, 1327 m.

Noblella cf. *myrmecoides*. Ecuador, Tungurahua: ZSFQ 1341, Río Negro, Reserva Río Zuñag, 1269 m.

Noblella coloma. Ecuador: Pichincha: QCAZ 7277, 7412, 8701, 11614, 26307, 32702, Reserva Ecológica Río Guajalito; 1800–2000 m.

Noblella heyeri. Ecuador, Loja: QCAZ 31470, 31471, 31473, Loja–Zamora road; 2385 m, QCAZ 22501, Zamora-Huaico; 2000 m.

Noblella worleyae. Ecuador, Imbabura: ZSFQ 345, 550, 551, 552, 2502, 2503, 2504, Reserva Manduriacu, 1184–1597 m.

Acta Herpetologica 16(2): 89-98, 2021
DOI: 10.36253/a_h-10402

So close so different: what makes the difference?

Dario Ottonello[1,7,*], Stefania D'Angelo[2], Fabrizio Oneto[3,6], Stefano Malavasi[1], Marco Alberto Luca Zuffi[4], Filippo Spadola[5]

[1] *Department of Environmental Sciences, Informatics and Statistics, Cà Foscari University of Venice, Via Torino 155, 30172 Venezia Mestre, Italy*
[2] *WWF Italia, via Po 25/c, 00195 Roma, Italy*
[3] *Centro Studi Bionaturalistici srl, Corso Europa 26, 16132 Genova, Italy*
[4] *Museum of Natural History, University of Pisa, via Roma 79, 56011 Calci (Pisa), Italy*
[5] *Department of Veterinary Sciences, University of Messina, Polo Universitario SS. Annunziata, 98128 Messina, Italy*
[6] *Università di Genova, Corso Europa 26, 16132 Genova, Italy*
[7] *ARPAL Ligurian Environmental Protection Agency, Via Bombrini 8, 16149 Genova, Italy*
**Corresponding author*. E-mail: dario.ottonello@arpal.liguria.it

Submitted on: 2021, 31st January; Revised on: 2021, 5th May; Accepted on: 2021, 22nd May
Editor: Emilio Sperone

Abstract. The introduction of alien fish species in wetland ecosystems could have a great impact on freshwater communities and ecological processes. Despite fish introduction has been noticed as one of the principal cause of freshwater extinctions, ecosystem processes alteration, and change in aquatic community assemblage, very few data about impact on freshwater reptiles are available. As study model we used two neighbour sub-populations of the endangered Sicilian pond turtle, *Emys trinacris*, inhabiting two small, close each other and very similar lakes, except for the presence of allocthonous fish, *Cyprinus carpio* and *Gambusia hoolbroki* in one of the two. The multi-year study allowed highlighting significant differences in abundance, growth and reproductive output between the two freshwater turtle sub-populations, suggesting their influence on phenotypic plasticity of the studied population. These results are discussed in the light of previous evidence about the impact of these alien species on abundance and assemblage of the invertebrate community with an evident impact on niche width, diet composition and therefore energy intake by *Emys trinacris*. These data may provide important information to address management strategies and conservation actions of small wetland areas inhabited by pond turtles, pointing out a threats never highlighted up to now.

Keywords. *Emys trinacris*, phenotypic plasticity, *Cyprinus carpio, Gambusia hoolbroki,* alien fishes impact.

INTRODUCTION

Phenotypic plasticity is an evolutionary adaptation to environmental variation often used to explain the intraspecific difference observed within various taxa, that could be influenced by local variation in abiotic and biotic factors associated with habitat type (Lubcke and Wilson, 2007). Nowadays, the introduction of alien species is one of the main stressor of freshwater ecosystem biodiversity (Genovesi, 2007), and it could have a great impact on freshwater communities causing cascading impacts on food webs and complex interactions among species (Ricciardi and MacIsaac, 2011). In the last decades, many species of fishes have been deliberately introduced worldwide to provide food or sport leisure, but also released from aquaria, bait buckets, and water gardens, as contaminants of fish intended for stocking, or in ballast water (Strayer, 2010). Despite fish introduction has been noticed as one of the principal cause of freshwater extinctions (Dextrase and Mandrak, 2006), ecosystem processes alteration (Pitcher and Hart, 1995) and change in aquatic community assemblage (Parkos et al.,

ISSN 1827-9635 (print)
ISSN 1827-9643 (online)

www.fupress.com/ah

2003), very few data about impact on freshwater reptiles are available.

Within this group, freshwater turtles are known to vary in different natural history traits among conspecific populations both over broad geographic area (Lovich et al., 1998; Joos et al., 2017) as well as among adjacent sites (Tucker at al., 1998). They usually follow a growth pattern that involves rapid growth from hatching to sexual maturity, followed by little or no growth once maturity is attained (e.g., Wilbur, 1975; Bury, 1979). Growth can be influenced both by different ecological factors, such as hatching size, food availability and habitat suitability (Mahmoud, 1969; Bury, 1979). Moreover, different growth patterns can lead to the same size (Bury, 1979; Andrews, 1982) or to different size at the maturity (Stearns and Koella, 1986). These differences can have also a direct impact on reproductive output in a taxon where clutch size often increases with maternal body size (Zuffi et al., 2004).

In particular, Ottonello et al. (2017a) showed how the presence of two alien fishes, *Cyprinus carpio* Linnaeus, 1758 and *Gambusia holbrooki* Girard, 1859, can alter the abundance and the assemblage of the invertebrate community with a considerable impact on niche width and diet composition of an endangered turtle. Local food availability and quality may indeed play a key role to regulate feeding strategy with consequences on growth, reproductive output and population density (Dunham and Gibbons, 1990; Parmenter and Avery, 1990). For these reasons we have aimed at investigating if the presence of alien fishes can have an impact at local scale on a population of an endangered turtle using as case study two neighbour wild sub-populations under similar climatic and environmental conditions. As model species we selected *Emys trinacris* Fritz et al., 2005, the only native freshwater turtle of Sicily, a large island off the coast of Italy. The Sicilian pond turtle lives in wetlands and slow-moving water bodies (e.g., lagoons, deltas, inland waters and mountain lakes) with soft bottoms and abundant aquatic vegetation, especially on the banks, from the sea level up to 1036 m a.s.l. (Marrone et al., 2016). However, the presence of the species at about 1250 m a.s.l. was recently observed (F. Marrone and R. Scardino, pers. obs.). In view of the low number of sicilian indigenous fish (Zerunian, 2004) and the absence of specialized aquatic vertebrate predators (Aa. Vv., 2008), it is likely to assume that *Emys trinacris* is one of the top aquatic predators in many of these environments in Sicily, with an opportunistic and generalist pattern oriented mainly towards aquatic invertebrates (Ottonello et al., 2017a).

Because of the introduction of non-native fish species, that are now the most represented non-indigenous taxon occurring in Sicily (Marrone and Naselli-Flores, 2015), new dynamics that can significantly alter and threaten the structure of the native biota have been established (Naselli-Flores and Barone, 2012) and top predators are likely to be valuable indicators of ecosystem health (Landres et al., 1988). Although some data and experimental studies highlighted the poorly competitive abilities of the genus *Emys* against some alien species, like *Trachemys scripta* (Cadi and Joly, 2003, 2004) and *Micropterus salmoides* Lacepède, 1802 (Lacomba and Sancho, 2004; Ayres and Cordero, 2007), robust evidence of interactions in the wild is still lacking (but see Polo-Cavia et al., 2010; Lambert et al., 2019). Moreover, Rakausas et al. (2016), studying the predator-prey interactions between a recent invader in Lituania, the Chinese sleeper (*Perccottus glenii* Dybowski, 1877) and the European pond turtle stated that this fish does not directly contribute to the decline of *E. orbicularis* because hatchlings turtles are resistant to *P. glenii* predation and, adults of *E. orbicularis* consumed juvenile *P. glenii,* but no data about indirect impacts (e.g., trophic resource competition) have been evaluated. Therefore, we assumed that Sicilian pond turtles in a habitat without alien fishes would have access to wider food availability than would individuals in a habitat with introduced alien fishes. We therefore hypothesized that this would affect their rates of energy intake and we predicted that turtles in a fish-less habitat would: (1) exhibit different patterns of growth, (2) have higher annual reproductive output, and (3) have higher abundance. To test this hypothesis in the wild, we compared the parameters of two *Emys trinacris* sub-populations inhabiting a fish-inhabited and a fish-less lakes during a multi-year study. The evidence of the negative impact of the presence of introduced fish fauna can provide additional information to further understand the effect of alien species on native fauna as well as promote adequate management plans.

MATERIALS AND METHODS

Study area

The Nature Reserve of the "Lake Preola and Gorghi Tondi" is a protected area of south-western Sicily, established in 1998 and currently managed by the Italian Association for the World Wildlife Fund. The Nature Reserve (medium point at 37°36'36.78"N 12°39'8.19"E) has a surface of 335 hectares and is surrounded by a homogeneous agricultural landscape (vineyards and olive groves). The Nature Reserve protects four distinct wetlands (Pantano Murana, Lake Preola, Gorghi Alto-Medio and Gorgo Basso), originating in a karstic depression. The basins do not have tributaries and the groundwater table is

located in the calcarenites and is fed by local meteoric recharge (Cusimano et al., 2006). Lake Preola is the widest water body of the area, with a surface of 33 ha approximately, filled with a thin layer of water occasionally deeper than two meters. The "Gorghi" are lake environments in a mature euthrophic status, with an average surface area of approximately 3 ha for the lake Gorgo Basso (altitude: 6 m a.s.l) and 5 ha for the lake Gorghi Alto-Medio (altitude: 3 m a.s.l.), and a maximum depth of 12 m. They are set on sink-holes and they are therefore immediately deep and surrounded by riparian helophytes [*Phragmites australis* (Cav.) Trin. ex Steud., *Typha latifolia* L. and *Cladium mariscus* (L.) Pohl], with some peripherals areas with a maximum depth of about 2 m. Comparison of water chemistry and benthic samples showed no significant difference between the two lakes and both showed high concentration of lead and arsenic (Bellante et al., 2015; Arpa Sicilia, 2016).

The Gorghi Alto-Medio is situated only 200 m away from the Gorgo Basso, but it is separated by an asphalt road and with a slight difference in elevation. Despite their proximity the two sites can be considered inhabited by two distinct sub-populations of *Emys trinacris*. Indeed, although no genetic data are available, capture-recapture data showed a very low migration rate between these lakes confirming what observed over the last fourteen years (D'Angelo, unpubl. data), when for instance only five individuals migrated between the two sites, three from the Gorgo Basso to the Gorghi Alto-Medio and two conversely.

Different non-indigenous species are reported for this territory, like the invasive Red swamp crayfish *Procambarus clarkii* Girard, 1852 (D'Angelo and Lo Valvo, 2003), and Eastern mosquitofish *Gambusia holbrooki* and Wild common carp *Cyprinus carpio* (Ottonello et al., 2017a). Red swamp crayfish is widespread in all the basins without significant difference in abundance and distribution (Maccarone et al., 2016), while fishes are limited only to the Gorghi Alto-Medio (Ottonello et al., 2017a). In the latter, fish presence affects the food web and the assemblage and abundance of the potential preys of *Emys trinacris* (Table 1; Ottonello et al. 2017a), in accordance with available results on the negative impacts that allocthonous species produce on local invertebrates communities (*Cyprinus carpio:* Parkos et al., 2003; as well as *Gambusia holbrooki:* Pyke, 2008).

Sampling

Individuals were captured by six fyke nets and 30 baited funnel traps in Gorgo Basso and Gorghi Alto-Medio located 50 m apart of each other. Fieldwork was carried out from 2014 to 2016 with 10 sampling occasions during the active season (March-October). Date of capture, sex, age (adult/juvenile), straight carapace length (SCL, sliding callipers to the nearest 0.1 mm), width (CW), height (CH) and body mass (BM, digital balance ± 1 g) were recorded on each capture according to a standardized procedure, and only individuals with evident sexual characters were considered as adults (Zuffi and Gariboldi, 1995). All captured turtles were individually marked by unique notch on their carapace (Servan et al., 1986) as a part of a long-term study on the ecology of the species (Ottonello et al., 2017b).

Abundance

The abundance of turtles in each site was measured indirectly by means of the Catch Per Unit Effort (CPUE) method. CPUE was calculated for each wetland and sampling occasion with effort measured as trap-day, and the number of traps on a site multiplied by the number of days set. Because animals were released after each capture we considered, within the same sampling occasion, only the first event for each individual to avoid pseudoreplication (Hurlbert, 1984). We used only data collected in 2015 and 2016 because the sampling was not carried out in Gorghi Alto-Medio in 2014. This method, usually applied in fisheries management (Maunder et al., 2006), can be used also for chelonians to infer the relative abundance and compare different groups (Selman et al., 2014).

Size and growth

Data and sites differences (Gorgo Basso *vs* Gorghi Alto-Medio) in size and body mass of turtles were firstly checked for normality with Shapiro-Wilk normality test and then analysed using a Student's *t* test. Females and males were analysed separately due to their difference in size and mass (Ottonello et al., 2017b). Recaptured animals were excluded from the analysis to avoid pseudoreplication. Population structure was analysed using a graphical approach by dividing SCL data in size classes of 10 mm. Individual variation in growth was assessed by the

Table 1. Comparative descriptive data of the two studied sites.

	Gorgo Basso	Gorghi Alto-Medio
Surface (ha)	3.1	4.9
Open deep water (ha)	2.1	4.4
Shallow water dominated by helophytes (ha)	1.0	0.5
Maximum Depth (m)	11	12
Fish	Absent	*Gambusia holbroki* *Cyprinus carpio*
Invertebrate alien species	*Procambarus clarckii*	*Procambarus clarckii*
Temperature (°C)[1]	27.9	26.6
Dissolved Oxygen (%sat)[1]	66.4	77.5
Chlorophyll alfa (µg/L)[1]	0.11	1.36
Total phosphorus (µg/L)[1]	6.9	13.3
Total nitrate (mg/L)[1]	2.21	0.87
N° of invetebrate sampled[2]	346	103
N° of invertebrate *taxa* sampled [2]	9	6
Food Niche Breadth of *E. trinacris*[2]	1.36	0.97
Average number of prey per faecal sample of *E. trinacris*[2]	15	1

[1] Arpa Sicilia 2016; [2] Ottonello et al. 2017a.

mean of the Relative Growth Rate (RGR) equation modified from Brody (1945) by Cox et al. (1991):

$$RGR = \frac{lnSCL_2 - \ln SCL_1}{t_2 - t_1}$$

where SCL_1 represents straight carapace length at first capture, SCL_2 represents straight carapace length at last recapture, and $t_2 - t_1$ represents the time interval in months between the two measurements. Juveniles at first and last capture were used in both groups (males and females), based on the assumption that early growth trajectories of the sexes do not differ (Dunham and Gibbons, 1990). Moreover, we considered only growing individuals (class 1, 2, 3) excluding aged (class 4) animals (see Olivier, 2002 for class definition), to avoid the possible bias due the presence or dominance of no or slow growing old animals in the two areas (Bury, 1979).

RGR analyses assume that growth is exponential, but this assumption is rarely valid (Cox et al., 1991). However, the regression between RGR and SCL_1 gives an estimate of growth rate at a specific carapace length, allowing direct comparison of growth rates both among individuals with different carapace lengths and among individuals with similar carapace lengths (Cox et al. 1991). We tested the effect of the site (Gorgo Basso *vs* Gorghi Alto-Medio) on the RGR using the Analysis of covariance (ANCOVA), separately for males and females. RGR has been identified as the dependent variable, SCL_1 as the independent variable and the site as the categorical variable.

The growth has been modelled for each site (Gorgo Basso and Gorghi Alto-Medio) using the von Bertalanffy Growth Model (VBGM), as previously used to estimate size-age relation in different species of chelonians (Lovich et al., 1990; Litzgus and Brooks, 1998; Çiçek et al., 2016). The general von Bertalanffy equation is:

$$SCL = a \cdot (1\text{-}be^{-kt})$$

where SCL is straight carapace length, a is asymptotic carapace length, b is a parameter related to length at hatching, e is the base of the natural logarithm, k is the intrinsic growth factor, and t is age in years. Since this is a non-linear model for the parameter estimation, non-linear statistic was used, by the estimation of parameters and their confidence interval (95%) with non-linear least-square regression method using the FSA package (Ogle, 2012) in R. The function "predict" was used to estimate the age at sexual maturity assuming the SCL of the smallest gravid female and of the smallest male showing secondary sex characteristics for each site. The age of individuals was estimated with the count of plastral growth rings (Keller et al., 1998), a reliable method for young European pond turtles as showed by Çiçek et al. (2016) in a comparative study with skeletochronology. The maximum number of growth rings that was possible to count was nine, after which the plastron abrasion does not allow a reliable estimate of the age of individuals. Because no wild new born of Sicilian pond turtle were captured, we used data of hatchlings from a local breeding centre – where eggs are incubated naturally – for the estimate of parameter b. Juveniles were used in both groups (males and females), based on the assumption that early growth trajectories of the sexes do not differ (Dunham and Gibbons, 1990).

Reproductive biology

The presence of oviductal eggs was verified by palpation of the inguinal region (Zuffi et al., 1999) directly at the capture site. Gravid females were transferred temporarily to the veterinary clinic of the University of Messina for X-ray examinations. In our experiment the exposure was made at 50 mA, 50 kV, 0.1 min, similar to that used by Zuffi et al. (1999) for *Emys orbicularis* (Linnaeus, 1758). As these latter authors, we presumed the absence of significant injuries at the gonadal level in our sampled females and in hatchlings (Hinton et al., 1997), although we recommended suspending this type of analysis within this population in next years as a precautionary measure. All individuals were released at the point of capture after the end of the procedures.

The size of the eggs has been recorded directly from the radiographic images. Due to the possibility that the eggs were not placed parallel on the radiographic plane we considered only the minimum diameter (D_{min}, ± 0.1 mm) in subsequent statistical analyses. The non-parametric Mann-Whitney U test was used to check any difference in the number of eggs between the two sites (Gorgo Basso *vs* Gorghi Alto-Medio). We tested the effect of the site on the number of eggs using the Analysis of covariance (ANCOVA) to avoid the "size effect". The number of eggs has been identified as the dependent variable, SCL as the independent covariate and the site as the categorical variable. The data collected in different years were treated uniquely to increase the accuracy of the statistical sample since a no significant inter-annual variability is known for the congeneric *Emys orbicularis* (Zuffi and Foschi, 2015). Only those females with oviductal eggs were considered certainly sexually mature. The reproductive phenology was considered as a whole, merging data of the two groups.

All above analyses were carried out with R 3.2.5 (R Development Core Team, 2015).

RESULTS

Abundance

A total of 1405 captures of 579 different turtles (493 in the Gorgo Basso, 86 in the Gorghi Alto-Medio) were made in 2015 and 2016. A strong site fidelity was confirmed as only two individuals were captured in both sites, and this happened only once during all sampling occasions. The sub-population of the Gorgo Basso was more abundant and reached a significant higher CPUE than the sub-population of the Gorghi Alto-Medio (Mann-Whitney U test = 42, $N_1 = N_2 = 6$, $P < 0.01$), respectively with an average of 3.02 and 0.80 turtles/trap/day.

Size and growth

The sub-population of the Gorgo Basso was characterized by a dominance of turtles (72%) with an SCL between 110 and 129.9 mm while the sub-population of Gorghi Alto-Medio is characterized by a dominance of turtles (76%) with an SCL between 100 and 119.9 mm (Fig. 1).

Females and males of Gorgo Basso were heavier ($t\text{-test}_{females}$= 8.73, df = 45.17, P < 0.001; $t\text{-test}_{males}$= -9.60, df = 68.20, P < 0.001) and bigger than individuals of Gorghi Alto-Medio, both in terms of carapace length ($t\text{-test}_{females}$= 9.61, df= 41.89, P < 0.001; $t\text{-test}_{males}$= 10.09, df= 66.31, P < 0.001), width ($t\text{-test}_{females}$= 5.50, df= 35.37, P < 0.001; $t\text{-test}_{males}$= 7.67, df= 77.63, P < 0.001), and height ($t\text{-test}_{females}$= 4.22, df= 28.13, P < 0.001; $t\text{-test}_{males}$= 6.48, df= 65.89, P < 0.001) (Table 2).

We used data on 79 males (61 from Gorgo Basso and 18 from Gorghi Alto-Medio) and 41 females (27 from Gorgo Basso and 14 from Gorghi Alto-Medio) to estimate relative growth rate (RGR). Individual variation in growth rate was high (range 0.0 – 0.0176), but with no significant difference between the sexes (t-test = -0.59, P = 0.5564). Considering independently the two sites, the models showed for both sexes (models 1 and 3, Table 3) that the interaction between the independent variable (SCL) and the categorical variable (site) was not significant, indicating that the slopes of

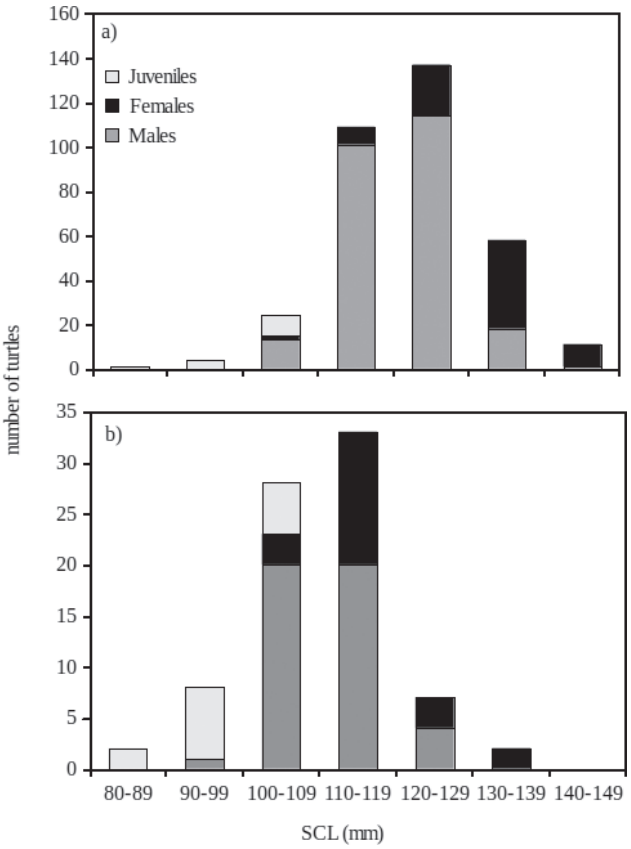

Fig. 1. Structure of sub-populations of *Emys trinacris* inhabiting the Gorgo Basso (a) and the Gorghi Alto-Medio (b).

Table 2. Mean values of biometric measurements for *Emys trinacris* in the two studied sites. SCL = straight carapace length; CW = carapace width; CH = carapace height; BM = body mass; n = number of individuals; S.E. = Standard Error.

Biometric measurement		GT Basso	GT Alto-Medio
SCL (mm) Adult females	Mean	131.5(n =144)	116.5 (n = 21)
	S.E.	0.7	0,05
	Min	110.0	4,42
	Max	150.9	5,5
SCL (mm) Adult males	Mean	120.1 (n = 291)	111.1 (n = 45)
	S.E.	0.4	0.9
	Min	101.3	99.7
	Max	141.1	124.9
CW (mm) Adult females	Mean	101.7 (n = 116)	93.7 (n = 21)
	S.E.	0.8	1.3
	Min	77.6	84.0
	Max	121.3	102.0
CW (mm) Adult males	Mean	94.0 (n = 282)	87.6 (n = 45)
	S.E.	0.4	0.7
	Min	69.4	71.4
	Max	112.0	101.5
PH (mm) Adult females	Mean	50.9 (n = 124)	47.0 (n = 21)
	S.E.	0.4	0.8
	Min	38.0	40.2
	Max	62.6	55.0
PH (mm) Adult males	Mean	42.6 (n = 271)	39.9 (n = 45)
	S.E.	0.2	0.4
	Min	25.4	34.6
	Max	53.5	46.3
BM (g) Adult females	Mean	401.1 (n = 144)	294.7 (n = 21)
	S.E.	7.7	12.8
	Min	217.0	221
	Max	658.0	422
BM (g) Adult males	Mean	281.2 (n = 290)	223.2 (n = 45)
	S.E.	3.4	5.7
	Min	143.0	154.0
	Max	453.0	310.0

the regressions were homogeneous. Therefore, in both sites, the growth rate is reduced progressively as the individual grows. The other models (models 2 and 4, Table 3) showed that the categorical variable (site) has a significant effect on the dependent variable (RGR), due to the significant difference of the intercept regression lines between the two sites. These models showed that individuals, despite having a growth rates that is inversely related to size, display a different growth rate: turtles from the Gorgo Basso are bigger than those of Gorghi Alto-Medio. The von Bertalanffy growth models showed that the Sicilian pond turtle of Lake Preola and Gorghi Tondi Nature Reserve appeared to mature sexually at approximately six years for males of Gorgo Basso (SCL_{min} = 102.8 mm) and of Gorghi Alto-Medio (SCL_{min} = 99.5 mm) and between seven and eight years for females of both sites, with a SCL_{min} of 112.1 mm and 106.2 mm respectively.

Table 3. Site effect on growth rate. RGR (relative growth rate) = dependent variable, SCL_1 (first capture straight carapace length) = independent variable, Site = categorical variable.

		F	d.f.	P
Male	Model 1 (interaction test)			
	SCL_1	20.03	1	< 0.001
	Site	13.17	1	< 0.001
	SCL_1 × Site	1.50	1	0.22
	Model 2 (no interaction)			
	SCL_1	19.89	1	< 0.001
	Site	13.08	1	< 0.001
Female	Model 3 (interaction test)			
	SCL_1	14.39	1	< 0.001
	Site	19.84	1	< 0.001
	SCL_1 × Site	0.69	1	0.41
	Model 4 (no interaction)			
	SCL_1	14.51	1	< 0.001
	Site	20.00	1	< 0.001

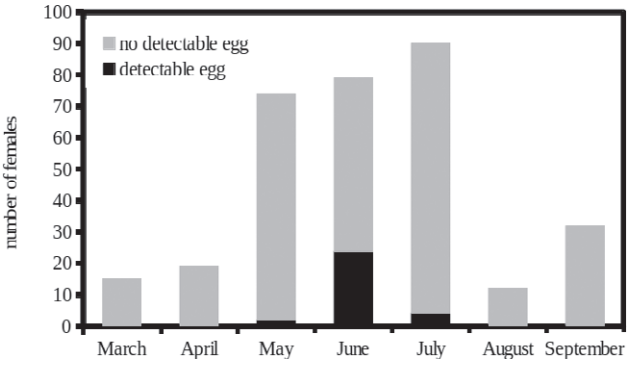

Fig. 2. Number of females of *Emys trinacris* with and without shelled eggs in the oviduct determined by inguinal palpation.

Allometry and reproductive biology

A total of 312 captures of 178 different females (152 in the Gorgo Basso and 26 in the Gorghi Alto-Medio) was made between 2014 and 2016. We collected 28 individuals with detectable eggs, 21 from the Gorgo Basso and seven from the Gorghi Alto-Medio. Reproductive females were found between May and July, with a peak in the first half of June (Fig. 2). In this period, the percentage of reproductive females collected over two-weeks interval ranged from 20% to 58.3%. We noticed also a double egg deposition of a female (SCL = 132.2 mm) captured on 10 June 2015 with four shelled eggs and on 7 July 2015 with five shelled eggs.

The average clutch size was 4.14 ± 0.23 (range 2 – 7, *n* = 28), with a positive correlation with the mother carapace length (F-statistic = 39.19, df = 27, P < 0.001) and a significant difference between the sites (Mann-Whitney U Test = 132.5, N_1 = 21, N_2 = 7, P < 0.01). The difference in the clutch size between the sites was significantly independent of the size of the females (Table 4). The average clutch size was 4.57 ± 1.07 (range 2 – 7, n = 21) for the sub-population of the Gorgo Basso and 2.86 ± 0.69 (range 2 – 4, n = 7) for the sub-population of the Gorghi Alto-Medio.

The average minimum diameter (D_{min}) was 19.46 ± 1.21 mm (range 16.0 – 21.5 mm, n = 89), with a not significant difference (t-test = 0.15, df = 24.23, P = 0.8843) between females of Gorgo Basso (D_{min} = 19.47 ± 0.94, n = 69) and those of Gorghi Alto-Medio (D_{min} = 19.42 ± 1.40, n = 20). The average minimum diameter (D_{min}) was positively correlated with the carapace length of the females ($r_{Pearson}$ = 0.70; t-test = 4.45, df = 21, P < 0.001), since the increase of the size allows a greater pelvic aperture width ($r_{Pearson}$ = 0.89; t-test= 8.75, df = 21, P < 0.001), that is a mechanical limiting factor for egg size in turtles.

Table 4. Site effect on number of eggs per female. Number of eggs = dependent variable, SCL (straight carapace length) = independent variable, Site = categorical variable.

	F	d.f.	P
Model	5.11	5	< 0.05
SCL	0.81	1	0.38
Site	0.48	2	0.63
SCL × Site	0.55	2	0.59

DISCUSSION

The growth of the Sicilian pond turtles in the Lake Preola and Gorghi Tondi Nature Reserve followed the general pattern described for other freshwater turtles: juveniles display a fast growth until sexual maturity, followed by a slowdown during ageing and at much larger size (Bury, 1979). The population studied seems to fall in the general rule noticed for the genus *Emys* (Zuffi et al., 2011) and for many others Emydidae (Iverson et al., 1993) as a typical southern ecotype with an advance in age at maturity at a smaller body size with respect to the northernmost populations, although regional fluctuations of temperature and precipitation are better predictors of body size than latitudinal temperature clines, especially in females of *Emys orbicularis* (Joos et al., 2017).

Moreover, the average clutch size is lower than that of similar sized population of the related *Emys orbicularis* in Italy (Zuffi et al., 1999; Zuffi et al., 2015), while no substantial variation in the nesting period and in the clutch frequency was noticed.

Despite these natural history traits, if we analysed separately the two sub-populations, a significant difference is noticeable: turtles in the Gorgo Basso reached higher body size, produced more eggs per clutch and had higher density than individuals in the Gorghi Alto-Medio.

Excluding both the presence of environmental and genetic effects due to the proximity and similarity of the sites, all these elements suggest the that phenotypic plasticity, driven by a stressor, may explain the observed difference. Furthermore, this hypothesis is supported by the different size at maturity reached in the two wetlands, following the pattern "five" described by Stearns and Koella (1986), where animals, that are forced to grow slowly by an inhibiting factor, mature at a same age, but a smaller size with respect to unstressed con-specific. This type of response is not uncommon in freshwater turtles at a local scale, such as noticed by Gibbons et al. (1981) for females of *Trachemys scripta* (Thunberg in Schoepff, 1792), while at a larger scale it can take over an adaptive process involving environmental and genetic components (Bernardo, 1993).

Indeed, turtles for the most part used energy resources, depending on age or period of year, for growth, maintenance of baseline metabolism and reproduction (Kuchling, 1999). In particular, during the juvenile stage of chelonians, almost all resources are dedicated to rapid growth to reach a body size and a strength of the shell that make them less susceptible to predation (Kuchling, 1999) and this is regulated mainly by the temperature and by the availability and quality of trophic resources (Kuchling, 1999) as well as by local factors related to the presence of contaminants that can alter the metabolic processes (Burger et al., 1998). Censi et al. (2013) speculated that smaller body mass of *Emys trinacris* living in Lake Preola and Gorghi Tondi Nature Reserve with respect to another Sicilian site can be associated to the supposed reduction of food disposal induced by lanthanide pollution of aquatic environment that influences the growth of aquatic micro-organisms, but no differences was observed within our study sites (D'Angelo, unpubl. data). In the same way, there are no substantial differences in the concentration of lead in the sediment - an inhibitor of growth in turtles (Burger et al. 1998) - between the two wetlands (Arpa Sicilia, 2016).

Therefore, the differences found could be explained in the light of the alteration of abundance and assemblage of the invertebrate community induced by the presence of alien fishes (Ottonello et al., 2017a) possibly exacerbated by the ubiquitous presence of *Procambarus clarkii*. In our opinion these differences in prey availability can definitely alter the energy intake by turtles affecting both the growth of individuals in the two sites, as already observed in other American Emydidae (Cagle, 1946; MacCulloch and Secoy, 1983; Dunham and Gibbons, 1990) and in *Chelydra serpentina* Linnaeus, 1758 (Brown et al., 1994) as well as the abundance (Congdon et al., 1986; Galbraith et al., 1988). These differences are likely to impact both the genetic variability of the population because males of *Emys* mate preferably with larger females (Poschadel et al., 2006), as well as the reproductive output, with females of the Gorgo Basso that laid twice as many eggs of the Gorghi Alto-Medio. These observations are concordant with the optimal egg size theory, according to which the major variation in the reproductive output due to different environmental conditions is in clutch size rather than in egg size, which has been optimized by natural selection (Brockelman, 1975).

In our opinion, these results highlighted how the introduction of non-native fish species can affect the ecology of the Sicilian pond turtle, also focusing on a often overlooked aspect, the problem of the interactions between alien fishes and turtles, on which data are lacking, in contrast to the more studied competition with non-native freshwater turtles (Cadi and Joly, 2003; 2004). Although further analyses are needed to confirm our finding with other wild populations, we believe that our data may provide important information for the management strategy of the Nature Reserve and for other similar areas and cases, in order to improve the conservation status of *Emys trinacris* and the quality of habitat in which it lives.

ACKNOWLEDGEMENTS

We are grateful to Nino Castelli, Michela Giribaldo, Maurizio Marchese, Nicola Napolitano, Gianpiero Pace for their help during field surveys and with Manuel Morici for his help during x-ray laboratory analysis. Capture and handling permits were released by the Ministero dell'Ambiente e della Tutela del Territorio e del Mare (DPN/2012/0003156 on 9.X.2012). D.O. was partially supported by Societas Europaea Herpetologica Grant in Herpetology 2014.

REFERENCES

Andreone, F., Corti, C., Ficetola, G.F., Razzetti, E., Romano, A., Sindaco, R. (2013): Liste rosse italiane, http: // www.iucn.it/scheda.php?id=1350576451. [*Accessed 1 June 2017*]

Andrews, R.M. (1982): Patterns of growth in reptiles. In: Biology of the Reptilia, vol. 13, p. 273–320. Gans C., Pough F.H., Eds, Academic Press, London.

Arpa Sicilia (2016): Monitoraggio Gorgo Basso 2015 - Classificazione dello stato ecologico e dello stato chimico in base al DM n. 260/2010. http: //www.arpa.sicilia.it/wp-content/uploads/2016/05/Relazione-GORGO-BASSO-TP-2015.pdf. [*Accessed 1 June 2017*]

Aa. Vv. (2008): Atlante della Biodiversità della Sicilia: Vertebrati terrestri. Studi e Ricerche, **6**, Arpa Sicilia, Palermo.

Ayres, C., Cordero, A. (2007): Site tenacity in European pond turtle (*Emys orbicularis*) hatchlings in Northwestern Spain. Amphibia-Reptilia **28**: 144-147.

Bellante, A., Maccarrone, V., Buscaino, G., Buffa, G., Filiciotto, F., Traina, A., Del Core, M., Mazzola, S., Sprovieri, M. (2015): Trace element concentrations in red swamp crayfish (*Procambarus clarkii*) and surface sediments in Lake Preola and Gorghi Tondi natural reserve, SW Sicily. Environ. Monit. Assess. **187**: 1–18.

Bernardo, J. (1993): Determinants of maturation in animals. Trends Ecol. Evol. **8**: 166–173.

Brockelman, W.Y. (1975): Competition, the fitness of offspring, and optimal clutch size. Am. Nat. **109**: 677–699.

Brody, S. (1945): Bioenergetics and growth. Reinhold Publishing Corp, New York.

Brown, G.P., Bishop, C.A., Brooks, R.J. (1994): Growth rate, reproductive output, and temperature selection of snapping turtles in habitats of different productivities. J. Herpetol. **28**: 405–410.

Burger, J., Carruth-Hinchey, C., Ondroff, J., McMahon, M., Gibbons, J.W., Gochfeld, M. (1998): Effects of lead on behaviour, growth, and survival of hatchling slider turtles. J. Toxicol. Environ. Health **55**: 495–502

Bury, R.B. (1979): Population ecology of freshwater turtles. In: Harless M, Morlock H (eds) Turtles perspectives and research. John Wiley, New York p. 571–602.

Cadi, A., Joly, P. (2003): Competition for basking places between the endangered European pond turtle (*Emys orbicularis galloitalica*) and the introduced red-eared slider (*Trachemys scripta elegans*). Can. J. Zool. **81**: 1392–1398.

Cadi, A., Joly, P. (2004) Impact of the introduction of the read-eared slider (*Trachemys scripta elegans*) on survival rates of the European pond turtle (*Emys orbicularis)*. Biodivers. Conserv. **13**: 1511–1518.

Cagle, F.R. (1946): The Growth of the Slider Turtle: *Pseudemys scripta elegans.* Miscellaneous Publications of the Museum of Zoology, University of Michigan.

Censi, P., Randazzo, L.A., D'Angelo, S., Saiano, F., Zuddas, P., Mazzola, S., Cuttitta, A. (2013): Relationship between lanthanide contents in aquatic turtles and environmental exposures. Chemosphere **91**: 1130–1135.

Çiçek, K., Kumaş, M., Ayaz, D., Varol Tok, C. (2016): A skeletochronological study of age, growth and longevity in two freshwater turtles, *Emys orbicularis* and *Mauremys rivulata*, from Mediterranean Turkey (Reptilia: Testudines). Zool. Middle East **62**: 29–38.

Congdon, J.D., Greene, J.L., Gibbons, J.W. (1986): Biomass of freshwater turtles: a geographic comparison. Am. Midl. Nat. **115**: 165–173.

Cox, W.A., Hazelrig, J.B., Turner, M.E., Angus, R.A., Marion, K.R. (1991): A model for growth in the musk turtle, *Sternotherus minor*, in a North Florida spring. Copeia **1991**: 954–968.

Cusimano, G., Hauser, S., Vassallo, M. (2006): Hydrogeochemistry of a wetland of south-western Sicily (Italy). E-Water. http: //www.ewa-online.eu/tl_files/_media/content/documents_pdf/Publications/E-Water/documents/43_2006_04.pdf. [*Accessed 1 June 2017*]

D'Angelo, S., Lo Valvo, M. (2003): On the presence of the red swamp crayfish *Procambarus clarkii* in Sicily. Naturalista siciliano **27**: 325–327.

Dextrase, A.J., Mandrak, N.E. (2006): Impact of alien invasive species on freshwater fauna at risk in Canada. Biol. Invasions **8**: 13–24.

Dunham, A.E., Gibbons, J.W. (1990): Growth of the slider turtle. In: Gibbons, JW (ed) Life History and Ecology of the Slider Turtle. Smithsonian Inst. Press, Washington, p. 135–145.

Fritz, U., Fattizzo, T., Guicking, D., Tripepi, S., Pennisi, M.G., Lenk, P., Joger, U., Wink, M. (2005): A new cryptic species of pond turtle from southern Italy, the

hottest spot in the range of the genus *Emys*. Zool. Scr. **34**: 351–371.

Galbraith, D.A., Bishop, C.A., Brooks, R.J., Simser, W.L., Lampman, K. (1988): Factors affecting the density of population of common snapping turtles (*Chelydra serpentina serpentina*). Can. J. Zool. **66**: 1233–1240.

Genovesi, P. (2007): Towards a European strategy to halt biological invasions in inland waters. In: Biological invaders in inland waters: profiles, distribution, and threats, Invading nature, pp. 627-638. Gherardi, F., Ed., Springer, Dordrecht, The Netherland.

Gibbons, J.W., Semlitsc, R.D., Greene, J.L., Schubauers, J.P. (1981): Variation in age and size at maturity of the slider turtle (*Pseudemys scripta*). Am. Nat. **117**: 841–845.

Hinton, T.G., Fledderman, P.D., Lovich, J.E., Congdon, J.D., Gibbons, J.W. (1997): Radiographic determination of fecundity: is the technique safe for developing turtle embryos? Chelon. Conserv. Biol. **2**: 409–414.

Hurlbert, S.H. (1984): Pseudoreplication and the design of ecological field experiments. Ecol. Monogr. **54**: 187–211.

Iverson, J.B., Balgooyen, C.P., Byrd, K.K., Lyddan, K.K. (1993): Latidudinal variation in egg and clutch size in turtles. Can. J. Zool. **71**: 2448–2461.

Joos, J., Kirchner, M., Vamberger, M., Kaviani, M., Rahimibashar, M. R., Fritz, U., Müller, J. (2017): Climate and patterns of body size variation in the European pond turtle, *Emys orbicularis*. Biol. J. Linn. Soc. **122**: 351–365.

Keller, C., Andreu, A.C., Ramo, C. (1998): Aspects of the population structure of *Emys orbicularis hispanica* from southern Spain. In: Fritz, U. et al. (eds), Proceedings of the *EMYS* Symposium Dresden 96. Mertensiella **10**: 147–158.

Kuchling, G. (1999): The Reproductive Biology of the Chelonia. Zoophysiology. Springer-Verlag Berlin Heidelberg.

Lacomba, I.A., Sancho, V.A. (2004): Advances in the action plan for Emys orbicularis in the Valencia region, Spain. Biologia **59**: 173-176.

Landres, P.B., Verner, J., Thomas, J.W., (1988): Ecological uses of vertebrate indicators species. A critique. Conserv. Biol. **2**: 316–328.

Lambert, M.R., McKenzie, J.M., Screen, R.M., Clause, A.G., Johnson, B.B., Mount, G.G., Shaffer, H.B., Pauly, G.B. (2019): Experimental removal of introduced slider turtles offers new insight into competition with a native, threatened turtle. PeerJ **7**: e7444.

Litzgus, J.D., Brooks, R.J. (1998): Growth in a cold environment: body size and sexual maturity in a northern population of spotted turtles, *Clemmys guttata*. Can. J. Zool. **76**: 773–782.

Lovich, J.E., Ernst, C.H., McBreen, J.F. (1990): Growth, maturity, and sexual dimorphism in the wood turtle, *Clemmys insculpta*. Can. J. Zool. **68**: 672–677.

Lovich, J.E., Ernst, C.H., Zappalorti, R.T., Herman D.W. (1998): Geographic variation in growth and sexual size dimorphism of Bog Turtles (*Clemmys muhlenbergii*). Am. Midl. Nat. **139**: 69–78.

Lubcke, G.M., Wilson, D. S. (2007): Variation in shell morphology of the western pond turtle (*Actinemys marmorata* Barid and Girard) from threee aquatic habitats in Northern California. J. Herpetol. **4**: 107–114.

Maccarrone, V., Filiciotto, F., Buffa, G., Stefano, V.D., Quinci, E.M., Vincenzi, G.d., Mazzola, S., Buscaino, G. (2016): An Invasive Species in a Protected Area of Southern Italy: the Structure, Dynamics and Spatial Distribution of the Crayfish *Procambarus clarkii*. Turkish J. Fish. Aquat. Sci. **16**: 401–412.

MacCulloch, R.D., Secoy, D.M. (1983): Demography, growth, and food of western painted turtles, *Chrysemys picta bellii* (Gray), from southern Saskatchewan. Can. J. Zool. **61**: 1499–1509.

Mahmoud, I.Y. (1969): Comparative ecology of the kinosternid turtles of Oklahoma. Southwestern Naturalist **14**: 31–66.

Marrone, F., Naselli-Flores, L. (2015): A review on the animal xenodiversity in Sicilian inland waters (Italy). Adv. Oceanogr. Limnol **6**: 2–12.

Marrone, F., Sacco, F., Arizza, V., Arculeo, M. (2016): Amendment of the type locality of the endemic Sicilian pond turtle *Emys trinacris* Fritz et al. 2005, with some notes on the highest altitude reached by the species (Testudines, Emydidae). Acta Herpetol. **11**: 59–61.

Maunder, M.N., Sibert, J.R., Fonteneau, A., Hampton, J., Kleiber, P., Harley, S.J. (2006): Interpreting catch per unit effort data to assess the status of individual stocks and communities. ICES J. Mar. Sci. **63**: 1373–1385.

Ogle, D.H. (2012): FSA: Fisheries Stock Analysis. R package version 0.2-8.

Naselli-Flores, L., Barone, R. (2012): Phytoplankton dynamics in permanent and temporary Mediterranean waters: is the game hard to play because of hydrological disturbance? Hydrobiologia **698**: 147–159.

Ottonello, D., D'Angelo, S., Oneto, F., Malavasi, S., Zuffi, M.A.L. (2017a): Feeding ecology of the Sicilian pond turtle *Emys trinacris* (Testudines, Emydidae) influenced by seasons and invasive aliens species. Ecol. Res. **32**: 71–80.

Ottonello, D., Oneto, F., Malavasi, S., Zuffi, M.A.L., D'Angelo, S. (2017b): Preliminary data on the popu-

lation of the Sicilian pond turtle, *Emys trinacris* Fritz et al., 2005 (Emydidae) inhabiting the Gorgo Tondo Basso in the "Lago Preola e Gorghi Tondi" Nature Reserve, Sicily, Italy. Acta zool. Bulgar., Supplement **10**: 121–128.

Parmenter, R.R., Avery, H.W. (1990): The feeding ecology of the slider turtle. In: Gibbons, J.W. (ed) Life History and ecology of the slider turtle. Sithsonian Institution Press, Whashington DC

Parkos, J.J., Santucci, V.J., Wahl, D.H. (2003): Effects of adult common carp (*Cyprinus carpio*) on multiple trophic levels in shallow mesocosms. Can. J. Fish. Aquat. Sci. **60**: 182–192.

Pitcher, T.J., Hart, P.J.B. (1995): The impact of species changes in African lakes. Chapman and Hall, London.

Polo-Cavia, N., López, P., Martín, J. (2010): Competitive interactions during basking between native and invasive freshwater turtle species. Biol. Invasions **12**: 2141–2152.

Poschadel, J.R., Meyer-Lucht, Y., Plath M. (2006): Response to chemical cues from conspecifics reflects male mating preference for large females and avoidance of large competitors in the European pond turtle, *Emys orbicularis*. Behaviour **143**: 569–587.

Pyke, G.H. (2008): Plague minnow or mosquitofish? A review of the biology and impacts of introduced *Gambusia* species. Annu. Rev. Ecol. Evol. Syst. **39**: 171–191.

Ricciardi, A., MacIsaac, H.J. (2011): Impact of biological invasions on freshwater ecosystems, pp. 211-224. In: Fifty Years of Invasion Ecology: The Legacy of Charles Elton, pp. 211-224. Richardson, D.M., Ed., Blackwell Publishing Ltd, Oxford, UK.

Selman, W., Baccigalopi, B., Baccigalopi, C. (2014): Distribution and abundance of Diamondback terrapins (*Malaclemys terrapin*) in Southwestern Louisiana. Chelon. Conserv. Biol. **13**: 131–139.

Servan, J., Baron, J., Bels, R., Bour, V., Lancon, M., Renon, G. (1986). Le marquage des tortues d'eau douce: application a la cistude d'Europe *Emys orbicularis* (Reptilia, Chelonii). Bull. Soc. Herp. Fr. **37**: 9–17.

Spadola, F., Insacco, G. (2009): Endoscopy of cloaca in 51 *Emys trinacris* (Fritz et al., 2005): morphological and diagnostic study. Acta Herpetol. **4**: 73–81.

Stearns, S.C., Koella, J.C. (1986): The evolution of phenotypic plasticity in li-history traits: prediction of reaction norms for age and size at maturity. Evolution **40**: 893–319.

Strayer, D.L. (2010): Aliens species in fresh waters: ecological effects, interactions with other stressors, and prospects for the future. Freshw. Biol. **55**: 152–174.

Tucker, J.K., Janzen F.J., Paukstis, G.L. (1998): Variation in carapace morphology and reproduction in the Red-Eared Slider *Trachemys scripta elegans*. J. Herpetol. **32**: 294-298.

Wilbur, H.M. (1975): The Evolutionary and Mathematical Demography of the Turtle *Chrysemys picta*. Ecology **56**: 64–77.

Zerunian, S. (2004): Pesci delle acque interne d'Italia. Quad Cons. Natura 20, Min Ambiente, Ist. Naz. Fauna Selvatica, Rome.

Zuffi, M.A.L., Citi, S., Foschi, E., Marsiglia, F., Martelli, E. (2015): Into a box interiors: clutch size variation and resource allocation in the European pond turtle. Acta Herpetol. **10**: 39–45.

Zuffi, M.A.L., Di Benedetto, F., Foschi, E. (2004): The reproductive strategies in neighbouring populations of the European pond turtle, *Emys orbicularis,* in central Italy. Ital. J. Zool. Suppl. **2**: 101–104.

Zuffi, M.A.L., Di Cerbo, A., Fritz, U. (2011): *Emys orbicularis* (Linnaeus, 1758). In: Fauna d'Italia, Reptilia, pp. 153-163. Corti, C., Capula, M., Luiselli, L., Razzetti, E., Sindaco, R., Eds, Edizioni Calderini, Bologna.

Zuffi, M.A.L., Gariboldi, A. (1995): Sexual dimorphism in Italian populations of the European pond terrapin, *Emys orbicularis*. In: Scientia Herpetologica, pp. 124–129. Llorente, G.A., Montori, A., Santos, X., Carretero, M.A., Eds, Associacion Herpetologica Espanola, Barcelona.

Zuffi, M.A.L., Foschi, E. (2015): Reproductive patterns of European pond turtles differ between sites: a small scale scenario. Amphibia-Reptilia **36**: 339–349.

Zuffi, M.A.L., Odetti, F., Meozzi, P. (1999): Body size and cluth size in the European pond turtle, *Emys orbicularis*, from central Italy. J. Zool. **247**: 139–143.

Acta Herpetologica 16(2): 99-108, 2021
DOI: 10.36253/a_h-11339

Hematological values of wild *Caiman latirostris* (Daudin, 1802) in the Atlantic Rainforest in Pernambuco, Brazil

Luciana C. Rameh-De-Albuquerque[1], Alexandre P. Zanotti[1], Denisson S. Souza[1], George T. Diniz[2], Paulo B. Mascarenhas-Junior[3,4,5,*], Ednilza M. Santos[3], Jozelia M.S. Correia[3]

[1] *Parque Estadual de Dois Irmãos, Recife, Pernambuco 52171-011, Brazil*
[2] *Fiocruz, Fundação Oswaldo Cruz - Instituto Ageu Magalhães, Recife, Pernambuco 50670-420, Brazil*
[3] *Laboratório Interdisciplinar de Anfíbios e Répteis da Universidade Federal Rural de Pernambuco, Recife, Pernambuco 52171-900, Brazil*
[4] *Programa de Pós-graduação em Biologia Animal da Universidade Federal de Pernambuco, Recife, Pernambuco 50670-901, Brazil*
[5] *Centro Universitário Brasileiro, UNIBRA, Recife, Pernambuco 50050-230, Brazil*
**Corresponding author*. E-mail: paulobragam16@gmail.com

Submitted on: 2021, 14th June; Revised on: 2021, 18th October; Accepted on: 2021, 29th October
Editor: Daniele Pellitteri-Rosa

Abstract. Hematological studies in crocodilians are important tools in the evolutionary diagnosis and control of sicknesses, such as anaemia, malnutrition, dehydration, inflammation, and parasitism, among others. We aimed to obtain reference intervals for the hemogram of *Caiman latirostris* in wild populations that inhabit Recife's Metropolitan Region, Pernambuco. We obtained blood samples from 42 caimans, from different sexes (22 males and 20 females) and ages classes (eight hatchlings, 24 subadults and 10 adults) in two areas of Atlantic Rainforest domain. We found that hematological parameters were included within the reference intervals for other crocodilian species. It was possible to observe differences between the areas for the mean corpuscular volume values, suggesting a possible difference between adult and juvenile individuals in the two study areas. When comparing sexes, there was no significant difference between the study parameters, but it was possible to observe differences in the mean corpuscular volume, mean corpuscular hemoglobin and hemoglobin in the Estação Ecológica de Tapacurá region. Although small differences have been observed between the two populations, we can infer that the hematological parameters are similar. We can use this information to evaluate animal's health in nature and for comparations with captive individuals, allowing the establishment of ideal maintenance conditions and assisting in the identification of possible pathologies.

Keywords. Broad-snouted Caiman, crocodilians, hematimetric indices, hematology.

INTRODUCTION

The broad-snouted caiman (*Caiman latirostris*) occurs in rivers, mangroves and flooded areas in Argentina, Bolivia, Brazil, Paraguay, and Uruguay. In Brazil, this species is found in the Cerrado, Caatinga, Atlantic Forest and Pampas biomes, from the coastal region of Rio Grande do Norte, distributed through the basins of the rivers São Francisco and Paraná/Paraguay to Rio Grande do Sul (Coutinho et al., 2013). In the wild, these caimans can live in large aggregations or in small groups and are always present in the mangrove areas of rivers, lagoons, wetlands, and lakes (Filogonio et al., 2010). This species, classified as Least Concern (LC), presents a large geographical area of distribution and an apparent ability to colonise anthropic environments (Júnior et al., 2018). However, anthropic pressure caused by the constant growth of human populations which, to a certain extent, triggers the destruction of their habitat, mainly through the drainage of water bodies, deforestation, pollution,

ISSN 1827-9635 (print)
ISSN 1827-9643 (online)

www.fupress.com/ah

intensive pesticide use, as well as illegal hunting in certain regions. These impacts can affect connectivity and consequently gene flow between populations on a micro and macrogeographic scale, with such processes resulting in the decline of populations (Coutinho et al, 2013; Bassetti and Verdade, 2014).

Reference hematological and blood biochemistry values are necessary for detecting the effects of environmental, infectious, parasitic, or toxicological stress in these animals, providing information on their health and therefore, can be used as a rapid diagnostic tool (Heatley and Russel, 2019). Hematological studies in wild or captive broad-snouted caimans have a scientific, educative and production improvement outcomes, and can be applied to conservation, reproduction, and reintroduction projects (Barboza et al., 2006; Adelakun et al., 2017). Blood analysis is a relatively non-invasive method which can provide important clinical data as well as information about the physiological conditions and health of animals (Padilha et al., 2011; Adelakun et al., 2017). The hemogram is comprised of the determination of the total erythrocyte count, hematocrit, hemoglobin concentration and hematological indices such as the mean corpuscular volume, mean corpuscular hemoglobin and mean corpuscular hemoglobin concentration (Saggese, 2009; Heatley and Russel, 2019). The erythrogram data serve to aid in the evolutionary diagnosis, characterisation, and control of sicknesses, such as anaemia, malnutrition, dehydration, inflammation, and parasitism among others (Barboza et al., 2007; Saggese, 2009; Heatley and Russel, 2019).

The clinical interpretation of the leukogram is challenging for many reasons, primarily because of the strict reference intervals, including the total leukocyte count and smear cell percentages which are not available for all species of healthy reptiles (Campbell, 2006; Saggese, 2009; Zayas et al., 2011). Normal hematological values for reptiles, including crocodilians, when determined by different laboratories, demonstrate ample inter and intraspecific variation due to the differences in blood sample collection, handling of the specimen, analysis techniques, physiological state of the reptiles, age, sex, nutrition, population dynamics, environmental conditions and use of anaesthetics (Stacy and Whitaker, 2000; Campbell, 2006; Saggese, 2009; Zayas et al., 2011). Reference intervals can be found for several reptile species, including crocodilians (Stacy and Whitaker, 2000; Padilha et al., 2011; Zayas et al., 2011). Since the mean hematological parameter values can vary between species, the reference values obtained for healthy animals can serve as a guide for dealing with sick animals (Stacy and Whitaker, 2000). Lastly, the effects on the leukocyte response to bacterial, fungal, viral, and parasitic infections or stress agents have been minimally investigated for this species (Heatley and Russel, 2019). Thus, when referring to a set of reference values, it is important to determine the conditions in which the blood samples were obtained. Understanding and recognising possible variations in hematological results for reptiles contributes to a critical interpretation of the published reference values and their clinical significance. Thus, the aim of this study was to describe the morphological characteristics of the peripheral blood of *C. latirostris* and establish erythrogram reference indices for this species in wild protected areas in Recife's Metropolitan Region.

MATERIAL AND METHODS

Study area

Between 2014 and 2015, we collected samples in water bodies located in the municipalities of Recife and São Lourenço da Mata, both belonging to the Recife's Metropolitan Region (RMR), the main socio-economic centre of the state of Pernambuco, Brazil. The region is dominated by Atlantic Forest and the climate is tropical and humid, with autumn-winter rains (Alvares et al., 2013). Furthermore, the area has a large water network (Carvalho, 2004) with the Capibaribe river, and great influence on RMR, occupying an area of 7,545.88 km^2, which represents 7.6% of Pernambuco (APAC, 2020).

In the municipality of São Lourenço da Mata, we collected samples in the Estação Ecológica de Tapacurá (EET) reservoir (8°2'S, 35°11'E), a lentic environment in a rural area, formed by the damming of the Tapacurá river. The water body is approximately 7.5 km^2 and is surrounded by sugar cane matrices (Almeida and Oliveira, 2009), open areas, agricultural areas, livestock, and riverside communities (Mascarenhas-Junior et al., 2020). It also has 5.35 km^2 of forest fragments, of which 1.72 km^2 belong to Conservation Units of Integral Protection (Mata do Camucim, Mata do Toró, Mata do Outeiro de Pedro) (CPRH, 2020) (Fig. 1). In the reservoir areas, there are also constant fishing activities, with recurring recordings of bycatch of local fauna (Mascarenhas-Junior et al., 2018; Santos et al., 2020).

Approximately 25 km from Tapacurá, we also collected samples from caimans located in the Parque Estadual de Dois Irmãos (PEDI) (8°0'S, 34°56'E), in the municipality of Recife, capital of Pernambuco. The area comprises approximately 11.6 km^2 of protected forests (Mata de Dois Irmãos, 3.8 km^2; Fazenda Brejo dos Macacos, 7.8 km^2) and in these fragments there is approximately 1.4 km^2 of water bodies forming the Prata microbasin, the Açude do Meio (~0.024 km^2), Açude do Prata (~0.025 km^2), Açude de Dentro (~0.015 km^2) and Açude de Dois Irmãos (~0.135 km^2). Despite this area is in an urban environment with anthropic pressures, the presence of a mature marginal forest aids in the maintenance of the water quality (Lima, 2004). In this study, we only accessed the Açude de Dentro and Açude de Dois Irmãos.

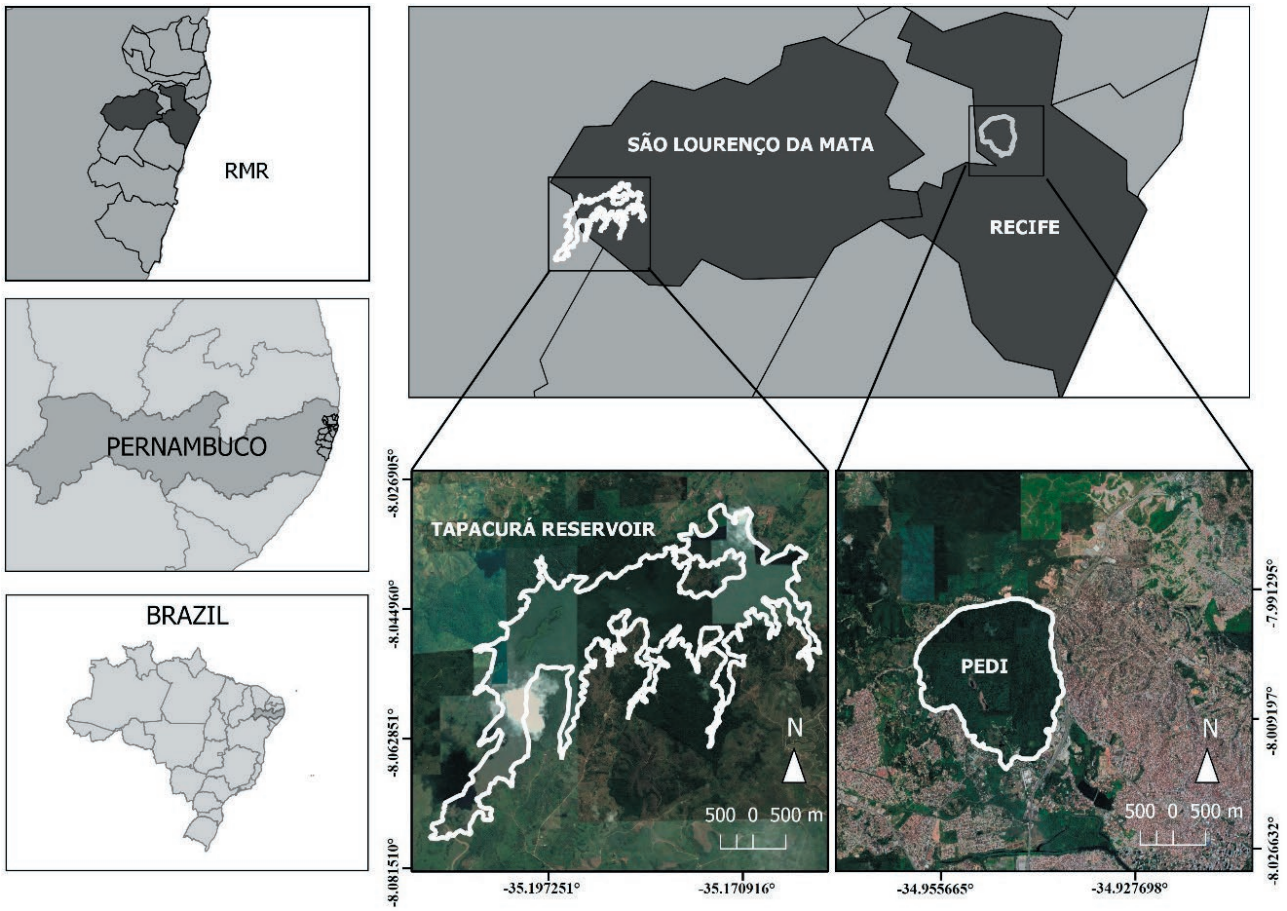

Fig. 1. Recife's Metropolitan Region (RMR) with Tapacurá reservoir and Parque Estadual de Dois Irmãos highlighted in white lines.

Data collection

Captures were performed bimonthly between 2014 and 2015, with active captures during the nocturnal period and with the aid of aluminium boats. The individuals were identified in the environment through the reflection of eyeballs (*tapetum lucidum*) from the interception of a beam of concentrated light using a spotlight (Magnusson, 1995). The captures were performed manually or with the use of cables snares connected to a telescopic pole (up to 5 m). Additionally, aquatic funnel traps with baits to attract the caimans were used. All physical post-capture restraint was performed using adhesive tapes.

The caimans were evaluated in terms of trauma, body scars and the absence of clinical signs and symptoms of diseases. Following this evaluation, blood samples were collected through supravertebral occipital venous sinus punctures using 20-gauge needles without anticoagulants and disposable needles. Immediately following the collection of samples, blood smears were prepared, air dried and stained with modified May-Grünwald-Giemsa colouration (Rosenfeld, 1947). A small volume of blood (0.5 mL) was collected in a microtube containing heparin for the determination of hematological parameters. The total hemocyte count (THC), total leukocyte count (TLC) and total thrombocyte count (TTC) were performed manually in a Neubauer chamber after 10 mL of blood being diluted in 2.0 mL of Natt and Herrick solution. The hematocrit (HT) was determined using the microhematocrit method, through the centrifugation of microcapillaries at 10000 rpm (Coles, 1986) and the hemoglobin concentration (HB) was determined using the cyanmethemoglobin method, mixing 20 mL of blood with 2.5 mL of Drabkin solution (Labtest Diagnostica®). Through conventional calculations, hematometric indices of mean corpuscular volume (MCV), mean corpuscular hemoglobin (MCH), mean corpuscular hemoglobin concentration (MCHC) were calculated. To count the differential leukocytes, a total of 100 cells were counted using a microscope under immersion (1000X).

After the collection of the blood material, the individuals were measured, weighed, sexed, and marked. The size class was determined through the snout-vent length (SVL), following the proposal by Leiva et al. (2019): Class I or hatchlings (< 25cm); Class II or subadults (25 cm to 67.9 cm); Class III (68 cm to 99.9 cm) and Class IV (over 99 cm) or adults. The weight was determined using scales with a limit of 40 kg. Furthermore, sex was determined for larger individuals using a cloacal palpation technique (Yanosky, 1990) and, in smaller caimans, surgical tweezers were inserted into the cloaca to separate the edges for

the observation of the genitalia (Webb et al., 1984). Lastly, all the individuals were marked with cuts in the scales of the single and double crests and with the subcutaneous implantation of microchips. At the end of data collection, caimans were released back into the water bodies from where they were captured.

Data analysis

To test the normality and homogeneity of the variables included in the study, we used Shapiro Wilk and Bartlett tests, respectively. For the analyses of the quantitative variables, we used a Bartlett test for homogeneity and the Shapiro Wilk test for the normality of the variables included in the study. The mean differences for the independent variables were evaluated using an ANOVA followed by Tukey's post-hoc test when observing the presumption of homogeneity. Otherwise, Kruskal-Wallis tests were used followed by the post-hoc test using Fisher's criteria of the lowest significant difference (LSD). A student t test was also used to observe when there was a presumption of normality, and when there was not, a Mann-Whitney test was used to evaluate the medians of the variables included in the study. We used categorical analyses for the comparative analysis between the qualitative variables, such as Pearson's χ^2 test andm when necessary, Fisher's exact test. All the conclusions were taken at a significance level of 5%. The R software (R Core Team, 2021) was used for the evaluation of the study results.

RESULTS

Cells morphological aspects

The erythrocytes presented an elliptical shape, with abundant cytoplasm, acidophilic, pinkish in colour, occupying approximately 80% of the cell. The nucleus presented condensed chromatin, basophilia, predominantly elliptical and occupies a central position in the cell. Larger erythrocytes with spherical nuclei and more rounded forms were also occasionally found (Fig. 2a). No intracellular inclusions or hemoparasites were observed.

The thrombocytes were predominantly elliptical with abundant cytoplasm, hyaline, also presenting a less elongated shape with little cytoplasm. Eventually, azurophilic granules were observed in the cytoplasm. The predominantly elliptical nucleus can present morphological variations, with chamfers, indentation or grooves, violet in colour with a central location (Fig. 2a, 2f and 2h).

The lymphocytes presented a large variation in terms of size and shape. The presence of irregularly shaped or spherical cells was common. The cytoplasm is scarce, basophilic, with azurophilic granules, commonly exhibiting cytoplasmic projections (Fig. 2a, 2b and 2g).

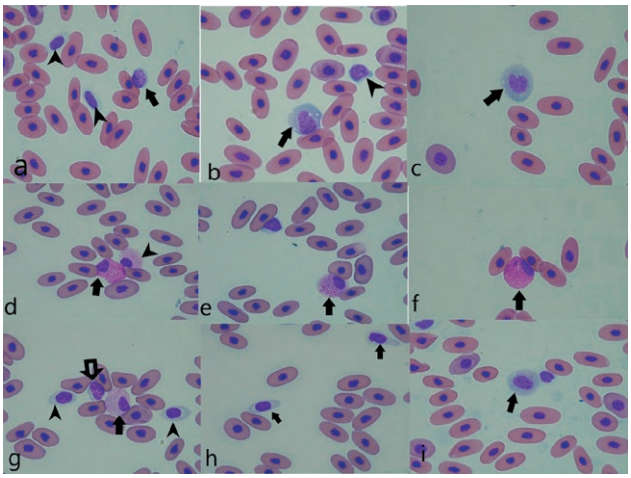

Fig. 2. Photomicrographs of *Caiman latirostris* blood cells coloured with modified May-Grunwald-Giemsa (Rosenfield, 1947) (magnification 1000X). (a) Mature erythrocytes in high quantity, lymphocytes (arrow), thrombocytes (head of arrow); (b) monocytes (arrow), lymphocyte (head of arrow); (c) monocyte; (d) eosinophil (arrow), heterophil (head of arrow); (e) heterophil; (f) eosinophil; (g) heterophile (arrow), thrombocytes (head of arrow), lymphocyte (outlined arrow); (h) thrombocytes; (i) monocytes with vacuoles.

The monocytes presented a spherical to oval shape, often presenting an irregular outline (Fig. 2b, 2c and 2i). The pale to moderately basophilic cytoplasm may contain cytoplasmic vacuoles of varying sizes. The nucleus may be spherical, oval or even U-shaped, generally with irregular outlines, occupying an off-centre position.

The eosinophils generally have a spherical shape. The cytoplasm is abundant and homogenously filled by acidophilic granules which are compact, spherical, oval or slightly elongated, pinkish in colour with a relatively homogenous colour. The nucleus is violet in colour and is generally spherical or lenticular and is in an off-centre position and may often be bilobulated (Fig. 2d and 2f).

The heterophils are large and are spherical, oval or irregular. The cytoplasm is generally abundant, full of compact granules whose acidophilia varies in its intensity, depending on the granule aspect and is of a dark pink or salmon colour. In terms of their morphology, the granules have varying aspects, both in terms of their colour intensity and their shape, where they can be spherical, fusiform with intense colouration or even stick, drumstick or oval shaped. There is a clear predominance of fusiforms compared to the others. The spherical nucleus is located off-centre or peripherally (Fig. 2d, 2e and 2g).

The basophils have a spherical shape and are smaller when compared to the other granulated leukocytes. The cytoplasm presents strongly basophilic spherical gran-

Table 1. Hematological reference values for wild *Caiman latirostris* and differences between the two study areas (Pernambuco, Brazil). SD (Standard deviation), P (p value), SVL (Snout-Vent Length), TL (Total Length), TEC (Total Erythrocyte Count), TLC (Total Leukocyte Count), HB (Hemoglobin), Ht (Hematocrit), MVC (Mean corpuscular volume), MCH (Mean Corpuscular Hemoglobin), MCHC (Mean Corpuscular Hemoglobin Concentration), TTC (Total Thrombocyte Count).

Parameter	PEDI (n = 22)			EET (n = 20)			P
	Mean	SD	Range	Mean	SD	Range	
SVL (cm)	47.2	36.14	17.3-100	58.88	25.5	17.8-100.04	0.09
TL (cm)	81.77	41.62	36-209	106.31	60.64	28-211	0.30
Weight (g)	5287	11934	125-51380	8140	12030	114.2-38300	0.42
TEC (10^3 cells/mm^3)	178.86	73.58	30-355	219.75	63.58	120-345	0.06
TLC (10^3 cells/mm^3)	5.23	2.87	0.75-11.75	3.84	2.01	1.25-8.25	0.07
HB (g/dl)	6.85	0.82	5.2-8.0	7.22	0.6	5.8-8	0.11
Ht (%)	20.18	6.13	3-29	21.5	3.61	15-29	0.40
MCV (fl)	1.53	1.18	0.76-5.45	1.02	0.18	0.75-1.42	**0.04**
MCH (pg)	0.5	0.4	0.22-2	0.35	0.09	0.22-0.59	0.15
MCHC (%)	42.66	40.91	25-223.3	33.9	4.33	22.3-41.76	0.67
TTC (10^3 cells/mm^3)	2.98	1.94	0.5-8.37	4.5	1.59	1.5-7	**0.01**
Lymphocytes (%)	54.32	12.37	33-81	51.5	12.95	31-77	0.48
Monocytes (%)	5.18	2.72	1.0-9.0	3	2.18	0-9	**0.01**
Basophils (%)	2.73	1.75	0-5	1.4	1.79	0-8	**0.01**
Heterophils (%)	34.82	12.94	6.0-60.0	41.8	13.83	9.0-63.0	0.10
Eosinophils (%)	2.95	1.73	0-6	1.8	1.4	0-5	**0.02**

ules of varying sizes and when located on top of the nucleus it can be impossible to distinguish between their outlines.

General parameters of caimans

Blood samples from 42 caimans were collected, with 22 from PEDI and 20 from EET. The sex proportions of the captured individuals were 22 males (PEDI = 12, EET = 10, 52.38%), 18 females (PEDI = 10, EET = 8, 42.86%) and 2 undetermined individuals (4.76%).

From the total number of animals, 10 were adults (PEDI = 3, EET = 7, 23.9%), eight hatchlings (PEDI = 5, EET = 3, 19.0%) and 24 subadults (PEDI = 14, EET = 10, 57.1%). Between the two locations it was possible to observe differences in the capture of different age classes, with a greater number of adults in the EET and more subadults in PEDI.

The biometric and hematological parameters collected for *Caiman latirostris* in the two locations are presented in Table 1. The SVL varied from 17.30 cm to 100.04 cm and the weight varied from 114.2 g to 51,380 g. It was possible to observe differences in the hematological parameters for the different areas for the values of MCV ($P = 0.04$), thrombocytes ($P \leq 0.01$), monocytes ($P = 0.01$), basophils ($P = 0.01$) and eosinophils ($P = 0.02$; Table 1).

The hematological data and their reference intervals for the different age groups are established in Table 2 and Table 3. The MCV values did not indicate difference between adult and subadult individuals ($P = 0.06$). In the comparisons between the areas, differences in the values for hatchling thrombocytes ($P = 0.04$) and adult eosinophils ($P = 0.03$) were identified (Table 2 and Table 3).

For the comparison between the sexes in the samples, there was no significant difference between the hematological parameters, with the only significant difference being for TL ($P = 0.04$). However, when performing this evaluation between individuals of the same area, it was possible to observe differences in the red blood cells ($P = 0.02$), MCV ($P < 0.01$), MCH ($P = 0.01$) and monocytes ($P = 0.01$) in Tapacurá and for the hemoglobin values in the PEDI ($P = 0.02$) with higher values for red blood cells in females. The other parameters, MCV, MCH, monocytes and hemoglobin, were higher for males (Table 4 and Table 5).

DISCUSSION

In general, the hematological parameters found for *Caiman latirostris* in wild environments in the State of Pernambuco fall within the reference intervals for other species of crocodilians (Stacy and Whitaker, 2000; Padil-

Table 2. Hematological reference values for different age groups of wild *Caiman latirostris* (Parque Estadual de Dois Irmãos, Pernambuco, Brazil). SD (Standard deviation), P (p value), SVL (Snout-Vent Length), TEC (Total Erythrocyte Count), TLC (Total Leukocyte Count), HB (Hemoglobin), Ht (Hematocrit), MVC (Mean corpuscular volume), MCH (Mean Corpuscular Hemoglobin), MCHC (Mean Corpuscular Hemoglobin Concentration), TTC (Total Thrombocyte Count).

Parameter	Adults (n = 3)			Hatchlings (n = 5)			Subadults (n = 14)			P
	Mean	SD	Range	Mean	SD	Range	Mean	SD	Range	
SVL (cm)	99.13	62.39	70-109	22.17	6.48	17.3-21.0	44.25	4.83	32.4-50.0	**<0.01**
Weight (g)	23553	21138	3834-51380	330	370.63	125-1140	1799	965.94	166-3210	**<0.01**
TEC (10^3 cells/mm^3)	171.25	101.77	30-255	175.71	26.21	150-210	183.64	88.29	55-355	0.28
TLC (10^3 cells/mm^3)	5.87	3.05	1.5-8.5	4.86	1.04	3.5-6.5	5.23	3.69	0.7-11.75	0.34
HB (g/dl)	6.45	0.7	6-7.5	7.11	0.73	5.8-8	6.84	0.91	5.2-8	0.44
Ht (%)	18.5	3.42	14-22	21.57	4.72	12-26	19.91	7.71	47178	0.80
MCV (fl)	1.88	1.87	0.76-4.67	1.24	0.28	0.80-1.73	1.58	1.31	0.82-5.45	0.22
MCH (pg)	0.73	0.85	0.26-2	0.41	0.03	0.37-0.46	0.48	0.3	0.22-1.21	0.16
MCHC (%)	35.45	5.74	30.5-42.86	34.21	6.8	26.54-48.34	50.66	57.78	25-223	0.86
TTC (10^3 cells/mm^3)	2.75	2.01	0.75-5.5	2.54	0.82	1-3.5	3.35	2.45	0.5-8.37	**0.04**
Lymphocytes (%)	43.25	8.88	35-55	59.29	8.12	48-68	55.18	13.82	33-81	0.22
Monocytes (%)	5.25	3.5	1-9	4.57	2.94	2-9	5.55	2.5	2-9	0.07
Basophils (%)	3.25	2.22	0-5	2.29	1.5	0-5	2.82	1.83	0-5	0.11
Heterophils (%)	44	7.12	38-52	30.43	9.25	18-45	34.27	15.41	6-60	0.28
Eosinophils (%)	4.25	0.96	3-5	3.43	1.62	2-6	2.18	1.72	0-4	**0.03**

Table 3. Hematological reference values for different age groups of wild Caiman latirostris (Estação Ecológica de Tapacurá, Pernambuco, Brazil). SD (Standard deviation), P (p value), SVL (Snout-Vent Length), TEC (Total Erythrocyte Count), TLC (Total Leukocyte Count), HB (Hemoglobin), Ht (Hematocrit), MVC (Mean corpuscular volume), MCH (Mean Corpuscular Hemoglobin), MCHC (Mean Corpuscular Hemoglobin Concentration), TTC (Total Thrombocyte Count).

Parameter	Adults (n = 7)			Hatchlings (n = 3)			Subadults (n = 10)			P
	Mean	SD	Range	Mean	SD	Range	Mean	SD	Range	
SVL (cm)	74.71	18.39	70-100.4	41.1	35.12	17.8-24.0	44.24	14.97	59.0-67.5	**<0.01**
Weight (g)	15495	13641	1015-38300	709.73	827.8	114-216	829	512.35	540-1740	**<0.01**
TEC (10^3 cells/mm^3)	223.64	47.17	130-290	246.25	70.28	185-345	190	89.93	120-345	0.28
TLC (10^3 cells/mm^3)	4.34	1.92	1.75-7.75	3.19	0.24	3-3.5	3.25	2.9	1.25-8.25	0.34
HB (g/dl)	7.19	0.65	5.8-8	7.4	0.54	6.9-8	7.12	0.61	6.2-7.8	0.44
Ht (%)	21.45	3.24	15-26	23.25	4.35	19-29	20.2	4.02	16-26	0.80
MCV (fl)	0.98	0.15	0.75-1.26	0.96	0.08	0.84-1.02	1.15	0.25	0.75-1.42	0.22
MCH (pg)	0.33	0.05	0.27-0.45	0.31	0.06	0.22-0.37	9.42	0.13	0.22-0.59	0.16
MCHC (%)	33.91	3.37	28.33-33.33	31.33	6.16	22.33-36.31	35.92	4.51	30-41.76	0.86
TTC (10^3 cells/mm^3)	4.02	1.5	1.5-6	6.12	0.77	5.25-7	4.25	1.61	1.75-5.75	**0.04**
Lymphocytes (%)	54.09	13.68	37-77	53.5	14.84	32-66	44.2	8.64	31-55	0.22
Monocytes (%)	2.18	1.54	0-5	4.25	1.5	3-6	3.8	3.27	1-9	0.07
Basophils (%)	1	1.1	0-3	1	0	1	2.6	3.13	0-8	0.11
Heterophils (%)	40.36	15.59	9-59	39	16.06	30-63	47.2	7.6	35-54	0.28
Eosinophils (%)	1.45	0.82	0-3	2.25	2.22	0-5	2.2	1.79	0-4	**0.03**

ha et al., 2011; Zayas et al., 2011; Bassetti and Verdade, 2014). Some factors that may have affected the results obtained in previous studies may be related to the methodology used, the environmental conditions and the diet of the population sampled.

Among the hematological parameters, it was possible to observe differences between the areas in the MCV values. These values suggest a possible difference between adult individuals and subadults between the two study areas. The causes of physiological changes in

Table 4. Hematological reference values for male and female wild *Caiman latirostris* (Parque Estadual de Dois Irmãos, Pernambuco, Brazil). SD (Standard deviation), P (p value), SVL (Snout-Vent Lenght), TL (Total Length), TEC (Total Erythrocyte Count), TLC (Total Leukocyte Count), HB (Hemoglobin), Ht (Hematocrit), MVC (Mean corpuscular volume), MCH (Mean Corpuscular Hemoglobin), MCHC (Mean Corpuscular Hemoglobin Concentration), TTC (Total Thrombocyte Count).

Parameter	Males (n=12)			Females (n=10)			P
	Mean	SD	Range	Mean	SD	Range	
SVL (cm)	37.77	25.43	17.3-100	49.51	13.3	42-86.50	0.07
TL (cm)	74.21	51.07	36-209	90.85	26.18	75.5-163	0.11
Weight (g)	5944	14631	125-51380	4498	8332	166-28000	0.22
TEC (10^3 cells/mm^3)	203.33	39.9	150-255	149.5	94.5	30-355	0.12
TLC (10^3 cells/mm^3)	5.77	2.3	2.75-11	4.57	3.45	0.75-11.7	0.36
HB (g/dl)	7.21	0.69	5.8-8	6.43	0.78	5.2-8	**0.02**
Ht (%)	22.25	4.22	12-28	17.7	7.3	3-29	0.10
MCV (fl)	1.12	0.27	0.76-1.73	2.01	1.64	0.82-5.45	0.12
MCH (pg)	0.36	0.07	0.26-0.46	0.67	0.56	0.22-2	0.21
MCHC (%)	33.3	5.6	25.71-48.34	53.9	60.09	25-223	0.62
TTC (10^3 cells/mm^3)	2.77	1.13	1-5.75	3.23	2.67	0.5-8.37	0.69
Lymphocytes (%)	56.17	12.38	38-81	52.1	12.64	33-73	0.46
Monocytes (%)	5.08	3	1-9	5.3	2.5	2-9	0.85
Basophils (%)	2.67	1.56	0-5	2.8	2.04	0-5	0.87
Heterophils (%)	32.92	13.06	6-52	37.1	13.09	17-60	0.46
Eosinophils (%)	3.16	1.99	0-6	2.7	1.42	0-4	0.53

Table 5. Hematological reference values for male and female wild *Caiman latirostris* (Estação Ecológica de Tapacurá, Pernambuco, Brazil). SD (Standard deviation), P (p value), SVL (Snout-Vent Lenght), TL (Total Length), TEC (Total Erythrocyte Count), TLC (Total Leukocyte Count), HB (Hemoglobin), Ht (Hematocrit), MVC (Mean corpuscular volume), MCH (Mean Corpuscular Hemoglobin), MCHC (Mean Corpuscular Hemoglobin Concentration), TTC (Total Thrombocyte Count).

Parameter	Males (n=10)			Females (n=8)			P
	Mean	SD	Interval	Mean	SD	Interval	
SVL (cm)	67.73	27.31	28.5-100.04	59.75	14.14	41-73.5	0.49
TL (cm)	104.33	78.14	28-211	124.3	25.24	82-147	0.50
Weight (g)	12032	15975	540-38300	5584	4447	1015-11260	0.57
TEC (10^3 cells/mm^3)	192.5	67.17	120-345	259.37	46.17	195-345	**0.02**
TLC (10^3 cells/mm^3)	3.72	2.34	1.25-8.25	4.15	1.9	1.75-7.75	0.67
HB (g/dl)	7.04	0.69	5.8-8	7.5	0.44	7-8	0.11
Ht (%)	20.8	4.29	15-29	22.75	2.87	18-26	0.27
MCV (fl)	1.12	0.17	0.84-1.42	0.89	0.11	0.75-1.02	**0.00**
MCH (pg)	0.39	0.1	0.22-0.59	0.29	0.04	0.22-0.35	**0.01**
MCHC (%)	34.21	5.54	22.33-41.76	33.28	3.16	30-40	0.66
TTC (10^3 cells/mm^3)	4.62	1.66	1.75-7	4.09	1.67	1.5-6	0.51
Lymphocytes (%)	47.1	10.88	31-66	58.75	12.52	44-77	0.06
Monocytes (%)	3.9	2.28	1-9	1.5	1.07	0-3	**0.01**
Basophils (%)	1.8	2.3	0-8	1.25	1.2	0-3	0.49
Heterophils (%)	45	10.87	30-59	36.25	15.56	9-54	0.20
Eosinophils (%)	2.2	1.69	0-5	2.25	0.89	0-3	0.15

erythrogram parameters for reptiles are numerous. With increasing age, the total erythrocyte count, the MCV, MCH, MCHC, hematocrit and hemoglobin, tend to increase (Heatley and Russel, 2019).

A relative increase in the total erythrocyte count, hemoglobin and/or hematocrit occurs in males of some

reptile species. However, many species may not correspond to this expectation (Heatley and Russel, 2019). In this study, most parameters did not present significant differences between males and females, but we observed differences in the MCV, MCH and hemoglobin values, which were higher in males, whereas the total erythrocyte count was higher in females in the EET region.

The main aims of the blood smear readings include the differentiation of cell types, the evaluation of cell morphology, the observation of anomalies in cell morphology and the observation of cell inclusions or extracellular anomalies, such as hemoparasites (Heatley and Russel, 2019). In this study, no intracellular inclusions nor hemoparasites were found.

This study corroborates the findings of Basset (2016) for *C. latirostris* and Moura et al. (1999) for *Caiman yacare*, in relation to the types of cells found in peripheral blood. The leukocytes were classified as lymphocytes, azurophilic monocytes, eosinophils, heterophils and basophils. For many authors, azurophils are a variation of monocytes, as can be observed (Zayas et al., 2011), for the same species, whereas other researchers recommend that these cells could be counted separately in snakes but should be grouped for other reptile species (Moura et al., 1999). In this study all the cells were grouped as as monocytes, and we observed we observed differences in the number of monocytes between areas, with the PEDI presenting higher values compared to the EET. Likewise, when comparing sexes within the same area, males in the EET presented higher values than females.

In relation to the morphological characteristics of the other leukocytes, this study corroborates the findings described for other species of crocodilians (Moura et al., 1999; Stacy and Whitaker, 2000; Padilha et al., 2011; Zayas et al., 2011). The reptile heterophile has larger cytoplasmic granules, despite being fewer in number, compared to lizards and snakes (Clever and Quaglia, 2009; Sacchi et al., 2011).

The lymphocytes are the most common leukocytes, accounting for up to 80% of the differential count in healthy reptiles (Heatley and Russel, 2019). In this study the lymphocytes were the most numerous leukocytes, followed by heterophils, monocytes, eosinophils, and basophils, which differs from the results found by Zayas et al. (2011), for the same species. They observed a higher number of lymphocytes followed by heterophils. However, they found more basophils compared to monocytes and eosinophils. Stress factors may be responsible for the increase in total leukocyte count and differential count; however, the extent of these changes has not been comprehensively investigated in reptiles. With a few exceptions, we lack fundamental knowledge on the timing of inflammation and associated cellular responses in reptiles (Heatley and Russel, 2019).

Although we attempted, in this study, to relate the differences found between ages, sex and sample areas, additional factors should be considered, as the influence of environmental parameters such as climate, seasonal period, nutritional state and population dynamics (Moura et al., 1999; Stacy and Whitaker, 2000; Heatley and Russel, 2019).

This study corroborates the idea presented by Basset (2016) where the results obtained from experiments involving blood hematology and biochemistry parameters should always be considered as a diagnostic tool for an animal's or even of a population's state of health.

As affirmed by Stacy and Whitaker (2000) in their study on *Crocodylus palustris*, the differences found may not be a true reflection of the differences between species, therefore making it difficult to come to any firm conclusion about the biological significance of these differences. However, it is still worth considering this data when interpreting the blood parameters of one species, since these are the best data available currently.

ACKNOWLEDGMENTS

We would like to thank the PEDI management and the EET manager and crew for making field trips and sample collections possible. We also thank the Fundação de Amparo a Ciência no Estado de Pernambuco (FACEPE) for funding's (APQ 0245/2.04-15), the Sistema de Autorização e Informação em Biodiversidade (SISBIO) for the sampling license (39929-2) and Ethics and Animal Use Committee from Universidade Federal Rural de Pernambuco (CEUA- UFRPE) for authorizing the execution of the project (license number 068/2014).

REFERENCES

Adelakun, K.M., Kehinde, A.S., Olaoye, O., Ihidero, A.A., Dalha, A. (2017): Blood biochemical of Nile crocodile (*Crocodylus niloticus*) in Kano zoological garden, Nigeria. Bull. Ani. Hea. Prod. Afr. **65**: 95-102.

Almeida, A.V., Oliveira, M.A. (2009): A história da Estação Ecológica do Tapacurá (São Lourenço da Mata, PE) baseada no relatório de Vasconcelos Sobrinho de 1976. Available at: http://www. ufrpe. br/ trabalho_ver. php. [*Acessed 12 November 2020*]

Alvares, C.A., Stape, J.L., Sentelhas, P.C., Gonçalves, J.D., Sparovek, G. (2013): Köppen's climate classification map for Brazil. Meteor. Zeits. **22**: 711-728.

APAC: Bacia do Capibaribe (2020): Available at http://200.238.107.184/bacias-hidrograficas/40-bacias-hidrograficas/193-bacia-do-rio-capibaribe. [*Accessed 10 September 2020*]

Barboza, N.N., Mussart, N.B., Coppo, J.A., Fioranelli, S.A., Koza, G.A. (2007): Oscilaciones del eritrograma en caimanes criados por sistema ranching. Rev. Vet. **18**: 84-91.

Barboza, N.N., Mussart, N.B., Prado, W.K., Gabriela, A., Coppo, J.A. (2006): Cambios del eritrograma durante el cautiverio de *Caiman latirostris* y *Caiman yacare*. Comum. Cient. Tecno. 1-4.

Basset, L.A.B. (2016): Estado sanitário do jacaré-de-papo-amarelo (*Caiman latirostris*) em paisagens antropizadas no Estado de São Paulo. Unpublished doctoral dissertation. Escola Superior de Agricultura Luiz de Queiroz, University of University of São Paulo, Piracicaba, Brazil.

Bassetti, L.A.B., Verdade, L.M. (2014): Crocodylia (Jacaré, Crocodilo). In: Tratado de Animais Selvagens – Medicina Veterinária, pp 18. Cubas, Z.S., Silva, J.C.R., Catão-Dias, J.L., Eds, São Paulo, São Paulo.

Campbell, T.W. (2006): Clinical pathology of reptiles, In: Reptile medicine and surgery, pp. 453-470. Mader, D.R., Ed., Saunders, St. Louis, Missouri.

Carvalho, L.E. (2004): Os descaminhos das águas no Recife: os canais, os moradores e a gestão. Unpublished master thesis, Universidade Federal Rural de Pernambuco, Recife, Brazil.

Claver, J.A., Quaglia, A.I. (2009): Comparative morphology, development, and function of blood cells in non-mammalian vertebrates. J. Exo. Pet. Med. **18**: 87-97.

Coles, E.H. (1986): Veterinary clinical pathology, 4th Edition. DE:CBS Press, New Delhi.

Coutinho, M.E., Marioni, B., Farias, I.P., Verdade, L.M., Bassetti, L., Mendonça, S.H.S.T., Vieira, T.G., Magnusson, W.E., Campos, Z. (2013): Avaliação do risco de extinção do jacaré-de-papo-amarelo *Caiman latirostris* (Daudin, 1802) no Brasil. Available at: https://www.icmbio.gov.br/portal/images/stories/biodiversidade/fauna-brasileira/avaliacao-do-risco/crocodilianos/Caiman_latirostris_BB.pdf. [*Accessed 1 August 2020*]

CPRH: Agência Estadual Do Meio Ambiente de Pernambuco. (2011): Unidades de Conservação de Proteção Integral. Available at: cprh.pe.gov.br/unidades_conservacao/Protecao_Integral/ Refugio_de_Vida_Silvestre/40032%3B56221%3B223705%3B0%3B0.asp. [*Accessed 12 November 2020*]

Filogonio, R., Assis, V.B., Passos, L.F., Coutinho, M.E. (2010): Distribution of populations of broad-snouted caiman (*Caiman latirostris*, Daudin 1802, Alligatoridae) in the São Francisco River basin, Brazil. Braz. J. Biol. **70**: 961-968.

Heatley, J.J., Russell, K.E. (2019): Hematology. In: Mader's Reptile and Amphibian Medicine and Surgery, pp. 301-318. Divers, S.J, Stahl, S.J, Eds, Saunders, St. Louis, Missouri.

Júnior, P.B.M., Santos, E.M., Correia, J.M.S. (2018): Diagnóstico dos resgates de jacarés na região metropoliana do Recife, Pernambuco. Ver. Ibero-Amer. de Ciênc. Ambientais. **9**: 138-145.

Leiva, P.M., Simoncini, M.S., Portelinha, T.C., Larriera, A., Piña, C.I. (2019): Size of nesting female Broad-snouted Caimans (*Caiman latirostris* Daudin 1802). Braz. J. Bio. **79**: 139-143.

Lima, Y.C. (2004): Dinâmica social e ambiental de capivaras (*Hydrochoerus hydrochaeris* Linnaeus, 1766) do Parque Estadual de Dois Irmãos, Recife-PE. Unpublished Barchelor's monograph. Universidade Federal Rural de Pernambuco, Recife, Brazil.

Magnusson, W.E. (1995): A conservação de crocodilianos na América Latina. In: La conservación y el manejo de caimanes e cocodrilos de America Latina, pp. 5-17. Larriera, A., Verdade, L.M., Eds, Santo Tomé, Santa Fé.

Mascarenhas-Junior, P.B., Anjos, H.R., Santos, E.M., Correia J.M.S. (2018): *Caiman latirostris* (Daudin, 1802) interaction with fishing nets in a lentic area, Northeast of Brazil. Herp. Not. **11**: 977-980.

Mascarenhas-Junior, P.B., Santos, E.M., Moura, G.J., Diniz, G.T., Correia, J.M. (2020): Space-time distribution of *Caiman latirostris* (Alligatoridae) in lentic area of Atlantic Forest, northeast of Brazil. Herp. Not. **13**: 129-137.

Moura, W.L., Matushima, E.R., Oliveira, L.W., Egami, M.I. (1999). Aspectos morfológicos e citoquímicos dos glóbulos sangüíneos de *Caiman crocodilus yacare* (Daudin, 1802) (Reptilia, Crocodilia). Braz. J. Vet. Res. Ani. Sci. **36**: 45-50.

Padilla, S.E., Weber, M., Jacobson, E.R. (2011): Hematologic and plasma biochemical reference intervals for Morelet's crocodiles (*Crocodylus moreletii*) in the northern wetlands of Campeche, Mexico. J. Wild. Dis. **47**: 511-522.

R Core Team. (2021): R: A language and environment for statistical computing. Available at https://cran.microsoft.com/snapshot/2014-09-08/web/packages/dplR/vignettes/xdate-dplR.pdf. [*Accessed 12 April 2021*]

Rosenfeld, G. (1947): Método rápido de coloração de esfregaços de sangue. Noções práticas sobre corantes pancrômicos e estudo de diversos fatores. Mem. Inst. Butantan. **20**: 315-328.

Saggese, M.D. (2009): Clinical approach to the anemic reptile. J. Exo. Pet. Med. **18**: 98-111.

Sacchi, R., Scali, S., Cavirani, V., Pupin, F., Pellitteri-Rosa, D., Zuffi, M.A.L. (2011). Leukocyte differential counts

and morphology from twelve European lizards. Italian J. Zool. **78**: 418-426.

Santos, R.L., Bezerra, T.L., Correia, J.M.S., Santos, E.M. (2020): Artisanal fisheries interactions and bycatch of freshwater Testudines at the Tapacurá reservoir, Northeast Brazil. Herp. Not. **13**: 249-252.

Stacy, B.A., Whitaker, N. (2000): Hematology and blood biochemistry of captive mugger crocodiles (*Crocodylus palustris*). J. Zoo. Wild. Med. **31**: 339-347.

Webb, G.J., Manolis, S.C., Sack, G.C. (1984): Cloacal sexual of hatchling crocodiles. Wild. Res. **11**: 201-202.

Yanosky, A.A. (1990): Histoire naturelle du Caiman à museau large (*Caiman latirostris*), un alligatoriné mal connu. Rev. Franc. D'aqua. **17**: 19-31.

Zayas, M.A., Rodríguez, H.A., Galoppo, G.H., Stoker, C., Durando, M., Luque, E.H., Muñoz-de-Toro, M. (2011): Hematology and blood biochemistry of young healthy broad-snouted caimans (*Caiman latirostris*). J. Herp. **45**: 516-524.

Acta Herpetologica 16(2): 109-121, 2021
DOI: 10.36253/a_h-10079

Bone histology of Broad-snouted Caiman *Caiman latirostris* (Crocodylia: Alligatoridae) as tool for morphophysiological inferences in Crocodylia

Paulo Braga Mascarenhas-Junior[1,2,3,6,*], Luis Antonio Bochetti Bassetti[4], Juliana Manso Sayão[5,6]

[1] *Laboratório Interdisciplinar de Anfíbios e Répteis, Universidade Federal Rural de Pernambuco (UFRPE), Recife, Pernambuco, Brazil*
[2] *Programa de Pós-Graduação em Biologia Animal, Universidade Federal de Pernambuco, Recife, Pernambuco, Brazil*
[3] *Laboratório de Herpetologia, Universidade Federal de Pernambuco (UFPE), Recife, Pernambuco, Brazil*
[4] *Laboratório de Ecologia Isotópica – CENA/USP, Piracicaba, São Paulo, Brazil*
[5] *Museu Nacional do Rio de Janeiro, Universidade Federal do Rio de Janeiro, Rio de Janeiro, Rio de Janeiro, Brazil*
[6] *Centro Acadêmico de Vitória (CAV), Universidade Federal de Pernambuco, Vitória de Santo Antão, Pernambuco, Brazil*
**Corresponding author.* E-mail:paulobragam16@gmail.com

Submitted on: 2020, 30th November; Revised on: 2021, 14th October; Accepted on: 2021, 26th October
Editor: Fabio M. Guarino

Abstract. Bone histology is an important tool for the interpretation of life patterns in animals of the past and extant fauna. The crocodylians have been studied as important inferential models for morphophysiological characteristics. We aimed to characterize the osteohistology of captive *Caiman latirostris*, identifying its microanatomy related to growth rates, ontogeny, and environmental conditions. We analyzed five pairs of humeri (proximal elements of the appendicular skeleton) and ribs (axial skeleton) of females' caiman. Ribs showed, in general, woven-fibered tissues, with low vascularization and parallel-fibered bone and many resorption and erosion cavities. It presented lines of arrested growth (LAGs) in three individuals, without skeletochronological compatibility. Humeri showed a gradient of woven-fibered to parallel-fibered and lamellar-zonal bone as the individuals aging. We observed compacted coarse cancellous bone (CCCB) and a higher number of LAGs in older specimens. Ribs remodel faster than humerus, showing an intra-individual histovariability. The humeri indicated an evident growth pattern with different ontogeny stages and growth rates in different ages. Fast-growing tissues are uncommon in crocodylians, but basal metabolism and optimal growth conditions can lead to this. Bone histology of *C. latirostris* shows patterns that can be used as inferential models for extant and extinct groups, but we encourage further studies for a better understanding, under different environmental conditions, such as temperature and food availability.

Keywords. Crocodylians, growth rate, ontogeny, osteohistology.

INTRODUCTION

The order Crocodylia is a monophyletic group of animals widely distributed in tropical regions, divided into three families: Alligatoridae, Crocodylidae, and Gavialidae (Zug, Vitt and Caldwell, 2001). They have great ecological importance within the ecosystems where they are inserted, as in the control of food chains (Fernández-Fernández, Arias and Khazan, 2015) and supply of nutrients from the aquatic environment (Fittkau, 1973), besides their economic relevance through meat and skin trade (Caldwell, 2017).

In South America, Broad-snouted Caiman *(Caiman latirostris* Daudin, 1801) is one of the most abundant species of Alligatoridae family, especially in Brazilian territory (Coutinho et al., 2013). It is considered as a medium-sized crocodylian with records of up to three and a half meters, although free-living specimens hard-

ISSN 1827-9635 (print)
ISSN 1827-9643 (online)

www.fupress.com/ah

ly exceed two and a half meters (Verdade, Larriera and Piña, 2010). It is commonly found in lentic freshwater ecosystems, such as dams and ponds (Filogonio et al., 2010), and is widely adapted to anthropized environments (Mascarenhas Júnior, Santos and Correia, 2018; Mascarenhas-Junior et al., 2020). It presents opportunistic and generalist feeding behavior, preying from invertebrates to fish, testudines, and small mammals (Diefenbach 1988; Melo, 2002). Its meat and skin have great commercial value, with its rearing being allowed for economic purposes, especially in the closed systems in Brazil (farming) and in ranching programs in Argentina (Coutinho et al., 2013).

As it is a well-known species, *C. latirostris* has an important potential for interpretive and inferential studies, especially in understand past species conditions. Knowledge at microscopic level of bone structures of crocodylians is an important tool for biological, behavioral, evolutionary, and ecological inferences through ontogenetic stages (Chinsamy, Codorniú and Chiappe, 2009). Due to physiological and morphological similarities between fossil and extant crocodylian taxa, the later are widely used as inferential histological models for past groups (Storrs, 1993; Andrade and Sayão, 2014; Woodward, Horner and Farlow, 2014; Sayão et al., 2016, Company and Pereda-Suberbiola, 2017). To understand the microstructural information of a fossilized bone, for example, a series of analyzes of comparative structures in existing organisms through osteohistology are necessary (Woodward, Horner and Farlow, 2014).

The histological methods of inference are complementary to the traditional models of morphological descriptions (Sayão et al., 2016), as the bone structure consists of biomineralized tissue, formed by deposition of hydroxyapatite and crystalline calcium phosphate, and its inner region consists of bone cells known as osteocytes and various blood and lymph canals (Andrade and Sayão, 2014). After death, all organic compounds are decomposed, the inorganic part is fossilized, and the shape of microstructures is preserved (Ricqlès, Horner and Padian, 1998), allowing their interpretation even in extinct organisms. However, although we can infer on the natural history of extinct groups with analyzes on extant crocodylians, individual skeletal variations may affect generalizations. Factors such as unfamiliarity of environmental influences, bone resorption and remodeling during growth can interfere in a determination of a pattern (Hutton, 1986).

Broad-Snouted Caiman is one of the extant species of Caimaninae subfamily, originally from the Cenozoic period (Brochu, 2010). Osteohistological information serving as inferential tool on the morphology, physiology, and environmental stresses in Caimaninae are still incipient, restricted to data of *C. yacare* (Andrade et al., 2018). Therefore, we aim to aggregate and refine information on microanatomical bone tendencies in Crocodylia by using bone elements from specimens of *C. latirostris* as a model for deducting structural responses to morphological, physiological, ontogenetic, and environmental questions.

MATERIAL AND METHODS

Sample study

Here we used skeletal elements of *C. latirostris*, kept in captivity and then slaughtered for commercial purposes. They were supplied by the Aruman Slaughterhouse Ltd, located in the municipality of Porto Feliz, São Paulo State, Brazil.

The slaughterhouse donated bone elements from ten females according to the availability, and we selected pairs from one to six years old (except for five years old specimens), totaling five pairs of different ages. All caimans were slaughtered in the same period and had their body mass weighted at slaughter, ranging from 6.99 kg to 21.35 kg. The individual classification of each specimen follows the control protocols used by the slaughterhouse (Table 1).

Like other crocodylians, *C. latirostris* exhibits temperature-dependent for sex determination. In captivity, eggs are generally incubated at temperatures ranging from 28 ºC to 34 ºC, to avoid embryonic death. For safety, the hatchery's incubation chamber in the caiman farm is adjusted to maintain constant temperature of 31 ºC, making 100% of females in its production (Parachú-Marcó et al., 2017, Simoncini et al., 2019).

Caiman farming

In the rearing pens, specimens were fed daily until reach two years old and three times a week at the beginning of the third year of life. Pens were formed by water tanks, dry areas, and rooftops, functioning as greenhouses for thermal retention and accelerating the growth of animals. Each pen has a total area of 7x5 m, of which 14 m² meters are dry and 21 m² meters are wet, with 80 cm deep pools. The walls measure 1.20 m from the surface of the tanks and the dry floor.

Abiotic data

We obtained the minimum and maximum daily temperatures of Porto Feliz city during the years that specimens lived in the rearing pens from data obtained from the National Meteorological Institute (INMET). We categorized temperatures considering each year of the animal's life as absolute minimum; average minimum; average; average maximum; and absolute average. We note that temperatures tend to be higher in the rearing pens for the use of greenhouses to retain heat and opti-

Table 1. Age, weight and morphometric data of the *Caiman latirostris* specimens from the Aruman Slaughterhouse Ltd. used in this study. IDnum = identification number; IDlabel = identification label; Humerus and Rib: L = length (mm); D = diameter (mm); S = Lenght of the sectioned sample.

IDnum	IDlabel	Age (year)	Weight (Kg)	Humerus			Rib		
				L	D	S	L	D	S
1	3VD4E259	6	15.08	84.07	9.20	6.40	111.65	5.65	6.71
2	3VD4E239	6	21.36	92.11	10.63	6.51	123.57	6.38	6.82
3	5VD2D348	4	19.17	87.54	8.84	6.80	122.84	5.38	7.15
4	5VD6D467	4	12.62	81.98	9.75	6.23	94.50	5.58	6.16
5	6VD3D568	3	10.00	72.56	8.66	4.23	105.62	5.39	6.39
6	6VD3D237	3	10.80	69.14	7.93	4.47	129.82	5.92	6.32
7	7VD5E248	2	8.49	70.55	8.02	4.51	105.43	6.66	5.52
8	7VD5D479	2	7.12	64.12	8.25	5.67	109.05	5.86	6.87
9	8VD7D9	1	6.99	67.49	7.27	3.83	118.90	5.24	5.11
10	8VD2E345	1	7.31	64.85	7.93	4.76	105.91	5.24	4.50

mize animal growth, especially in the hottest periods of the year (Sarkis-Gonçalves et al., 2001).

Inside greenhouses, the temperature is not constant, forming microclimates in different areas, such as on the dry floor, on the surface, and at the bottom of the water tanks. To determine the temperatures estimated in these three microhabitats, we used the study by Fincatti and Verdade (2002) as reference for presenting similar rearing pens to those applied by the caiman farm in Porto Feliz City. We performed temperature estimates for this study based on the difference between the averages measured by Fincatti and Verdade (2002) in the rearing pens and the approximate local temperature of the external environment, based on data from INMET (2018).

The difference between the three microclimates (dry area, tank surface, and tank bottom) and the external environment, considering the physical conditions of the rearing pens, ranges in approximately 8 °C, 10 °C, and 10 °C in the absolute minimum data; 8 °C, 10 °C, and 9 °C in the average minimum data; 9 °C, 4 °C, and 0.1 °C in the maximum averages; and 14 °C, 11 °C, and 0.4 °C in the absolute maximum temperatures (Fincatti and Verdade, 2002) (Available in supplementary material). Each same age pair of individuals were subjected to different temperature variations, considering that some of them spent more time in the farm for being older.

Bone elements

We selected 20 bones, one axial (rib) and one appendicular (humerus) element of each specimen, which we removed from the same anatomical position (Fig. 1). We measured each bone according to its length, diameter, and the length of the sample used. We defined rib length by the distance between proximal and distal portions.

The humeri presented maximum length and diameter ranging between 64.12 mm and 103.34 mm and 7.27 mm and 11.36 mm, respectively. The ribs indicated length ranging between 94.5 mm and 129.82 mm and diameter gradient ranging between 5.24 mm and 8.01 mm. The average length of the sectioned sample were 5.35 mm and 6.08 mm for humerus and rib, respectively (Table 1).

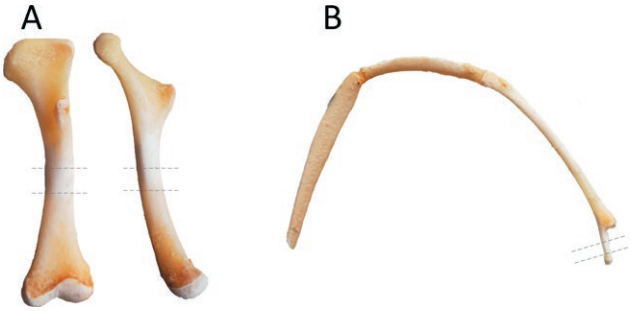

Fig. 1. Bone elements selected for osteohistological description. Section location highlighted between dashed lines. A: Humerus; B: Rib.

Sample preparation

We prepared all the material in the Laboratory of Paleobiology and Microstructures of the Academic Center of Vitória (CAV), advanced campus of Federal University of Pernambuco (UFPE).

For preparation of histological slides, we performed thin sections from the medial regions of the bone diaphysis (Fig. 1), using standard osteohistological techniques (Chinsamy and Raath, 1992; Lamm, 2013). Sampled portions were removed using a Dremel 400 rotary tool, embedded in epoxy clear resin RESAPOL T-208 and catalyzed with BUTANOX M50, using a ratio of 1 mL of catalyst for every 100 mL of resin. The samples were adhered to microscopy slides with glue and Epoxy Araldite hardener. The blocks were roughed and polished using a metallographic polishing machine (ARAPOL VV) with Arotec abrasive paper of increasing grit size (grain sizes 60/ P60, 120/P120,

320/P400, 1200/P2500) until a final thickness of 30 to 60 μm was reached.

Analysis of histological material

We analyzed the bone sections using an AxioImager M2 transmitted and polarized light microscope equipped with AxioCam digital sight camera. Inferences and descriptions followed the study by Francillon-Vieillot et al. (1990). We selected all the structures of interest observable in sections of the bone cortex. We evaluated humeri together in pairs of the same age for presenting similarities between the observed patterns. Ribs were not described in pairs for not presenting microanatomical similarities between same-aged individuals. Images of all histological sections are available in the supplementary material.

Growth curve

Older specimens presented lines of arrested growth (LAGs), enabling to estimate the initial growth curves of these animals based on the distances between lines and the medullary cavity. We also calculated the artithmetic means of distances between LAGs.

Data analysis

For the lack of information on animal size, relationships between specimens were tested according to age, weight, humerus lengths, and rib length. Notably, we tested the significance of the bivariate Pearson's correlation coefficient (r_P) between all the possible pairs. Analyzes were performed using the BioStat 5.9.8 software. The level of significance was set 0.05.

RESULTS

We observed a significant positive correlation between caimans' weight and humerus length (r_P = 0.962; t-test: t = 9.897; df = 8; P <0.001). On the other hand, we did not observe this relationship between weight and rib length (r_P = 0.396; t-test: t = 1.221; df = 8; P = 0.257) and between humerus and rib lengths (r_P = 0.192; t-test: t = 0.552; df = 8; P = 0.596).

Humeri

One-year-old specimens: we observed a highly vascularized cortex, mainly on endosteal portion, with presence of woven-fibered tissue. Anastomosed vascular canals have a reticular pattern, with the presence of simple longitudinal canals and primary osteons distributed throughout the cortex, forming a fibrolamellar bone (Fig. 2A).

Two-year-old specimens: the bone cortex of specimen 8 indicated the presence of fibrolamellar complex. At the endosteal level it shows a woven-fibered bone followed by a lower vascularized transition zone of parallel-fibered tissue towards the subperiosteal region (Fig. 2 B). We could observe a similar pattern of decreased vascularization in the medullary-cortex direction in specimen 7, with evidence of secondary lamellar tissue in perimedullary portion (Fig. 3 A), woven-fibered and parallel-fibered bone at inner the cortex. Simple and anastomosed canals are found inside the cortex, with the presence of primary osteons throughout the cortex and opening towards the periosteum (Fig. 2 B).

Three-year-old specimens: we observed moderate vascularization in the matrix, with mostly simple and few anastomosed canals, presenting longitudinal and reticular patterns and primary osteons (Figs. 2 C, 3 B). We noticed an anisotropic tissue in perimedullary portion, indicating secondary remodeling bone with the presence of a compacted coarse cancellous bone (CCCB). We also observed parallel-fibered and woven-fibered in medial (Fig. 3 B) and parallel-fibered in endosteal portions of the cortex (Fig. 2 C).

Four-year-old specimens: perimedullary portion of both individuals presented remodeling bone, with CCCB in specimen 4 (Fig. 3 C) and lamellar remodeling tissue in specimen 3 (Fig. 3 D), both with mineral erosion cavities, opening to medullary cavity in specimen 4. Also, in medullary-periosteum direction, both bones presented a decrease of primary osteons and vascularization, woven-fibered tissue in medial portion of matrix and parallel-fibered tissue in periosteal region (Fig. 2 D), with an erosion cavity in specimen 3 (Figs.2 E,3 D). We observed simple and anastomosed vascular canals pattern in both samples and plexiform canals in specimen 3 (Fig. 2 F). The most external portion of both bones presented LAGs (three in specimen 4, Fig. 2 D, and two in specimen 3).

Six-year-old specimens: both specimens 1 and 2 presented remodeling bone in perimedullary portion (lamellar in specimen 2 and CCCB in specimen 1, Fig. 3 E). We observed woven-fibered and parallel-fibered tissue (Figure 2 G), besides primary osteons throughout the cortex (Fig. 2 H), with simple vascular canals and reticular anastomoses within the matrix and low vascularization in periosteal portion. In addition, we observed four LAGs in specimen 2 (Fig. 2 G) and three in specimen 1.

Ribs

Specimen 10 (one-year-old): cortex is composed of woven-fibered tissue low vascularized, with few simple

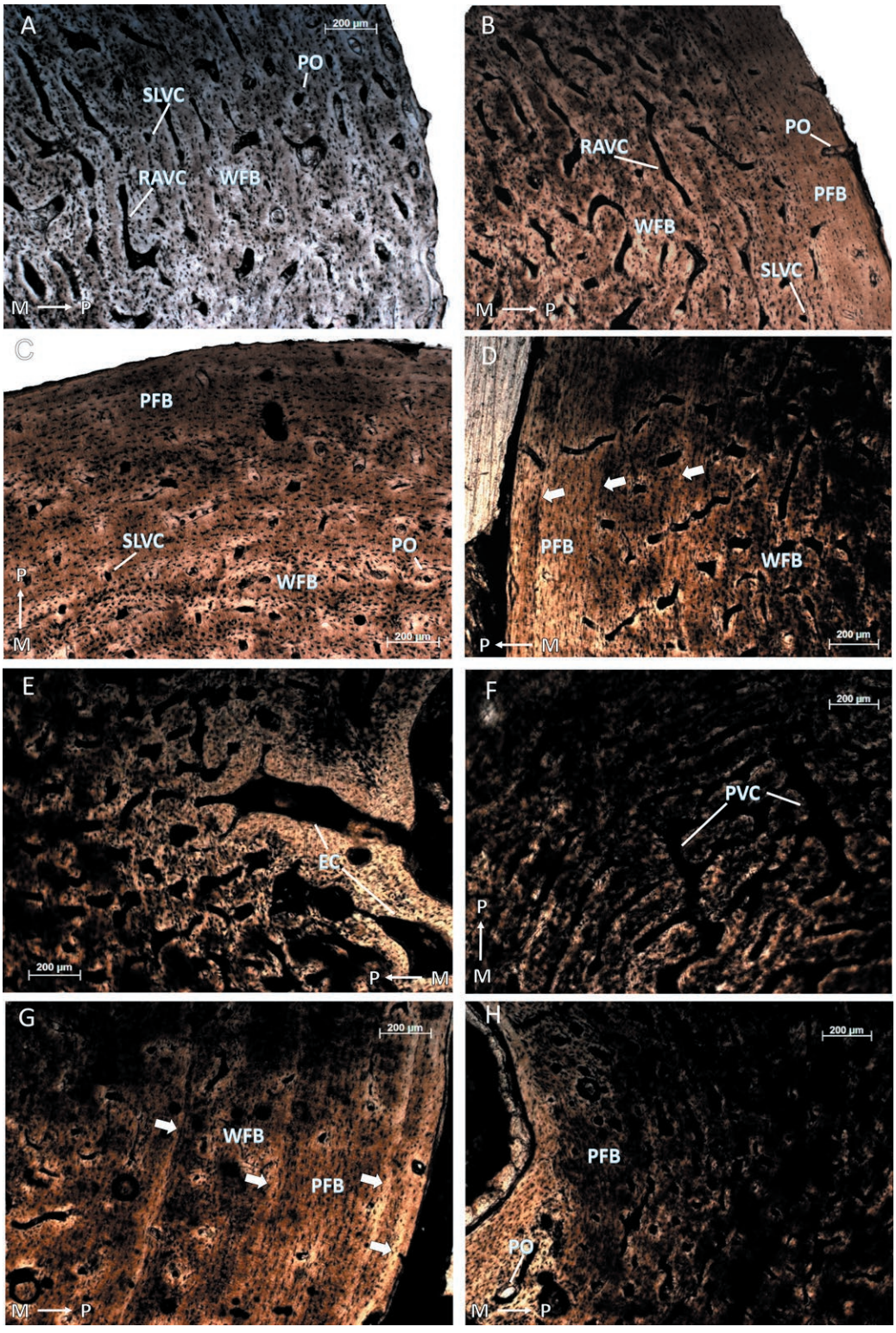

Fig. 2. Histology under transmitted light of humeri of *Caiman latirostris* specimens in captivity slaughtered in a rearing pen in the municipality of Porto Feliz, São Paulo. The specimens were one year old (A), two years old (B), three years old (C), four years old (D, E, and F), and six years old (G and H) at the time of slaughter. EC: erosion cavity; M: medullary portion; P: periosteal portion; PFB: parallel-fibered bone; PO: primary osteon; PVC: plexiform vascular canal; RAVC: reticular anastomosing vascular canal; SLVC: simple longitudinal vascular canal; WFB: woven-fibered bone. White arrows show lines of arrested growth (LAGs).

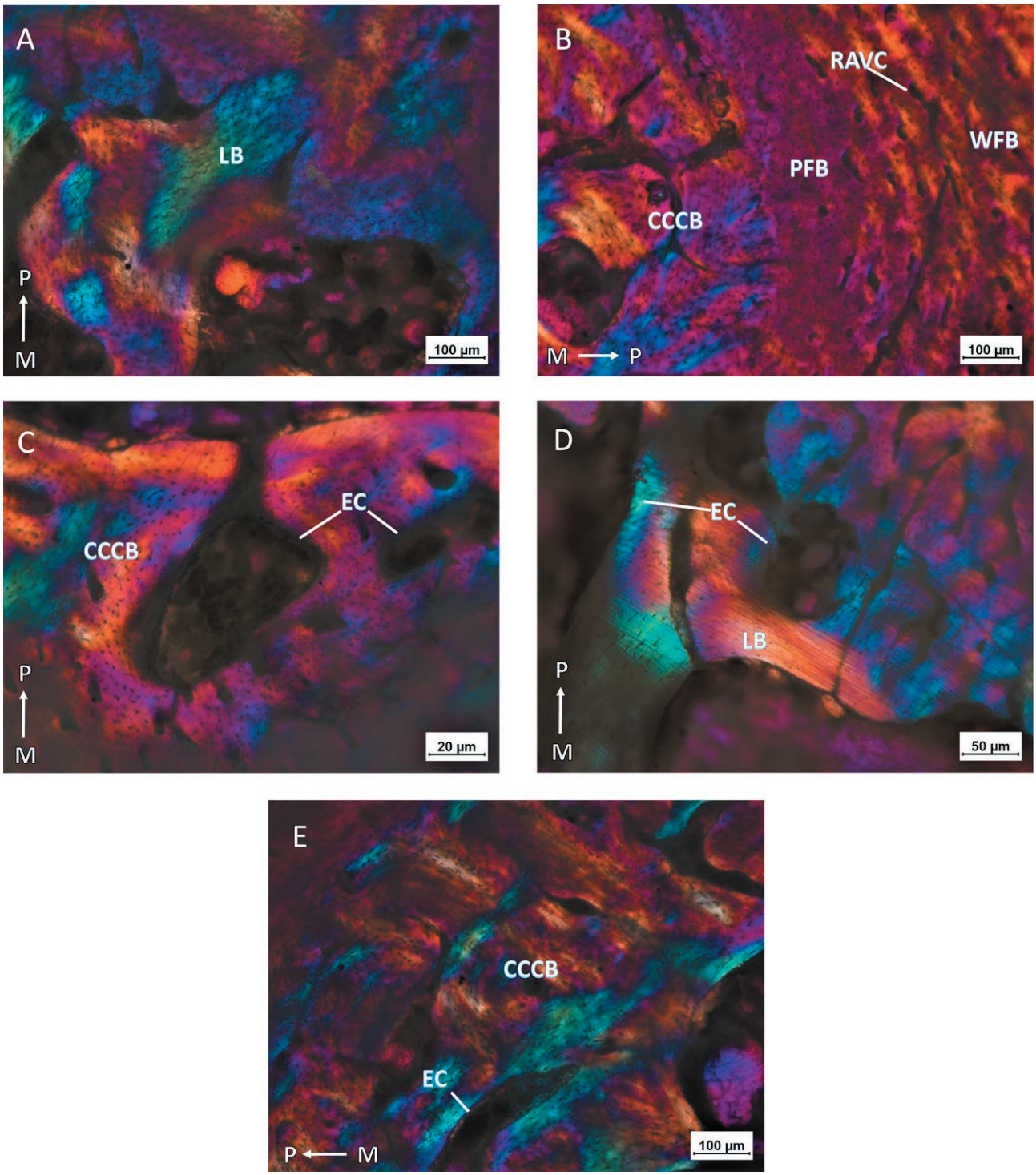

Fig. 3. Histology under polarized light combined with gypsum filter of humeri of *Caiman latirostris* specimens in captivity slaughtered in a rearing pen in the municipality of Porto Feliz, São Paulo. The specimens were two years old (A), three years old (B), four years old (C and D) and six years old (E). CCCB: compacted coarse cancellous bone; EC: erosion cavity; LB: lamellar bone; M: medullary portion; P: periosteal portion; PFB: parallel-fibered bone; RAVC: reticular anastomosing vascular canal; WFB: woven-fibered bone.

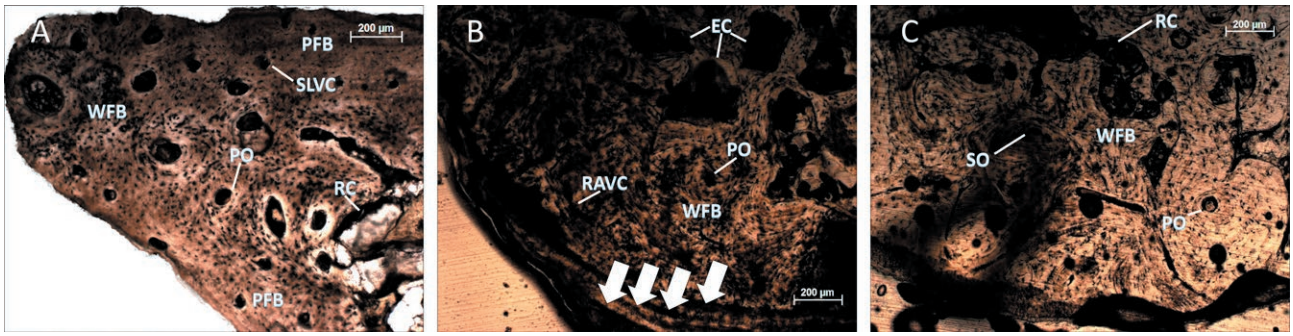

Fig. 4. Rib histology under transmitted light of three specimens of *Caiman latirostris* in captivity slaughtered in a rearing pen in the municipality of Porto Feliz, São Paulo. The individuals were two (A), three (B) and four (B) years old at the time of slaughter. EC: erosion cavity; PFB: parallel-fibered bone; PO: primary osteon; RAVC: reticular anastomosing vascular canal; RC: resorption cavity; SLVC: simple longitudinal vascular canal; SO: secondary osteon; WFB: woven-fibered bone. White arrows indicate lines of arrested growth (LAGs).

and anastomosed vascular canals, and few primary osteons. Large resorption cavities appear in the endosteal bone.

Specimen 9 (one-year-old): the tissue is predominantly woven-fibered, with a matrix vascularized mainly through simple canals and presenting primary osteons. Within the cortex, we found secondary osteons. Resorption cavities are also visible.

Specimen 8 (two-years-old): woven-fibered bone is observed at endosteal level and parallel-fibered bone evidenced in the periosteal layer, with simple longitudinal vascular canals presenting primary osteons. Resorption cavities present mainly within the cortex (Fig. 4A).

Specimen 7 (two-years-old): we found little vascularization in the cortex, presenting simple longitudinal and reticular anastomosing canals with primary osteons. The tissue exhibits woven-fibered pattern and two possible LAGs in the cortex.

Specimen 6 (three-years-old): we noticed a large amount of erosion cavities, found in the bone structure until close to the periosteal region. We evidenced woven-fibered tissue in the regions between erosion cavities, comprising most of the tissue and parallel-fibered tissue in the periosteal region. We found little vascularization, with simple longitudinal and reticular anastomosing canals and primary osteon.

Specimen 5 (three-years-old): we found tissue of woven-fibered type with moderate vascularization, presenting simple longitudinal and reticular anastomosing vascular canals, as well as primary osteons. In the region of the inner cortex, we identified several bone resorption cavities. In one of the periosteal portions, we identified three LAGs.

Specimen 4 (four-years-old): we found woven-fibered tissue in this bone with moderate vascularization, presenting simple longitudinal and reticular anastomosing vascular canals. We observed primary osteons and erosion cavities. In addition, it presents four LAGs in the periosteal region (Fig. 4B).

Specimen 3 (three-years-old): cortex is composed of woven-fibered tissue full of resorption cavities, comprising most of the bone. Vascularization is low, composed by primary osteons and simple longitudinal vascular canals.

Specimen 2 (six-years-old): presence of several bone resorption cavities with woven-fibered bone. The cortex is poorly vascularized, with small amounts of simple longitudinal and reticular anastomosing vascular canals and primary osteons.

Specimen 1 (six-years-old): primary and secondary osteons compose the cortex. Vascularization is low with simple longitudinal and reticular anastomosing canals. Bone resorption cavities concentrated endosteal region and woven-fibered tissue is present within the cortex (Fig. 4C).

Distance between lines of arrested growth

LAGs are present only in older specimens. We calculated distances between intervals among lines, as well as the total thickness of the cortex. The distances between the medullary cavity and periosteum ranged between 8,040 µm in specimen 3 and 9,830 µm in specimen 2. The minimum and maximum distances observed between LAGs ranged from 105 µm to 475 µm. The average spacing between LAGs was 282.2µm, ranging between 35 µm from the first to the second LAGs in specimen 1 and 475 µm from the second to the third LAGs in the same specimen (Fig. 5).

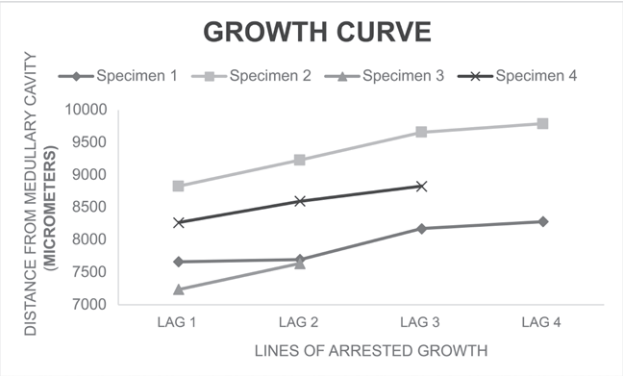

Fig. 5 Distance between highlighted lines of arrested growth (LAGs) in humeri of specimens 1, 2, 3, and 4.

DISCUSSION

In general, we observed a fast-growth pattern in ribs than in humeri. Younger specimens presented mostly woven-fibered (fast-growing) tissues in the humeri, and during their ontogenetic development, began to form parallel-fibered tissue, indicating growth stabilization. The ribs demonstrated a prevalence of woven-fibered tissue in all ages, with reduced vascularization. This information may be related to a lack of relationship in the growth trend between these bone elements, leading us to believe that the ribs may have a faster growth and remodeling than humeri (Enlow and Brown, 1958), demonstrating histovariability in axial and appendicular bone elements the same specimen (Sayão et al., 2016; Sena et al., 2018). This also corroborates what has already been described in Alligatoridae crocodylians: *Alligator* and *Caiman* (Lee, 2004; Woodward, Horner and Farlow, 2014; Andrade et al., 2018).

The ribs showed major remodeling in the medullary region, which expanded over a large part of the bone cortex, as already observed in other Crocodylomorpha (Andrade et al., 2015; Sayão et al., 2016; Sena et al., 2018). These remodeling processes can directly influence determinations by skeletochronology. Specimens 7, 5, and 4 (two, three and four years old respectively) were the only with LAGs, showing the same number of lines as its age, as found by Waskow and Mateus (2017). On the other hand, the other ribs showed no evidence of LAGs, indicating that the bone had possibly been remodeled and the lines lost during the processes of bone absorption and redeposition throughout its development. Deficiency to determine ages from axial elements has also been previously reported in the literature in both living (Hutton, 1986) and fossil specimens (Sayão et al., 2016; Sena et al., 2018). For the inconsistency in microanatomical patterns, ribs are not the most suitable elements for skeletochronology (Padian, 2011), although having already been used in skeletochronological studies in other groups of archosaurs, especially in fossils, such as Dinosauria (Gallina, 2012; Waskow and Sander, 2014; Waskow and Mateus, 2017; Woodruff, Fowler and Horner, 2017; Brum et al., 2021). Also, Waskow and Sander (2014) stated that the posteromedial side of the proximal shaft of the ribs record best growth information in osteohistological observations. It was suggested that in studies without promising results, samples were collected from distal portions of the ribs, not showing lines or other growth marks (Waskow and Sander, 2014). However, in this study all samples were collected from the proximal portions of ribs (see material and methods), and we identified LAGs in three of our samples, contradicting this idea, at least for the group under study. We did not identify significant relationship between rib length increase and animals aging, although we found association between the size of the axial element and the presence of LAGs. The three specimens that presented LAGs (specimens 4, 5, and 7) had the smallest ribs, being related to bone tissue remodeling, which had not been enough remodeled for the destruction of the lines.

The humeri showed tendencies in microanatomy and osteohistology related to animal age. The youngest caimans (10 and 9) presented a homogeneous pattern in tissue composition, being of woven-fibered type. This tissue is quite common in young specimens, with high metabolic rates and rapid growth, presenting great vascularization and primary osteons (Huttenlocker, Woodward and Hall, 2013). The presence of woven-fibered tissue with primary osteons, as already reported in crocodylians, indicate physiological strategies of rapid growth, forming a fibrolamellar complex (Ricqlès, 1983; Reid, 1984, 1990, 1997; Ricqlès, Padian and Horner, 2001; Chinsamy and Hillenius, 2004; Tumarkin-Deratizan, Vann and Dodson 2007; Woodward, Horner and Farlow, 2014; Andrade et al., 2018). This bone composition supports the hypothesis that crocodylians retain an ancestral characteristic of Archosauria (Cubo et al., 2012), evidenced in young animals.

We did not expect the presence of fibrolamellar bones in crocodylians, although it has already been identified in young specimens with optimal growth conditions in farms, constant feeding, and ideal temperature of approximately 30 °C to 33 °C (Lang, 1987; Woodward, Horner and Farlow, 2014). During the day, caimans tend to move within the pens, being exposed to the temperature ranges close to the ideal for growth (Verdade, 1995). Generally, during winter and days of lower temperatures, caimans remain in the dry areas in

sun periods and in humid areas at night for the different rates of heat accumulation between air and water, as the air is a better heat disperser than water. During summer or in periods with high temperatures, the animals will follow the opposite, preferring wet microenvironments during sun periods and the dry ones at night (Verdade et al., 1994). Despite lower temperatures, the pens have greenhouses that tend to retain heat, leaving the environment with a higher temperature in relation to the outside (Fincatti and Verdade, 2002). It is possible that, through thermal stimuli and constant feeding, individuals tend to maintain higher rates of basal metabolism, consequently accelerating their growth with longer lasting strategies of rapid growth. This fact is understandable, since crocodylians spend less energy producing heat, living with a low metabolic rate. Therefore, we assume that the physiological demand for energy, especially glucose, for the growth and maintenance of ectothermic animals is low if compared to that of endothermic carnivores, since there is no need to produce heat from this sugar to maintain temperature body. Consequently, a large part of its energy supply is invested in growth and reproduction. This result is obtained rather through predominantly behavioral mechanisms than physiological mechanisms by seeking the ideal temperature range for their metabolic activities, which in general are eight to ten-fold lower than that of endothermic animals, somehow explaining their dependence on room temperature (Smith, Robertson and Davies, 1978; Staton, 1988; Silva, 2000).

Specimens 8 and 7, despite being the same age (two years old), presented differences in metabolic growth strategies, observed in the bone. During animal aging, the tendency is the reduction of growth rate, with a transition between tissues that demonstrate fast-growing metabolism strategies (woven-fibered bone) and slow-growing tissues (Ricqlès, Padian and Horner, 2003; Huttenlocker, Woodward and Hall, 2013). With maturation, we observed parallel-fibered tissue, especially in the periosteal region, and secondary remodeling bone, such as CCCB and lamellar bone in endosteal portion. There is a gradient associated with age which reflects the start of slow-growth strategy, although without finalization of definitive bone growth, evidenced by the absence of an External Fundamental System and the opening of primary osteons in the cortex towards the periosteum (Ricqlès et al., 2003; Woodward et al., 2011; Andrade et al., 2018). The decreasing presence of fibrolamellar complexes implies the reduce of fast-growth rates, a baseline characteristic of tetrapods in general (Woodward, Horner and Farlow, 2014).

In some specimens CCCB in response of secondarily remodeling processes can be observed, mainly in older individuals or breeding females (Hutton, 1986; Schweitzer et al., 2007). In female crocodylians, bone remodeling can occur faster than in males due to calcium mobilization for the formation of eggshells (Hutton, 1986). The beginning of the reproductive stage in the life of crocodylians is related to their growth, also influenced by temperature, and feeding. Females of *C. latirostris* reaches sexual maturity with approximately 68 centimeters of snout-vent length (Leiva et al., 2019) or between four and five years of age in captivity (Verdade et al., 2003). In commercial farms, caimans are maintained in greenhouses under high temperatures to reduce their time for slaughter and sexual maturation. We observed a high remodeling bone in females over 10 kg (three years old), which can be an important indicator of reproductive stage beginning. Klein, Scheyer and Tütken (2009) suggest that captive females have great absorption in long bones due to mineral mobilization to form eggshells or due to nutritional deficiencies, and, associated with secondary remodeling bone, the cyclic growth marks may be destroyed. For free-living animals, Schweitzer et al. (2007) stated that long bones in wild female *Alligator mississipiensis* do not show major remodeling activities, which may indicate histovariability between wild and captive animals, even in similar ontogenetic stages.

As in other reptiles, LAGs provide clues to both skeletochronology and the growth rates of specimens on an annual basis (Castanet et al., 1993; Guarino et al., 2020). These thin lines that occur parallel to the periosteum margin (Wilson and Chin, 2014) are observed in greater quantities with increasing age. According to Castanet et al. (1993), the deposition of LAGs occurs annually in crocodylians, regardless of food, temperature, or photoperiod. Tucker (1997) suggested that the appearance of LAGs is associated with winter periods (food shortages and decreased metabolism). In this study, specimens that were in the first, second, and third years of life did not present evident lines and specimens that were in the fourth and sixth years of life presented underestimated numbers of growth marks regarding age.

Considering the deposition of one LAG per year, we could identify the growth speed of animals that showed these marks. Four-year-old specimens had a relatively similar spacing between LAGs, which may indicate a similar growth rate between the first and second years. The third line of Specimen 4 is close to the periosteum, indicating that the animal died before formation of the fourth LAG. On the other hand, six-year-olds had different intervals between lines. Specimen 2 presented a large

spacing between the first and second LAG and between the second and third. Between the third and fourth, the distance reduced, leading us to believe that the caiman grew at high rates between the first three years and had a decline in the growth curve in the fourth year. Specimen 1 had little spacing between the first and second LAG, with a larger distance between the second and third one. It also had a reduction between the third and fourth lines, probably indicating a low growth rate until reaching the third year of life, growing quickly until reaching the fourth year, in which apposition decreased again. Both specimens 1 and 2 may have been slaughtered before the formation of the fifth line. These differences in growth patterns can be related both to the intrinsic physiological conditions that influence growth and external factors, such as dominance in the competition for food and the selection of thermal ranges in the pens (Hutton, 1986; Verdade et al., 1994).

Scarcity of osteohistological studies conducted with a significant sample of specimens and taxa hinders the confirmation that LAGs are necessarily formed annually in crocodylians. Based on our observations, it is likely that this concept is not consistent with the patterns observed in captive specimens of living taxa or even with those of the genus *Caiman* or of the species *C. latirostris*. In general, studies that performed osteohistological interpretations in extant crocodylians are restricted to less than ten specimens sampled (Schweitzer et al., 2007; Woodward, Horner and Farlow, 2014; Andrade et al., 2018), the only exception was a study conducted with 30 different individuals of *A. mississipiensis* (Woodward, Horner and Farlow, 2011). Researches with larger samples are still scarce (Hutton, 1986; Tumarkin-Deratzian, Vann and Dodson, 2007) and must be incentivized. So far, any other research has been performed with crocodylians from the subfamily Caimaninae, which elucidates the incipience of concrete data on the pattern of growth marks in crocodylians.

ACKNOWLEDGEMENTS

This project has a license from the Environmental Company of the State of São Paulo (CETESB) for the effluent, number 61000099. The Aruman slaughterhouse is authorized by the Secretariat of Environment for the use and management of *C. latirostris* through license number 000001409, with process number 000762, 2016. All the material used in this research was delivered with the issuance of invoice number 000000097. ICMBio authorization was also issued to conduct this work, legally supported under license number 59048-1.

The authors would like to thank Dr. Mariana Sena, Dr. Rafael Araújo, Esaú Victor, and Haggy Rodrigues for helping with the first processing of material for this research. Dr. José Adauto de Souza Neto for the access to petrographic microscope at Laboratório de Geoquímica Aplicada ao Petróleo (LGAP) and Dr. Mariana Sena for helping in polarized microscope imaging. To Dr. Holly Woodward (Oklahoma State University) and an anonymous reviewer for the suggestions and questions that improved the final version of this manuscript. We would like to express our gratitude to the Aruman Slaughterhouse, responsible for donating the bone material that enabled this work. This project was partially funded by the National Council for Scientific and Technological Development - CNPq (proc. N. # 311715/2017-6 and 314222/2020-0 to JMS) and Coordination for the Improvement of Higher Education Personnel - CAPES (MsC fellowship to PBMJ).

REFERENCES

Andrade, R.C.L.P., Bantim, R.A.M., Lima, F.J., Campos, L.S., Eleutério, L.H.S., Sayão, J.M. (2015): New data about the presence and absence of the external fundamental system in archosaurs. Cad. Cult. Cienc. **14**: 200-211.

Andrade, R.C.L.P., Sayão, J.M. (2014): Paleohistology and lifestyle inferences of a dyrosaurid (Archosauria: Crocodylomorpha) from Paraíba Basin (Northeastern Brazil). PloS one **9**: 1:11.

Andrade, R.C.L.P., Sena, M.V.A., Araújo, E.V., Bantim, R.A.M., Riff, D., Sayão, J.M. (2018): Osteohistological study on both fossil and living Caimaninae (Crocodyliformes, Crocodylia) from South America and preliminary comments on growth physiology and ecology. Hist. Biol. **32**: 346-355.

Brochu, C.A. (2010): A new alligatorid from the lower Eocene Green River Formation of Wyoming and the origin of caimans J. Vert. Paleontol. **30**: 1109-1126.

Caldwell, J. (2017): World trade in crocodilian skins 2013-2015.The Louisiana Alligator Advisory Council, Louisiana, USA.

Castanet, J., Francillon-Vieillot, H., Meunier, F.J., Ricqlès, A. de (1993): Bone and individual aging. In: Bone, Vol. 7, pp. 245-283. Hall, B.K., Ed, CRC Press, Boca Raton (FL).

Chinsamy, A., Codorniú, L., Chiappe, L. (2009): Palaeobiological implications of the bone histology of *Pterodaustro guinazui*. Anat. Rec.**292**: 1462-1477.

Chinsamy, A., Hillenius, W.J. (2004): Physiology of nonavian dinosaurs. In: The dinosauria, pp. 643-659.

Weishampel, D.B., Dodson, P., Osmólska H. Eds. University of California Press, Berkeley.

Chinsamy, A., Raath, M.A. (1992): Preparation of fossil bone for histological examination. Paleontol. Africana **29**: 39-44.

Company, J., Pereda-Suberbiola, X. (2017): Long bone histology of a eusuchian crocodyliform from the Upper Cretaceous of Spain: Implications for growth strategy in extinct crocodiles Cretac. Res. **72**: 1-7.

Coutinho, M.E., Marioni, B., Farias, I.P., Verdade, L.M., Bassetti, L.A.B., Mendonça, S.H.S.T., Vieira, T.Q., Magnusson, W.E., Campos, Z. (2013): Avaliação do risco de extinção do jacaré-de-papo-amarelo *Caiman latirostris* (Daudin, 1802). Brasil Biodiversidade Brasileira **3**: 4-12.

Cubo, J., Le Ro, N., Martinez-Maza, C., Montes, L. (2012): Paleohistological estimation of bone growth rate in extinct archosaurs. Palaeobiol. **38**: 335-349.

Diefenbach, C.O.D.C. (1988): Thermal and feeding relations of *Caiman latirostris* (Crocodylia: Reptilia). Comp. Biochem. Phys. Part A **89**: 149-155.

Enlow, D.H. (1969): The bone of reptiles. In: Biology of the Reptilia, pp. 45-80,. Gans, C., Bellairs, A.d'A., Parsons, T.S., Eds, Academic Press, New York.

Enlow, D.H., Brown, S.O. (1958): A comparative histological study of fossil and recent bone tissues. Part III. Tex. J. Sci. **10**: 187-230.

Fernández-Fernández, L.M., Arias, M., Khazan, E.S. (2015): Analysis of population density and distribution of spectacled caiman (*Caiman crocodilus*) in Caño Palma, northeast Costa Rica. Herpetol. Cons. Biol. **10**: 959-968.

Filogonio, R., Assis, V.B., Passos, L.F., Coutinho, M.E. (2010): Distribution of populations of broad-snouted caiman (*Caiman latirostris*, Daudin 1802, Alligatoridae) in the São Francisco River basin, Brazil. Brazil. J. Biol. **70**: 961-968.

Fincatti, C.R., Verdade, L.M. (2002): Variação térmica microclimática em estufa plástica e sua aplicação para crescimento de filhotes de jacarés. In: Conservação e Manejo de Jacarés e Crocodilos da América Latina, Piracicaba: Fundação de Estudos Agrários Luiz de Queiroz **1**: 75-83.

Fittkau, E.J. (1973): Crocodiles and the nutrient metabolism of Amazonian waters. Amazoniana **4**: 103-133.

Francillon-Vieillot, H., Buffrénil, V., Castanet, J., Meunier, G.F.J. (1990)**:** Microstructure and mineralization of vertebrate skeletal tissues. In: Skeletal Biomineralization Patterns, Processes and Evolutionary Trends, pp. 471-458. Carter, J.G., Ed., Van Nostrand Reinhold, New York.

Gallina, P.A. (2012): Histología ósea del titanosaurio *Bonitasaura salgadoi* (Dinosauria: Sauropoda) del Cretácico superior de Patagonia. Ameghiniana **49**: 289-302.

Guarino, F.M, Nocera, F.D., Pollaro, F., Galiero, G., Iaccarino, D., Iovino, D., Mezzasalma, M., Petraccioli, A., Odierna, G., Maio, N, (2020): Skeletochronology, age at maturity and cause of mortality of loggerhead sea turtles *Caretta caretta* stranded along the beaches of Campania (south-western Italy, western Mediterranean Sea). Herpetozoa **33**: 39–51.

Huttenlocker, A.K., Woodward, H.N., Hall, B.K. (2013): The biology of bone. In: Bone histology of fossil tetrapods, pp. 13-34, Padian, K., Lamm, E., Eds, University of California Press, Berkeley.

Hutton, J.M. (1986): Age determination of living Nile crocodiles from the cortical stratification of bone. Copeia, **1986**: 332-341.

INMET- Instituto Nacional de Meteorologia. (2018): Dados históricos: Banco de Dados Meteorológicos para Ensino e Pesquisa. Brasília. Available on: <*http://www.inmet.gov.br/portal/index.php?r=bdmep/bdmep*>. [*Accessed 3 October 2018*], 2018.

Klein, N., Scheyer, T., Tütken, T. (2009): Skeletochronology and isotopic analysis of a captive individual of *Alligator mississippiensis* Daudin, 1802. Foss. Rec. **12**: 121-131.

Lamm, E.T. (2013**)**: Preparation and sectioning of specimens. In: Bone histology of fossil tetrapods: advancing methods, analysis, and interpretation, pp 55-160. Padian, K., Lamm, E., Eds, University of California Press, Berkeley.

Lang, J.W. (1987): Crocodilian thermal selection. In: Wildlife management: crocodiles and alligators, pp 301-317. Webb, G.J.W., Manolis, S.C., White, P.J., Eds. Surrey Beautty and Sons press, Sydney.

Lee, A.H. (2004): Histological organization and its relationship to function in the femur of *Alligator mississippiensis*. J. Anat. **204**: 197-207.

Leiva, P.M.D.L., Simoncini, M.S., Portelinha, T.C.G., Larriera, A. and Piña, C.I., (2019): Size of nesting female Broad-snouted Caimans (*Caiman latirostris* Daudin 1802). Braz. J. Biol. **79**: 139-143.

Mascarenhas-Junior, P.B., Santos, E.M., Moura, G.J.B., Diniz, G.T.N., Correia, J.M.S. (2020): Space-time distribution of *Caiman latirostris* (Alligatoridae) in lentic area of Atlantic Forest, northeast of Brazil. Herpetol. Notes **13**: 29-137.

Mascarenhas Júnior, P.B.M., Santos, E.M., Correia, J.M.S. (2018): Diagnóstico dos resgates de jacarés na região metropoliana do Recife, Pernambuco. Revista Ibero-Americana de Ciências Ambientais **9**: 138-145.

Melo, M.T.Q. (2002): Dieta do *Caiman latirostris* no sul do Brasil. In: La conservación y manejo de los Croco-

dylia de America Latina, Vol. 2, pp. 119-125. Verdade, L.M., Larriera, A., Eds, CN Editoria, Piracicaba (Brasil).

Padian, K. (2011): Vertebrate palaeohistology then and now: A retrospective in the light of the contributions of Armand de Ricqlès. C. R. Palevol **10**: 303-309.

Parachú-Marcó, M.V., Leiva, P.M.D.L., Iungman, J.L., Simoncini, M.S., & Piña, C.I. (2017): New evidence characterizing temperature-dependent sex determination in broad-snouted caiman, *Caiman latirostris*. Herpetol. Cons. Biol. **12**: 78-84.

Reid, R.E.H. (1984): Primary bone and dinosaurian physiology. Geol. Mag. **121**: 589-598.

Reid, R.E.H. (1990): Zonal "growth rings" in dinosaurs. Mod. Geol. **15**: 19-48.

Reid, R.E.H. (1997): How dinosaurs grew. In: The Complete Dinosaur, pp. 403-413. Brett-Surman, M.K., Holtz, T.H., Farlow, J.O., Eds. Indiana University Press, Bloomington (US).

Ricqlès, A. de, Padian, K., Horner, J.R. (2001): The bone histology of basal birds in phylogenetic and ontogenetic perspectives. In: New perspectives on the origin and early evolution of birds: proceedings of the international symposium in honor of John H. Ostrom, pp 411-426. Gauthier, J.A., Gall, L.F., Eds, Peabody Museum of Natural History, Yale University, New Haven.

Ricqlès, A. de (1983): Cyclical growth in the long limb bones of a sauropod dinosaur. Acta Paleont. Pol. **28**: 225-232.

Ricqlès, A. de, Horner, J.R., Padian, K. (1998): Growth dynamics of the hadrosaurid dinosaur *Maiasaura peeblesorum* J. Vert. Paleont. **18:** 72A.

Ricqlès, A.de, Padian, K., Horner, J.R. (2003): On the bone histology of some Triassic pseudosuchian archosaurs and related taxa. Annal. de Paléont., **89**: 67-101.

Sarkis-Gonçalves, F., Miranda-Vilela, M.P., Bassetti, L.A.B., Verdade, L.M. (2001): Manejo de jacarés-de-papo-amarelo (*Caiman latirostris*) em cativeiro. In: A produção animal na visão dos brasileiros, pp. 565-579. Matos, W.R.S., Ed. Soc. Brazil. Zoot., Piracicaba (Brazil).

Sayão, J.M., Bantim, R.A.M, Andrade, R.C.L.P., Lima, F.J., Saraiva A.A.F., Figueiredo R.G., Kellner, A.W.A. (2016): Paleohistology of *Susisuchus anatoceps* (Crocodylomorpha, Neosuchia): comments on growth strategies and lifestyle. Plos One **11**: e0155297.

Schweitzer, M.H., Elsey, R.M., Dacke, C.G., Horner, J.R., Lamm, E.T. (2007): Do egg-laying crocodilian (*Alligator mississippiensis*) archosaurs form medullary bone? Bone **40**: 1152-1158.

Sena, M.V.A., Andrade, R.C.L.P., Sayão, J.M., Oliveira, G.R. (2018): Bone microanatomy of *Pepesuchus deiseae* (Mesoeucrocodylia, Peirosauridae) reveals a mature individual from the Upper Cretaceous of Brazil. Cret. Res. **90**: 335-348.

Silva, R.G. (2000): Introdução à bioclimatologia animal. São Paulo Nobel press, São Paulo (Brazil).

Simoncini, M.S., Leiva, P.M., Piña, C.I., Cruz, F.B. (2019): Influence of temperature variation on incubation period, hatching success, sex ratio, and phenotypes in *Caiman latirostris*. J. Exp. Zool. Part A **331**: 299-307.

Smith, E.N., Robertson, S., Davies, D.G. (1978): Cutaneous blood flow during heating and cooling in the *American alligator*. Amer. J. Physiol., Regulat. Integrat. Comp. Physiol. **235**: 160-167.

Staton, M.A. (1988): Studies on the use of fats and carbohydrates in the diet of American alligators (*Alligator mississippiensis*). Thesis (Ph.D)- Graduate Faculty of the University of Georgia, Georgia, 151p.

Storrs, G.W. (1993): Function and phylogeny in sauropterygian (Diapsida) evolution. Am, J. Sci. **293**: 63.

Tucker, A.D. (1997): Validation of skeletochronology to determine age of freshwater crocodiles (*Crocodylus johnstoni*). Mar. Freshw. Res. **48**: 343-351.

Tumarkin-Deratzian, A.R., Vann, D.R., Dodson, P. (2007): Growth and textural ageing in long bones of the American alligator *Alligator mississippiensis* (Crocodylia: Alligatoridae). Zool. J. Linnean Soc. **150**: 1-39.

Verdade, L.M. (1995): Biologia reprodutiva do jacaré-de-papo-amarelo (*Caiman latirostris*) em São Paulo, Brasil, pp. 57-79. In: Conservación y manejo de los Crocodylia de America Latina, Larriera, A. Verdade, L. M., Eds, Fundación Banco Bica, Santa Fé.

Verdade, L.M., Larriera, A., Piña, C.I. (2010): Broad-snouted caiman *Caiman latirostris*. Croc. Stat. Surv. and Cons. Act. Plan **18**: 22.

Verdade, L.M., Packer, I.U., Michelotti, F., Rangel, M.C. (1994): Thermoregulatory behavior of broad-snouted caiman (*Caiman latirostris*) under different thermal regimes. In: Memorias del IV Workshop sobre conservación y manejo del yacare overo *Caiman latirostris*, pp. 84-89. "La Región" - Fundación Banco Bica - Santo Tomé. Santa Fé, Argentina

Verdade, L.M., Sarkis-Goncalves, F., Miranda-Vilela, M.P., Bassetti, L.A.B. (2003): New record of age at sexual maturity in captivity for *Caiman latirostris* (Broad-snouted caiman). Herpetol. Rev. **34**: 225-271.

Waskow, K., Mateus, O. (2017): Dorsal rib histology of dinosaurs and a crocodylomorph from western Portugal: skeletochronological implications on age determination and life history traits. Comptes. Rendus. Palevol. **16**: 425-439.

Waskow, K., Sander, P.M. (2014): Growth record and histological variation in the dorsal ribs of *Camarasaurus* sp. (Sauropoda). J. Vert. Paleont. **34**: 852-869.

Wilson, L.E., Chin, K. (2014): Comparative osteohistology of *Hesperornis* with reference to pygoscelid penguins: the effects of climate and behaviour on avian bone microstructure. R. Soc. Open Sci. **1**: 140245.

Woodruff, D.C., Fowler D.W., Horner, J.R. (2017): A new multi-faceted framework for deciphering diplodocid ontogeny. Paleont. Electron **20**: 1-53.

Woodward, H.N., Horner, J.R., Farlow, J.O. (2011): Osteohistological evidence for determinate growth in the *American alligator*. J. Herpetol. **45**: 339-342.

Woodward, H.N., Horner, J.R., Farlow, J.O. (2014): Quantification of intraskeletal histovariability in *Alligator mississippiensis* and implications for vertebrate osteohistology. PeerJ. **2**: 1-34.

Zug, G.R., Vitt, L., Caldwell, J.P. (2001): Herpetology: an introductory biology of amphibians and reptiles. Academic press, Boston.

Acta Herpetologica 16(2): 123-128, 2021
DOI: 10.36253/a_h-10229

Is the Northern Spectacled Salamander *Salamandrina perspicillata* aposematic? A preliminary test with clay models

Giacomo Barbieri, Andrea Costa, Sebastiano Salvidio*

DISTAV, University of Genova, Corso Europa 26, I-16132 Genova, Italy
**Corresponding author.* E-mail: sebastiano.salvidio@unige.it

Submitted on: 2020, 29th December; Revised on: 2021, 11th May; Accepted on: 2021, 3rd October
Editor: Dario Ottonello

Abstract. Aposematism is a visual communication system in which bright and contrasted coloured prey warn predators about their unprofitability. The Northern Spectacled Salamander *Salamandrina perspicillata*, a small terrestrial salamander endemic to Italy, displays a uniform dark dorsal colouration and a contrasted ventral side in which a bright red colour is displayed by coiling the tail over the body. In amphibians, this behaviour, known as "*Unkenreflex*", is usually considered to be aposematic. In this study, we used realistic plasticine replicas to test this aposematic hypothesis in the Northern Spectacled Salamander. Of the 199 clay models placed in a natural habitat, 165 (83%) were recovered and 39 (24%) showed some sign of predation. The head of the models was more attacked than expected by chance (P = 0.042), suggesting that potential predators were perceiving models as real prey. However, there were no differences in the proportion of dorsal (18/83 = 22%), and ventral (21/82 = 26%) models attacked by predators. Therefore, contrary to expectations our experiment did not support the aposematic hypothesis. However, predation experiments with clay models have limitations and our results should be considered as preliminary, deserving further research to better understand the Northern Spectacled salamander prey-predator system.

Keywords. Animal replicas, plasticine, predation, salamander, *Unkenreflex*.

Many animal taxa evolved conspicuous colourations associated with different mechanisms of antipredator defence such as claws, beaks, teeth, spines, stings and a variety of toxic compounds that are actively inoculated or passively delivered to predators (Stevens, 2013; Caro and Allen, 2017). This visual communication system is known as aposematism (Steven, 2013), a widespread phenomenon that independently evolved many times in different amphibians lineages (Wells, 2007). Aposematic colourations are usually associated with a variety of toxic compounds that are produced or sequestered and stored in specialised glandular skin glands (e.g., Wells, 2007; Rojas, 2017; Demori et al., 2019). Several species of aquatic and terrestrial salamanders exhibit a variety of combinations of red, orange yellow or white marks usually displayed on brown or black backgrounds. In salamanders, conspicuous colourations are typically assumed to act as aposematic warning anti-predatory signals (e.g., Wells, 2007; Lüddecke et al., 2018). In fact, several alkaloids (e.g., tetradoxins) and other toxic compounds are isolated from the skin of newts and salamanders, reinforcing the assumption that these contrasted colourations are associated with unpalatability (e.g., Yotsu-Yamashita et al., 2007, 2017; Preissler et al., 2019).

Usually, bright colour patterns are usually displayed on the dorsal surface of amphibians. However, some salamanders are dorsally cryptic while possessing aposematic colourations on the underside. These species display their ventral bright colours by exposing the venter by coiling laterally (e.g., the Asian newt *Paramesotriton deloustali*) or coiling the tail above the body (e.g., the North American newt *Taricha rivularis* and the Alpine

ISSN 1827-9635 (print)
ISSN 1827-9643 (online)

newt *Ichthyosaura alpestris*) (see Fig. 14.30 in Wells, 2007). This latter anti-predatory behaviour is known as "*Unkenreflex*", first described in the fire-bellied toad *Bombina bombina* (Hinsche, 1926). This peculiar behaviour, i.e. exposing bright ventral colouration by arching the body, is displayed also by the two species of Spectacled salamander belonging to the genus *Salamandrina* Fitzinger, 1826: *S. perspicillata* and *S. terdigitata* (Angelini et al., 2007). However, Lanza (1967) casted doubts on the aposematic function of *Unkenreflex* in *Salamandrina*, because this genus does not possess the parotoid glands typical of many toxic salamanders, while Utzeri et al. (2005) presented some anecdotal evidence for unpalatibility. Therefore, the function of the black, white and red coloured ventral side and of the red tail of *Salamandrina* remains uncertain, although no alternative explanation has been proposed.

To better understand if the ventral colouration of *S. perspicillata* could represent an aposematic signal, we made a predation experiment by using of clay replicas representing the dorsal and ventral patterns of the focal species. Experiments using this technique are non-invasive and easy to perform in natural habitats, but problems and limitations should be also taken into consideration (Bateman et al., 2017; Rössler et al., 2018). In the present study, clay models were exposed in the species' natural habitat and predation rates on different model types compared. If the aposematic hypothesis holds true, we expected that models with a conspicuous red colouration typical of the body underside and tail would be attacked less frequently than those bearing a dark dorsal appearance.

Salamandrina perspicillata (Savi, 1821), the Northern Spectacled Salamander, is endemic to central and northern Italy (Angelini et al., 2007). This species is found from the sea level up to about 1900 m, in Mediterranean vegetation areas and in humid broadleaf woodlands (Angelini et al., 2007; Romano et al., 2009). Adults usually range from 70 to 100 mm in total length and are fully terrestrial, with the exception of gravid females that enter water bodies for spawning (Angelini et al., 2007). The dorsal colouration is characterised by a very dark or black dorsal pattern with, during the terrestrial phase, a matt appearance. On the salamander' head the presence of a characteristic whitish or yellowish mark between the eyes suggested the common species name "spectacled" (Fig. 1). The ventral surface displays a conspicuous combination of black and white in its central and anterior part, while the posterior part of the abdomen, cloaca and tail, and the inferior part of all four limbs is brightly coloured in red (Angelini et al., 2007; Fig. 1). When disturbed, *S. perspicillata* sometimes displays its conspicuous ventral colouration by coiling its tail above the body in an *Unkenreflex* posture (Lanza, 1967; Angelini et al., 2007).

The Northern Spectacled Salamander' replicas were made from plasticine, a soft material prepared from clay, wax and oil. Clay models are malleable, retain predatory marks (Kuchta, 2005; Salvidio et al., 2017) and have been used to analyse predation in relation to colour polymorphism and aposematism in amphibians (e.g., Kraemer et al., 2016; Paluh et al., 2014).

Clay models were obtained from a 3D printer template. We imported a photographic image of *S. perspicillata* in the software "Rhinoceros". The template was printed in PLA (a plastic material) with the "Wanhao Duplicator 6" printer (Supplementary Material Fig. S1). Models, possessing a total length of 79 mm, were hand painted with acrylic water-soluble red, black and white colours (Maimeri Polycolor # 220, 530 and 021, respectively). The model head, torso and tail surfaces were measure by ImageJ software (Schneider et al., 2012) giving these relative proportions: head (17.35%), torso (27,33%) and tail (55.32%).

The experiment took place, from October 26th to November 1st 2020, in North-western Italy, Province of Genova, in a mixed humid deciduous forest at about 900 m a.s.l. (44°34'00"N; 9°08'10"E). In this area the Northern Spectacled salamander is widespread along forest streams and in the leaf litter. During autumn, Northern Spectacled Salamanders can be found active on the forest floor also during daytime (Salvidio et al., 2012). Models showing the ventral or dorsal coloration were alternatively placed every 2 m on stones, fallen branches and moss. After 6 days, models were examined in the field with the aid of a ×20 geologist lens and removed. Clay models were scored as attacked, if they showed evident predatory marks on any body part, excluding the limbs. In many cases, predators could be identified as mammals, if tooth marks were evident, or as birds, if V-shaped peck marks were observed (Fig. 1). In some cases, however, the predator could not be identified. Predations on dorsal and ventral-coloured models were compared by means of Fisher exact test or χ^2, while absolute frequencies of attacks on the different body parts were compared to the expected frequencies, proportional to the relative surfaces of the model parts, by means of a χ^2 goodness-of fit test (Zar, 2005). We set the significance level at $\alpha = 0.05$ and all tests were performed with PAST 4.03 software (Hammer et al., 2001).

Of the 199 models placed on the forest floor (99 dorsal and 100 ventral), 165 (83%) were recovered (82 dorsal and 83 red). The total number of models attacked was 39 (24%), 18 dorsal and 21 ventral models (Table 1). Head, torso and tail of the dorsal and ventral-coloured models

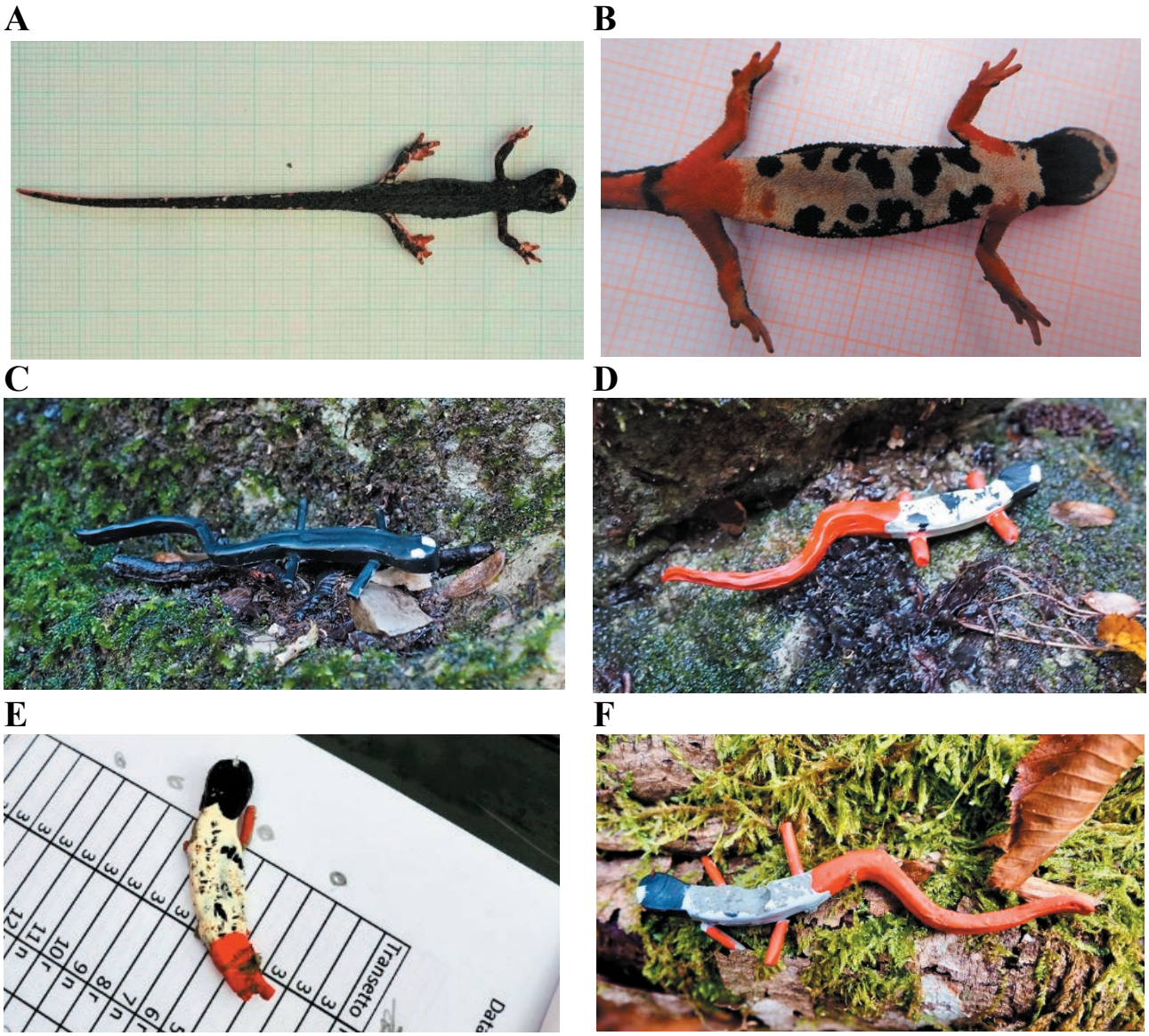

Fig. 1. Dorsal (A) and ventral (B) view of live Norther Spectacled Salamander *Salamandrina persicillata*; dorsal (C) and ventral (D) view of clay models displayed in the field; E) clay model showing a bird V-shaped beak mark on the tail; F) clay model showing mammal teeth marks on the torso.

received a similar number of attacks (χ^2 = 3.25, df = 2, P = 0.172). Overall, there was a tendency that more attacks were aiming to the head than expected by chance (16 observed versus 9.19 expected attacks; Fig. 2), this difference being statistically significant (head vs torso + tail: goodness-of-fit χ^2 = 4.147, df = 1, P = 0.042). Dorsal and ventral-coloured models were attacked with similar frequencies: 18 dorsal and 21 ventral models (Fisher exact test, P = 0.715; Table 1).

In our experiment the models' head was attacked more than expected by chance. Therefore, potential predators were perceiving the salamander replicas as real prey, suggesting that our experimental setting was successful. Contrary to expectations in case of aposematic colouration, clay models painted with conspicuous colours and representing the contrasted ventral side of the Northern Spectacled Salamander were attacked with similar frequencies as clay models displaying the dorsal colouration. This finding may be surprising, given that to date no alternative hypothesis to aposematism has been discussed in detail for this species. However, Utzeri et al. (2005) described the occurrence

Table 1. Distribution of attacks and supposed predators on the different body parts of *Salamandrina perspicillata* clay models.

Body part attacked/predator	Model		
	Black	Red	All
Head/bird	2	0	2
Head/mammal	4	3	7
Head/unidentified	0	0	0
Torso/bird	0	0	0
Torso/mammal	2	3	5
Torso/unidentified	1	0	1
Tail/bird	2	2	4
Tail/mammal	4	8	12
Tail/unidentified	1	0	1
Entire model/bird	0	0	0
Entire model /mammal	2	5	7
Entire model/unidentified	0	0	0
Intact models	64	62	126
Missing models	17	17	34
Total	99	100	199

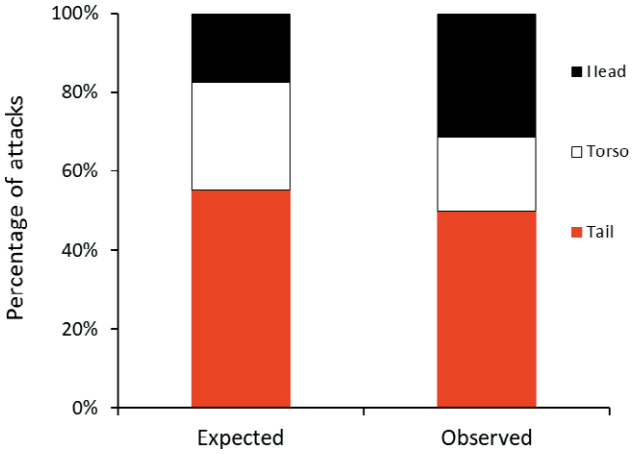

Fig. 2. Percentages of expected and observed attacks on different body parts of clay models of the Northern Spectacled Salamander *Salamandrina persicillata*. Expected percentages are proportional to the relative surfaces of the model parts (see text).

of salamanders showing their ventral coloration in the field, during male-male contests and possibly during sexual encounters. Moreover, a possible deimatic function for *Salamandrina* unkenreflex was suggested during the review process by both reviewers. Deimatism is a behaviour by a sender that produces a sudden change in shape, colour or emits noises. This unexpected behaviour of the prey may cause hesitation or recoil in the predator (Umbers et al. 2017). Unlike aposematism, deimatism does not require predator learned aversion and may be unrelated to unpalatability or armed defence. These alternative hypotheses should deserve attention in future studies on the colourations of the Spectacled salamanders.

In any case, predations trials using motionless animal replicas have several shortcomings and should be always interpreted with caution (Bateman et al., 2017; Rössler et al., 2018; Costa et al., 2020). Actually, studies using clay modes in well-established prey-predator systems, as in the Amazonian poisonous frog *Adelphobates galactonotus* (Rojas et al., 2015) and the Brazilian venomous coral snake *Micrurus corallinus* (Banci et al., 2020), were not able to validate the aposematic function of bright and conspicuous colourations. In fact, many predators use prey movements to search, spot and select their preferred prey items (Paluh et al., 2014). Therefore, it is possible that movement is playing a relevant role in the prey-predator system involving the Norther Spectacled Salamander, and that motionless models were not recognised as aposematic by predators. For example, red models of the Dendrobatid Poison Frog *Oophaga pumilio* equipped with a moving mechanism were attacked less frequently than moving brown models, suggesting that in this species aposematic warning signals need to be broadcasted through an association of colour and behaviour to become effective (Paluh et al., 2014). Indeed, combined factors may increase the specific recognition of visual signals as aposematic and reinforce learning abilities of predators (Stevens, 2013). Unfortunately, we do not have enough information about the prey-predator system of the Norther Spectacled Salamander in its natural habitat and, in particular, if the main predators are birds or mammals (Angelini et al., 2007). However, starting from our results, it could be possible to perform new and more accurate experiments to tests for aposematism (i.e., with moving models and displaying the replicas in different positions), or for alternative explanations such as deimatism or intra-specific communication, that could explain the significance of the bright ventral colouration and of the peculiar behaviour of *S. perspicillata* known as *Unkenreflex*.

ACKNOWLEDGMENTS

We are grateful to Luigi Cuneo (3D INK POINT Genova, affiliated to 3D INK) for the aid with 3D template and print, to Giacomo Bruni and a second anonymous reviewer for suggesting the deimatic defensive behaviour hypothesis, during the review process.

SUPPLEMENTARY MATERIAL

Supplementary material associated with this article can be found at <htttp://www.unipv.it/webshi/appendix> manuscript number 10229

REFERENCES

Angelini, C., Vanni, S., Vignoli, L. (2007): *Salamandrina terdigitata* (Lacépède, 1788) - *Salamandrina perspicillata* (Savi, 1821). In: Fauna d'Italia Amphibia, XLII, pp. 228-237. Lanza, B., Andreone, F., Bologna, M. A., Corti C., Razzetti, E., Eds, Edizioni Calderini, Bologna.

Banci, K.S.C., Eterovic, A., Marinho, P.S., Marquez, O.A.V. (2020): Being a bright snake: Testing aposematism and mimicry in a neotropical forest. Biotropica **3**: 1-13.

Bateman, P.W., Fleming, P.A., Wolfe A.K. (2017): A different kind of ecological modelling: the use of clay model organisms to explore predator-prey interactions in vertebrates. J. Zool. **301**: 251-262.

Caro, T., Allen, W.L. (2017). Interspecific visual signalling in animals and plants: a functional classification. Phil. Trans. R. Soc. B **372**: 20160344.

Costa A., Coroller S., Salvidio S. (2020): Comparing day and night predation rates on lizard-like clay models. Herpetol. Cons. Biol. **5**:198-203.

Demori, I., El Rasheb, Z., Corradino, V., Catalano, A., Rovegno, L., Queirolo, L., Salvidio, S., Biggi, E., Zanotti-Russo, M., Canesi, L., Catenazzi, A., Grasselli, E. (2019). Peptides for skin protection and healing in amphibians. Moleculs, **24**: 347.

Hinsche, G. (1926): Vergleichende untersuchungen zum sogenannten "unken" reflex. Biol. Zentralblatt. **46**: 296-305.

Kraemer, A.C., Serb, J.M., Adams, D.C. (2016): Both novelty and conspicuousness influence selection by mammalian predators on the colour pattern of *Plethodon* cinereus (Urodela: Plethodontidae). Biol. J. Linn. Soc. **118**: 889-900.

Kuchta, S.R. (2005): Experimental support for aposematic coloration in the salamander *Ensatina eschscholtzii xanthoptica*: implications for mimicry of Pacific newts. Copeia **2005**: 267-271.

Lanza, B. (1967): Reazione di tipo *Unkenreflex* in un Urodelo (*Salamandrina terdigitata*). Z. Tierpsyshol. **23**: 855-857.

Hammer, Ø., Harper, D.A.T., Ryan, P.D. (2001): PAST: Paleontological statistics software package for education and data analysis. Palaeontol. Electron. **4**: 9.

Lüddecke, T., Schulz, S., Steinfartz, S., Vences, M. (2018): A salamander's toxic arsenal: review of skin poison diversity and function in true salamanders, genus *Salamandra*. Sci. Nat. **105**: 9-10.

Paluh, D.J., Hantak, M.M., Saporito, R.A. (2014): A test of aposematism in the dendrobatid poison frog *Oophaga pumilio*: the importance of movement in clay model experiments. J. Herpetol. **48**: 244-254.

Preissler, K., Gippner, S., Lüddecke, T., Krause, E. T., Schulz, S., Vences, M., Steinfartz, S. (2019): More yellow more toxic? Sex rather than alkaloid content is correlated with yellow coloration in the fire salamander. J. Zool. **308**: 293-300

Rojas, B. (2017): Behavioural, ecological, and evolutionary aspects of diversity in frog colour patterns. Biol. Rev. **92**: 1059-1080.

Rojas, D.P., Stow, A., Amézquita, A., Simões, P.I., Lima, A.P. (2015). No predatory bias with respect to colour familiarity for the aposematic *Adelphobates galactonotus* (Anura: Dendrobatidae). Behaviour **152**: 1637-1657

Romano, A., Mattoccia, M., Marta, S., Bogaerts, S., Pasmans, F., Sbordoni, V. (2009): Distribution and morphological characterization of the endemic Italian salamanders *Salamandrina perspicillata* (Savi, 1821) and *S. terdigitata* (Bonnaterre, 1789) (Caudata: Salamandridae). It. J. Zool. **76**: 186-187.

Rössler, D., Pröhl, H., Lötters, S. (2018): The future of clay model studies. BMC Zool. **3**: 6.

Salvidio, S., Romano, S., Oneto, F., Ottonello, D., Michelon, R. (2012): Different season, different strategies: feeding ecology of two syntopic forest-dwelling salamanders. Acta Oecol. **43**: 42-50.

Salvidio, S., Romano, A., Palumbi, G., Costa, A. (2017): Safe caves and dangerous forests? Predation risk may contribute to salamander colonization of subterranean habitats. Sci. Nat. **104**: 20.

Schneider, C.A., Rasband, W.S., Eliceiri, K.W. (2012): NIH Image to ImageJ: 25 years of image analysis. Nat. Met. **9**: 671-675.

Stevens, M. (2013): Sensory ecology, behaviour, and evolution. Oxford University Press, Oxford.

Umbers, K.D., De Bona S., White, T.E., Lethonen, J., Mappes, J., Endler, J.A. (2017). Deimatism: a neglected component of antipredator defence. Biol. Lett. **13**: 20160936.

Utzeri, C., Antonelli, D., Angelini, C. (2005). Notes on behaviour of the Spectacled Salamander *Salamandrina terdigitata* (lacèpède, 1788). Herpetozoa, **18**: 182-185.

Wells, K. D. (2007): The ecology and behaviour of amphibians. University of Chicago Press, Chicago.

Yotsu-Yamashita, M., Mebs, D., Kwet, A., Schneider, M. (2007): Tetrodotoxin and its analogue 6-epitetrodotoxin in newts (*Triturus* spp.: Urodela, Salamandridae) from southern Germany. Toxicon **50**: 306-309.

Yotsu-Yamashita, M., Toennes, S. W., Mebs, D. (2017): Tetrodotoxin in Asian newts (Salamandridae). Toxicon **134**: 14-17.

Zar, J.H. (2014): Biostatistical analysis, 5th ed. Pearson Education Limited, London.

Acta Herpetologica 16(2): 129-131, 2021
DOI: 10.36253/a_h-10306

Sexual size dimorphism in the tail length of the Caspian Whip Snakes, *Dolichophis caspius* (Serpentes, Colubridae), in south-western Hungary

György Dudás[1], Krisztián Frank[2,*]

[1] *Danube-Dráva National Park Directorate, Tettye tér 9, 7625 Pécs, Hungary*
[2] *Szekszárd District Office of the Government Office of Tolna County, Dr. Szentgáli Gyula u. 2, 7100 Szekszárd, Hungary*
**Corresponding author.* E-mail: krisz.frank.biol@gmail.com

Submitted on: 2021, 3rd January; Revised on: 2021, 5th May; Accepted on: 2021, 11th May
Editor: Marco Sannolo

Abstract. Sexual size dimorphism is widespread among snakes and has also been observed in lengths of body appendages such as in tails. Males typically possess longer tails than females and this dimorphism in tail length has generally been attributed to the importance of the tail in mating and reproduction. We used body size measurements, snout-vent length (SVL) and tail length (TL) as well as a body condition index (BCI) as a measure of quality in Caspian Whip Snakes from Hungary, in order to shed light on sexual dimorphism patterns. The SVL of males (1061 ± 133 mm, n = 25) were significantly longer than that of females (887 ± 208 mm, n = 41). However, the proportion of TL to total length was lower in males than in females (0.257 ± 0.018 and 0.274 ± 0.017, respectively). The BCI of females (386 ± 10) was significantly higher than that of males (343 ± 15). Females having proportionally longer tails compared to males seems to be the reverse of the usual trend. Selective pressures on the tails of female snakes are less obvious, as tail length may be linked to more than one function, and hence be simultaneously subjected to more than one type of selective force.

Keywords. Colubridae, Hungary, sexual size dimorphism, tail length.

Sexual size dimorphism (SSD) is a common phenomenon and has been studied in snakes for decades (Klauber, 1943; Shine, 1978; King, 1989; Shine, 1994). Intersexual differences could be attributed to several evolutionary and ecological factors (Shine, 1978; King, 1989; Luiselli, 1996; Sheehy et al., 2016; Sivan et al., 2020). Dimorphism may result from sexual selection (e.g., male-male combat or female choice), may occur when natural selection favours different traits in females and males, additionally, morphological constraints imposed on members of one sex or another may also result in sexual dimorphism (King, 1989; Sivan et al., 2020). Though these mechanisms are not mutually exclusive, morphological traits may be simultaneously subjected to more than one type of selective force.

Tails are important for a variety of functions in snakes, including locomotion (Jayne and Bennett, 1989; Shine and Shetty, 2001; Sheehy et al., 2016), predation (Heatwole and Davison, 1976) and reproduction (King, 1989; Shine et al., 1999; Sivan et al., 2020). Snakes are sexually dimorphic, and differences in relative tail lengths between sexes have been described in various species (King, 1989; Shine et al., 1999). The difference in tail length was initially attributed to structural differences between sexes, as males possess a hemipenis in an elongated pocket at the base of the tail (Klauber, 1943). Later on, tail length has been shown to be a sexual selective trait, at least by some species, where males with relatively longer tails would have an advantage in reproduction (King, 1989; Luiselli, 1996; Shine et al., 1999; Sivan et al., 2020). This could be because longer tails are advantageous when competing with other males during ball mating (Luiselli, 1996; Shine et al., 1999), or because the length of

ISSN 1827-9635 (print)
ISSN 1827-9643 (online)

www.fupress.com/ah

the tail is an index signal by choosing mating partners (Sivan et al., 2020).

The Caspian Whip Snake, *Dolichophis caspius*, is a large-sized colubrid with a distribution area ranging from the Carpathian Basin to the west side of the Caspian Sea and covering most of the Balkan Peninsula and several neighbouring Near East countries (Puky et al., 2005). At the north-western edge of its distribution, populations tend to be fragmented and isolated (Tóth, 2002; Puky et al., 2005). A major part of scientific literature concerning the species deals with its geographic distribution and occurrence data. Life-history traits have been studied in the main distributional range in Frontier Asia and Balkans, studies conducted on north-western populations were less prominent.

We analysed body size measurements of Caspian Whip Snakes from Hungary, in order to shed light on sexual dimorphism patterns. At the north-western edge of its distribution, in south-western Hungary, the largest remnant Caspian Whip Snake population is harbouring Szársomlyó Hill, a strictly protected nature reserve (Tóth, 2002; Frank et al., 2012). During the period 1998-2003 road surveys were carried out from April to September. Snakes were captured by hand, weighed to the nearest 1 g by a digital balance and measured for snout-vent length (SVL) and tail length (TL) to the nearest 1 mm by stretching the animal out along a measuring tape. Snakes were probed to determine the sex of the animal. After measuring, snakes were released at the location of capture. Recaptures were not included in the statistical analyses. Two snakes had damaged tails and were omitted from the analyses.

Differences in body measurements (SVL and TL) and BCI between sexes were compared using t-tests. To examine the difference between the two regression estimates of TL on SVL in males and females an ANCOVA was used. Measurements are presented as means ± SE and $P < 0.05$ was accepted as the level of significance. All statistical analyses were performed with the software PAST (Hammer et al., 2001).

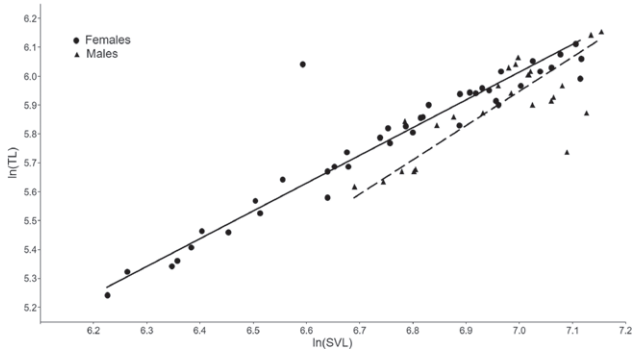

Fig. 1. The effect of snout-vent length (SVL) on tail length (TL) in female (circles, solid line) and male (triangles, dashed line) free-ranging Caspian Whip Snakes, *Dolichophis caspius*.

Average SVL of males (n = 25), 1061 ± 133 mm, was significantly longer than that of females (n = 41), 887 ± 208 mm ($t = -4.091$, $P = 0.0001$). However, average TL in males, 367 ± 54 mm, and females, 333 ± 72 mm was only marginally different ($t = -1.997$, $P = 0.0501$). The regression of TL on SVL (Fig. 1) was calculated in males as $\ln(TL) = 1.1734 \times \ln(SVL) - 2.2721$, ($R^2 = 0.597$, $F = 5.840$, $P = 0.0002$); and in females as $\ln(TL) = 0.9503 \times \ln(SVL) - 0.6407$ ($R^2 = 0.896$, $F = 18.339$, $P = 0.0001$). The proportion of TL to total length was lower in males than in females (0.257 ± 0.018 and 0.274 ± 0.017, respectively). Both size (as SVL) and sex affected TL ($F_{1,64} = 8.129$, $P = 0.0059$).

Size dimorphism between sexes is widespread among snakes; in a list of 129 species of the family Colubridae compiled by Shine (1994), males were the larger sex in 24% of species. Within the group of longer males, SSD ranged between -0.01 and -0.50 (Shine, 1994), the calculated SSD of *D. caspius* (Frank and Dudás, 2018) lies in the middle of this range. All 31 colubrids with longer males than females were oviparous (Shine, 1994), as is *Dolichophis*.

Difference in relative tail length between sexes is very widespread in snakes, and relative tail length might be a biologically relevant trait that affects reproduction (King, 1989; Shine, 1994; Shine et al., 1999; Sivan et al., 2020). Dimorphism in TL is usually male-biased, i.e. male snakes typically possess longer tails than females. This has generally been attributed to the importance of the tail in mating and reproduction (King, 1989; Luiselli, 1996; Shine et al., 1999; Shine and Shatty, 2001; Sivan et al., 2020). As pointed out by King (1989), males might benefit from a longer tail because it may provide space for larger hemipenes ("morphological constraint hypothesis") or because it confers an advantage in mating success ("male mating ability hypothesis"). Additionally, females might increase reproductive output due to an increase in body capacity and a secondary reduction of TL ("female reproductive output hypothesis").

Females having proportionally longer tails compared to males seems to be the reverse of the usual trend (King, 1989; Shine et al., 1999); thus, has been reported substantially less. In a list of 103 colubrid species compiled by King (1989), females had relatively longer tails than males in seven cases (King, 1989). Selective pressures on the tails of female snakes are less obvious (Shine and Shetty, 2001), as tail length may be linked to more than one function, and hence be simultaneously

subjected to more than one type of selective force. Sexual selection of longer tails in females would imply that individuals with longer tails have a higher reproductive output than females with shorter tails. Unfortunately, there are no data to confirm this hypothesis in *D. caspius*, and no finding of selective forces acting on the tails of female snakes has been published in any other species.

Relative tail length may also be influenced by ecological factors when, for example, males and females use different microhabitats, or have different defensive tactics. Arboreal snakes have been shown, in general, to have relatively longer tails than non-climbing species (Sheehy et al. 2015), but this trend was not investigated intraspecifically before. Besides, it is not likely that female *D. caspius* are more arboreal than males. However, this is the first study in which the sexual dimorphism in tail length in Caspian Whip Snakes was investigated and as for now the influence of tail length on female reproductive output or any other life-history trait remains unexplained.

ACKNOWLEDGEMENTS

We are grateful to all volunteers who participated in the fieldwork. This work was supported by Birdlife Hungary. Collecting and measuring the animals was done with permissions from the Danube-Dráva National Park Directorate.

REFERENCES

Frank, K., Dudás, Gy. (2018): Body size and seasonal condition of Caspian Whip Snakes, *Dolichophis caspius* (Gmelin, 1789), in southwestern Hungary. Herpetozoa **30**: 131-138.

Frank, K., Majer, J., Dudás, Gy. (2012): Capture-recapture data of large Whip Snakes *Dolichophis caspius* (Gmelin, 1789), in southern Transdanubia, Hungary. Herpetozoa **25**: 68-71.

Hammer, Ø., Harper, D. A. T., Ryan P. D. (2001): PAST: Paleontological statistics software package for education and data analysis. Palaeontol. Electron. **4**: 9.

Heatwole, H., Davison, E. (1976): A review of caudal luring in snakes with notes on its occurrence in the Saharan sand viper, *Cerastes vipera*. Herpetologica **32**: 332-336.

Jayne, B. C., Bennett, A. F. (1989): The effect of tail morphology on locomotor performance of snakes: a comparison of experimental and correlative methods. J. Exp. Zool. **252**: 126-133.

King, R. B. (1989): Sexual dimorphism in snake tail length: sexual selection, natural selection, or morphological constraint? Biol. J. Linn. Soc. **38**: 133-154.

Klauber, L. M. (1943): Tail-length differences in snakes with notes on sexual dimorphism and the coefficient of divergence. Bull. Zool. Soc. San. Diego. **18**: 1-60.

Luiselli, L. (1996): Individual success in mating balls of the grass snake, Natrix natrix: size is important. J. Zool. **239**: 731-740.

Puky, M., Schád, P., Szövényi, G. (2005): Magyarország herpetológiai atlasza / Herpetological Atlas of Hungary. Varangy Akciócsoport Egyesület, Budapest.

Sheehy, C. M. III, Albert, J. S., Lillywhite, H. B. (2016): The evolution of tail length in snakes associated with different gravitational environments. Funct. Ecol. **30**: 244-254.

Shine, R. (1978): Sexual size dimorphism and male combat in snakes. Oecologia **33**: 269-278.

Shine, R. (1994): Sexual size dimorphism in snakes revisited. Copeia **1994**: 326-346.

Shine, R., Olsson, M. M., Moore, I. T., LeMaster, M. P., Mason, R. T. (1999): Why do male snakes have longer tails than females? Proc. Roy. Soc. B **266**: 2147-2151.

Shine, R., Shetty, S. (2001): The influence of natural selection and sexual selection on the tails of sea-snakes *(Laticauda colubrina)*. Biol. J. Linnean Soc. **74**: 121-129.

Sivan, J., Hadad, S., Tesler, I., Rosenstrauch, A., Degen, A.A., Kam, M. (2020): Relative tail length correlates with body condition in male but not in female crowned leafnose snakes (*Lytorhynchus diadema*). Sci. Rep. **10**: 4130.

Tóth, T. (2002): Data on the north Hungarian records of the Large Whip Snake *Coluber caspius*. Herpetozoa **14**: 163-167.

Acta Herpetologica 16(2): 133-136, 2021
DOI: 10.36253/a_h-11502

Semi-automated photo-identification of Bahamian Racers (*Cubophis vudii vudii*)

Sebastian Hoefer[1,*], Andreu Rotger[2], Sophie Mills[1], Nathan J. Robinson[1,3]

[1] *Cape Eleuthera Institute, The Cape Eleuthera Island School, Eleuthera, The Bahamas*
[2] *Animal Demography and Ecology Unit (GEDA), IMEDEA, CSIC-UIB, 07190 Esporles, Spain*
[3] *Fundación Oceanogràfic, Oceanogràfic De Valencia, 46013 Valencia, Spain*
**Corresponding author*. E-mail: sebastianhoefer@outlook.com

Submitted on: 2021, 14th July, Revised on: 2021, 17th September; Accepted on: 2021, 18th September.
Editor: Marco Mangiacotti

Abstract. Photo-identification is a non-invasive option for mark-recapture. Here, we tested the effectiveness of APHIS, a semi-automated photo-identification software, to distinguish between individual Bahamian Racers (*Cubophis vudii vudii*) on the island of Eleuthera, The Bahamas. Over 10 months, we photographed 50 Bahamian Racers. We first identified individuals by manually comparing colouration and scale patterns in the pileus and labial regions. Next, we used APHIS to identify recaptured individuals after manually identifying the locations of intersections of the scales in the pileus and labial regions. In addition, we assessed whether images taken with a hand-held camera or by a smart phone affected the accuracy of APHIS. All recaptured snakes were correctly identified using APHIS from both camera or phone images as validated by our manually derived results. We conclude that APHIS is an effective tool for photo-identification in snakes.

Keywords. APHIS, I[3]S, Mark-recapture, non-invasive, Snake, Dipsadidae, Colubridae, The Bahamas.

Mark-recapture studies require individuals to be reliably identified upon repeat encounters. This enables researchers to monitor specific individuals over time and this can allow for the estimation of ecological relevant information such as growth or survival rates (Pradel, 1996; Besbeas et al., 2002). In snakes, long-term marking is typically achieved by scale clipping (Brown and Parker, 1976), branding (Winne et al., 2006), passive integrated transponder tags (PIT tags) (Gibbons and Andrews, 2004), and/or visible implant elastomers (VIE) (Hutchens et al., 2008; Major et al., 2020). As each method has different advantages and disadvantages, researchers must critically assess which method is most appropriate for their study. Branding and scale clipping is generally inexpensive but can leave lasting physical damage (Weary, 1969; Brown and Parker, 1976). In contrast, PIT tags or VIE are highly reliable but are associated with considerable financial cost (Gibbons and Andrews, 2004; Major et al., 2020) and can be unsuitable for smaller individuals (Gibbons and Andrews, 2004). An alternative method that has the benefit of being both non-invasive and relatively inexpensive is the use of photo-identification (Sacchi et al., 2016).

Photo-ID has been successfully applied to numerous snake species (e.g., Carlström and Edelstam, 1946; Vaughan, 1999; Creer, 2005; Bauwens et al., 2018; Lunghi et al., 2019). Photos can be processed manually but this can be time consuming. In contrast, pattern recognition software offers a fast and robust approach to compare patterns in photos and distinguish between individual animals (Sacchi et al., 2010). One such pattern recognition software is the Automated Photo-Identification Suite (APHIS), developed by Moya et al. (2015). APHIS enables users to choose between two image matching

ISSN 1827-9635 (print)
ISSN 1827-9643 (online)

methods; the Image Template Matching, (ITM) a pixel-based colour comparison, and the Spots Pattern Matching (SPM) procedure that compares user-defined spot patterns. We selected to use APHIS because images can be processed in batches due to the independence of the manual pre-processing and automated photo-matching which allows substantial time saving (see Moya et al., 2015). APHIS also creates log files that can be used to track the analyses and allow for successive examinations. In addition, APHIS offers the use of two image matching methods. Initially, we wanted to compare both matching methods but decided to discard the ITM method because of quality issues in some of our images and, in addition, we were concerned about potential colour changes of the snakes over the course of the study. So far, APHIS has been used to differentiate between individual horseshoe whip snakes (*Hemorrhois hippocrepis*) (Rotger et al., 2019) but it has not yet been applied to other snake species. Here, we tested the efficacy of the Spots Pattern Matching (SPM) procedure implemented in APHIS (see Moya et al., 2015 for details) to identify individual Bahamian Racers (*Cubophis vudii vudii*). Specifically, we investigated (1) whether APHIS was able to accurately identify individuals based on scale patterns in the pileus and labial regions, and (2) if image quality influenced the successful identification.

Bahamian Racers are colubrid snakes endemic to the eastern parts of the Great Bahama Bank (Henderson and Powell, 2009). These opportunistic snakes feed on a wide variety of vertebrate prey (Hoefer et al., 2020; 2021), are diurnally active and frequently encountered around human settlements.

On opportunistic encounters with Bahamian Racers, we observed that head colouration and scalation was notably variable, particularly in the labial and pileus region (Fig. 1). Thus, we selected these areas for photo-ID. We did not use colour patterns as there are several examples of ontogenetic colour change in snakes (Creer, 2005; Lunghi et al., 2019). Consequently, we used only head scalation for identification purposes, as it is generally considered to be robust throughout a snakes' life (Bauwens et al., 2018). Upon capture, we measured snout-vent length (SVL) and tail length (TL) to the nearest millimetre using a flexible measuring tape, weighed the snake to the nearest gram using a weighing scale (DAPHA DWS Weighing Scale) and determined the sex via probing. Using a Nikon D3300 DSLR camera and Sigma 105 mm 1:2.8 DG Macro HSM EX lens in combination with an external flash and flash diffuser, we took photos of the pileus and the right and left labial regions. We assumed that both labial regions were identical for the use in APHIS and so we combined them when comparing to the pileus region. We initially identified recaptures via visual examination of colour, scale patterns, unique scarring and scale counts. We selected APHIS for our recapture matching analyses because pictures can be processed in batches due to the independence of the manual pre-processing and automated photo-matching, which allows for great time savings (Moya et al., 2015). In addition, APHIS creates log files that can be used to track the analyses and allow for successive examinations.

From August 2019 to June 2020, we opportunistically captured a total of 50 Bahamian Racers including 11 recaptures from five unique individuals. All snakes were found in small shrubs or leaf litter close to walking paths and buildings, which is likely the result of a detection bias due to the opportunistic nature of sampling. For the recaptures, we used 10 pileus, 10 right labial, 9 left labial images. In addition, we used 11 iPhone 7 images of a selection of the same recaptures (4 pileus, 4 right labial, 3 left labial) to compare to the DSLR photos and assess the usability of phone quality images in APHIS. The angle and composition for DSLR and phone images were consistent across photos, but overall image quality and resolution differed (DSLR: 300 PPI 6000 x 4000 px, iPhone 7: 72 PPI 4032 x 3024 px). For each snake, we marked between 35 to 45 reference points on the corners of the scales (Fig. 1) and analysed the images using the I^3S procedure in an automated process described by Moya et al. (2015). We considered a successful match of a recapture when APHIS suggested the correct images for an individual within the top 10 candidates (i.e., top 20% of photos) (Gatto et al., 2018) and a top match when it was the first suggestion in the list. The candidate list created in APHIS is based on a similarity score where images that differ very little, i.e., photos of the same snake, produce a low score and are ranked at the top. Images that differ considerably result in a high score and are ranked at the lower end of the list. The similarity score represents the difference between photos in the relative distances of the reference points.

When comparing the combined labial and pileus regions, we found that all of the labial and pileus images were correctly identified as recaptures, with 100% (19/19) of the labial photos and 90% (9/10) of the images in the pileus region resulting in a top match, making either area suitable to use in APHIS. When only using photos collected via the DSLR camera (n = 29) across all head regions combined, recaptures were correctly identified 100% (29/29) of the time and 97% (28/29) were suggested as top matches. Images of recaptures taken with an iPhone 7 were successfully identified 100% (11/11) of the time when compared to the DSLR database photos, with 82% (9/11) of top match sugges-

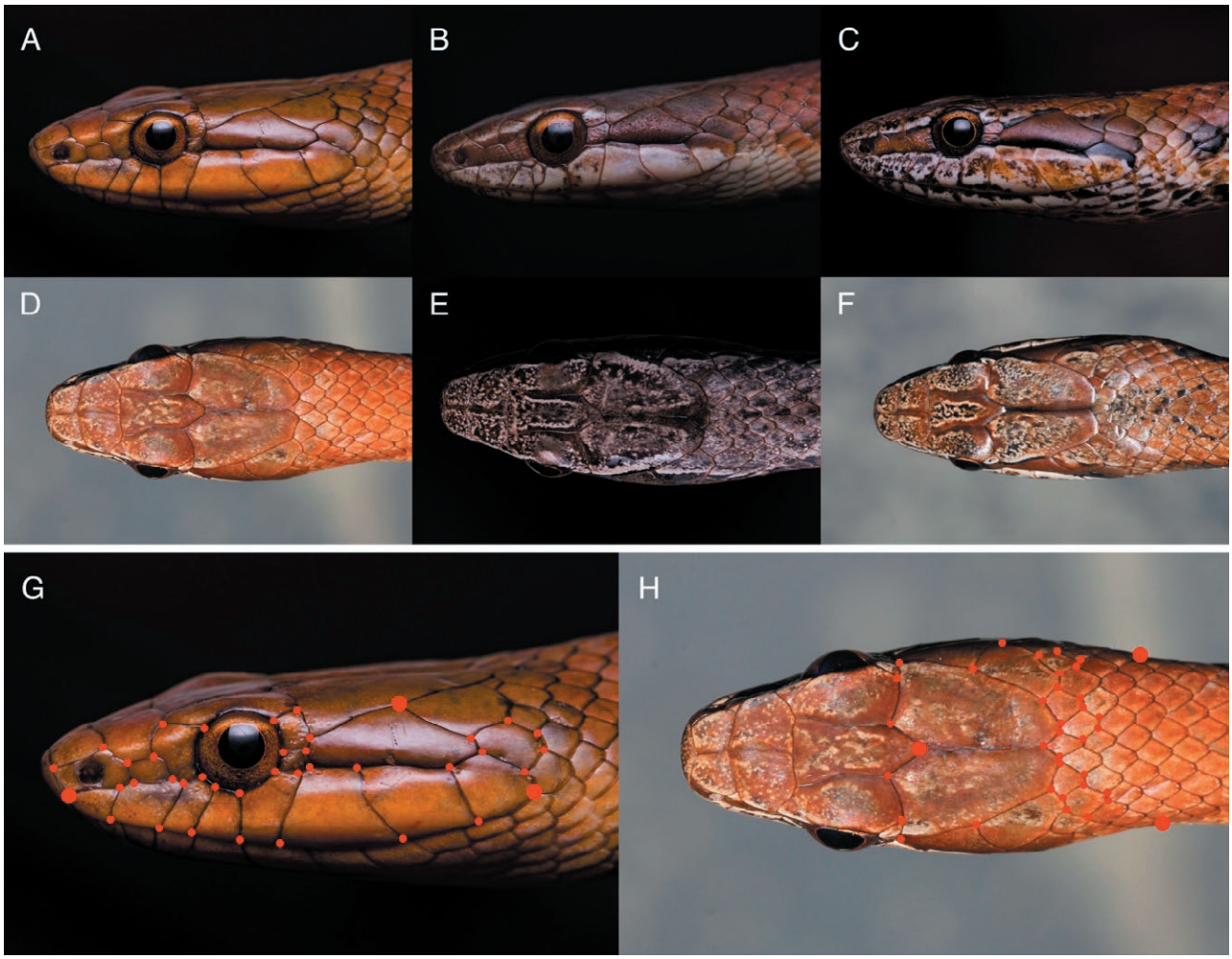

Fig. 1. Photographs of three different Bahamian Racers: A) – C) shows the labial region; D) – F) shows the pileus region. G) and H) shows an example of the reference points selected within APHIS marking the intersection of the scales in the labial and pileus region, respectively.

tions. When the top match was incorrectly identified, the difference in score between the incorrect first candidate and the correct candidate was marginal. Even when the two images that were compared differed substantially in resolution and composition, APHIS was able to successfully match recaptures. In addition, we did not observe any colour or scale pattern changes in neither the labial nor the pileus region of any individual Bahamian Racer over the course of this study (duration between captures ranging from 6 days to 216 days, Figs. S1 and S2). However, 10 months likely only provides a glimpse into the lives of these snakes and, furthermore, all the recaptured individuals were adult snakes and thus ontogenetic changes in colouration or scalation cannot be dismissed.

In conclusion, we were able to use APHIS to correctly identify and successfully match all our recaptured Bahamian Racers. The software provided accurate results even when the image quality differed substantially between the photos compared and the recaptures were up to seven months apart. The semi-automated analysis resulted in high matching probability when using images taken from a smartphone, which is likely more accessible in the field than a dedicated camera. The use of pattern recognition software in recapture studies allows for short handling times in the field and only requires taking a photograph. This likely increases the time available for searching and recording new individuals, thus enhancing data collection. Particularly for studies on snakes, where detectability of animals can be quite low, maximising the time to find snakes could enable researchers to gather more crucial information for many of these understudied species. Even though this study has its limitations due to low sample sizes, we provide

further support for the use of APHIS to effectively distinguish between individual animals.

ACKNOWLEDGMENTS

We would like to thank the Cape Eleuthera Institute for providing the resources to conduct research in The Bahamas. We also thank the many interns, staff, and visitors for reporting live snake sightings and helping with data collection and photos. Research was conducted under the Cape Eleuthera Institute research permit number MAMR/FIS/2/12A/17/17B.

SUPPLEMENTARY MATERIAL

Supplementary material associated with this article can be found at <htttp://www.unipv.it/webshi/appendix> manuscript number 11502.

REFERENCES

Bauwens, D., Claus, K., Mergeay, J. (2018): Genotyping validates photo-identification by the head scale pattern in a large population of the European adder (*Vipera berus*). Ecol. Evol. **8**: 2985-2992.

Besbeas, P., Freeman, S.N., Morgan, B.J.T., Catchpole, E.A. (2002): Integrating mark-recapture-recovery and census data to estimate animal abundance and demographic parameters. Biometrics **58**: 540-547.

Brown, W.S., Parker, W.S. (1976): A ventral scale clipping system for permanently marking snakes (Reptilia, Serpentes). J. Herpetol. **10**: 247-249.

Carlström, D., Edelstam, C. (1946): Methods of marking reptiles for identification after recapture. Nature **158**: 748-749.

Creer, D.A. (2005): Correlations between ontogenetic change in color pattern and antipredator behavior in the racer, *Coluber constrictor*. Ethology **111**: 287-300.

Gatto, C.R., Rotger, A., Robinson, N.J., Santidrián Tomillo, P. (2018): A novel method for photo-identification of sea turtles using scale patterns on the front flippers. J. Exp. Mar. Biol. Ecol. **506**: 18-24.

Gibbons, W.J., Andrews, K.M. (2004): PIT tagging: simple technology at its best. BioScience **54**: 447-454.

Henderson, R.W., Powell, R. (2009): Natural history of west Indian reptiles and amphibians. University Press of Florida, Gainesville (US).

Hoefer, S., Mills, S., Pinou, T., Robinson, N.J. (2021): What the dead tell us about the living: using roadkill to analyse diet and endoparasite prevalence in Bahamian snakes. Ichthyol. Herpetol. **109**: 685-690.

Hoefer, S., Robinson, N. J., Jones, A. (2020): *Cubophis vudii vudii* (Bahamian Racer). Diet. Herpetol. Review **51**: 346-347.

Hutchens, S.J., Deperno, C.S., Matthews, C.E., Pollock, K.H., Woodward, D.K. (2008): Visible implant fluorescent elastomer: a reliable marking alternative for snakes. Herpetol. Review **39**: 301-303.

Lunghi, E., Giachello, S., Mulargia, M., Dore, P.P., Cogoni, R., Corti, C. (2019): Variability in the dorsal pattern of the Sardinian grass snake (*Natrix natrix cetti*) with notes on its ecology. Acta Herpetol. **14**: 141-145.

Major, T., Alkins, D.R., Jeffrey, L., Wüster, W. (2020): Marking the un-markable: visible implant elastomer in wild juvenile snakes. Herpetol. J. **30**: 173-176.

Moya, Ó., Mansilla, P.L., Madrazo, S., Igual, J.M., Rotger, A., Romano, A., Tavecchia, G. (2015): APHIS: a new software for photo-matching in ecological studies. Ecol. Inform. **27**: 64-70.

Pradel, R. (1996): Utilization of capture-mark-recapture for the study of recruitment and population growth rate. Biometrics **52**: 703-709.

Rotger, A., Colomar, V., Moreno, J.E., Parpal, L. (2019): Photo-identification of horseshoe whip snakes (*Hemorrhois hippocrepis*, Linnaeus, 1758) by a semi-automatic procedure applied to wildlife management. Herpetol. J. **29**: 304-307.

Sacchi, R., Scali, S., Mangiacotti, M., Sannolo, M., Zuffi, M.A.L. (2016): Digital identification and analysis. In: Reptile ecology and conservation. A handbook of techniques, pp. 59-72. Dodd, C.K., Ed. Oxford University Press, Oxford.

Sacchi, R., Scali, S., Pellitteri-Rosa, D., Pupin, F., Gentilli, A., Tettamanti, S., Cavigioli, L., Racina, L., Maiocchi, V., Galeotti, P., Fasola, M. (2010): Photographic identification in reptiles: a matter of scales. Amphibia-Reptilia **31**: 489-502.

Silvy, N.J., Lopez, R.R., Peterson, M.J. (2012): Techniques for marking wildlife. In: The wildlife techniques manual, 7th ed., Vol. 1, pp. 230-257. Silvy, N.J., Ed, James Hopkins University Press, Baltimore (US).

Vaughan, R. (1999): Provisional results from study of facial features as a means of individual identification in *Natrix natrix*. Herpetol. Bulletin **69**: 39-46.

Weary, G.C. (1969): An improved method of marking snakes. Copeia **1969**: 854-855.

Winne, C.T., Willson, J.D., Andrews, K.M. (2006): Efficacy of marking snakes with disposable medical cautery units. Herpetol. Review **37**: 52-54.

Finito di stampare da
Logo s.r.l. – Borgoricco (PD) – Italia

Cover: Mindo Leaf Frog (*Noblella mindo*), adult female. Photo by Melissa Costales.

Università degli Studi di Firenze
Firenze University Press
via Cittadella 7, 50144 Firenze, Italy
http://www.fupress.com/
E-mail: journals@fupress.com

Periodicità: semestrale
ISSN 1827-9643 (online)
ISSN 1827-9635 (print)
Registrata al n. 5450 del 3.11.2005
del Tribunale di Firenze

ACTA HERPETOLOGICA

CONTENTS

December 2021 Vol. 16 – N. 2

15,00 €